2011

Analysis and Modelling of Seismic Surface Wave for Studying the Crustal Structure of the South-Eastern Region of Bangladesh

Faruk, Md. Omar

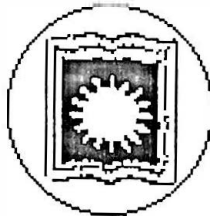University of Rajshahi

ANALYSIS AND MODELLING OF SEISMIC SURFACE WAVE FOR STUDYING THE CRUSTAL STRUCTURE OF THE SOUTH-EASTERN REGION OF BANGLADESH

MD. OMAR FARUK

A THESIS

SUBMITTED TO THE DEPARTMENT OF APPLIED PHYSICS AND ELECTRONIC ENGINEERING, FACULTY OF ENGINEERING OF THE UNIVERSITY OF RAJSHAHI FOR THE DEGREE OF DOCTOR OF PHILOSOPHY.

Geophysics Research Laboratory
Department of Applied Physics and Electronic
Engineering, University of Rajshahi, Rajshahi-6205
Bangladesh
November 2011

Declaration

I do, hereby, declare that this thesis entitled *ANALYSIS AND MODELLING OF SEISMIC SURFACE WAVE FOR STUDYING THE CRUSTAL STRUCTURE OF THE SOUTH-EASTERN REGION OF BANGLADESH* has been done by me and the work described here, is entirely of my own unless otherwise explicitly stated in the text. It is prepared for the degree of Doctor of Philosophy, in the Geophysics Laboratory, Department of Applied Physics and Electronic Engineering, Faculty of Engineering, University of Rajshahi, Bangladesh. No part of this work has been submitted in any university or institution for any degree.

Md. Omar Faruk

(Md. Omar Faruk)
Ph. D. Fellow
Department of Applied Physics and Electronic Engineering
University of Rajshahi
Bangladesh.

Certificate of the Supervisors

The undersigned certify that the thesis entitled *ANALYSIS AND MODELLING OF SEISMIC SURFACE WAVE FOR STUDYING THE CRUSTAL STRUCTURE OF THE SOUTH-EASTERN REGION OF BANGLADESH* has been composed by him under our joint supervision. To the best of our knowledge, it has not formed the basis for any degree or award elsewhere.

(Dr. Md. Abul Hashem)
Professor
Department of Applied Physics and
Electronic Engineering, University of Rajshahi,
Rajshahi-6205, Bangladesh.

(Dr. Syed Mustafizur Rahman)
Associate Professor
Department of Applied Physics and
Electronic Engineering, University
of Rajshahi, Rajshahi-6205,
Bangladesh.

Abstract

Earthquake is one of the catastrophic events of the natural disasters that are prone to cause great damage to life and property. In order to decrease the damages, it is essential to gain knowledge for studying the crustal structure of the earth.

In this dissertation crustal structure of the south-eastern region of Bangladesh is estimated by using seismic surface wave data. The parameters of the recorded earthquake data are ideally related to the subsurface geology. Geologic properties beneath a region have a major impact on the ground motion by modifying the amplitude, phase, duration, and shape of seismic waves. The main purpose of our work is to study the crustal structure, particularly major crustal boundaries and thicknesses of the structures.

Three earthquake events of the south-eastern region of Bangladesh have been deliberated in this research. The events are respectively of magnitude 5.6 occurred on 26 July 2003 at the south-west of Daluchari, Chittagong, Bangladesh, magnitude 5.1 occurred on 27 July 2003 at Kolabunia, Chittagong, Bangladesh and magnitude 5.6 occurred on 21 September 2003 at the south of Meiktila, Myanmar nearer to the study area.. The events were recorded at Dhaka University seismic station located at $23^0 44.10' \, N$ and $90^0 23.45' \, E$.

In order to make a relationship between earthquake wave and crustal structure of an area, time frequency to amplitude analysis which is an extension of time frequency analysis is brought for the analysis of synthetic and real data. Analyses have well marked the sequences over the recorded earthquake wave, however, it lacks to make a meaningful relation with crustal parameters though it is revealed that the technique can be further used for characterization of the geology of the earth.

The research work is then extended to dispersion analysis of the earthquake wave. A realistic relation between seismic wave analysis and crustal variables, in the form of models which are proposed in this work, is being tried to be incorporated using the application of group velocity dispersion estimation. Group velocity dispersions are developed for both the earthquake data and the model parametric data.

Dispersions are computed using graphical method for three earthquake events. Modified Haskell matrix method has been introduced to compute the dispersions for the crustal model parameters. Group velocity dispersions by graphical method are then interpreted from model parameters. Sensitivity and the statistical errors of the model have also been studied. Interpreted results have shown that the crustal structure of the south-eastern region of Bangladesh is consisted of four major subsurface layers of thickness 1.5 km, 5.0 km, 6.0 km and 8.0 km to a total depth of 20.5 km. Seismic surface wave analysis and modelling with subsurface variables presented in this thesis are seemed to be effective and can be further used for the other recorded waves in different stations for studying detailed crustal structure of an area.

Acknowledgements

Contents

List of Figures

List of Tables

Chapter 1
Introduction

1.1 Background

Seismic wave investigation is using as the only and prime tool to determine the internal structure of the earth since long. The study of the earth's internal structure is made possible through the analysis and interpretation of seismic waves produced by earthquakes. Indirect seismic wave research is becoming increasingly popular as it is blended with mathematical techniques for the determination of earth's internal structure. Direct measurements of the internal earth of the deeper depth are almost impossible or limited. Scientists have investigated the earth's interior with a depth of 12.262 km so far highest from the earth's surface by means of direct observation (Kozlovsky, 1987 and Bowler, 1990) that is less than 0.2% of the average radius of the earth of 6371 km (NASA, 2011). Hence most of the contributions about the structure of the earth are put together from indirect measurement of seismic waves, which originate from the sudden release of energy by the occurrence of earthquakes or explosions and can be detected at the earth's surface with the sensitive devices.

Seismic surface wave is a type that propagates along the earth's surface. Most of the energy in this wave is confined to the close vicinity of the surface, similar to waves propagating on the surface of water. It is only through the crust with a slower speed, lower frequency, longer duration and larger amplitude than other type seismic wave and is easily distinguished on a detected record as known as seismogram. Seismogram contains information about the earthquake as an energy source and the medium through which propagates or energy-radiates. The present research is intended to analyze the detected seismic surface wave for studying the regional crustal structure of the earth.

1.2 Seismic Wave and Earth's Structure

The nature of seismic surface wave has been investigated by many seismologists and it has been seen from various analyses that the dispersion of this wave is strongly influenced by the crustal structures (Ewing et al., 1957 and Satŏ et al., 1960). In a homogeneous medium surface waves are found to be non dispersive. In the earth, however, due to the general increase in velocity with depth, the longer wavelength components of a surface wave train penetrate deeper and hence travel faster (Campillo and Paul, 2003). This effect is the basis for the widely used surface wave dispersion analysis to infer horizontally layered earth structure (Knopoff, 1961; Dorman and Ewing, 1962 and Snieder, 1987) and shallower geotechnical applications (Park et al., 1999; Xia et al., 1999; Ritzwoller and Levshin, 2002).

The application of dispersion curves for subsurface characterization was originally proposed during the 1950s (Aki, 1957). Surface wave dispersion curve development for flat-layered earth model began with Thomson (1950) and Haskell (1953) whom used a matrix to solve the eigen value problem of the system of differential equations. The original Thomson-Haskell formulation was unstable and had many numerical difficulties that are associated with numerical overflow and loss of precision at high frequencies (Kennett, 1983; Buchen and Ben-Hador, 1996). Later improvements on the formulation are being observed to overcome such problems. Delta matrix (Pestel and Leckie, 1963), reduced delta matrix or modified Haskell matrix (Watson, 1970), fast delta matrix (Buchen and Ben-Hador, 1996), Schwab–Knopoff method (Schwab and Knopoff, 1970, 1972), fast Schwab–Knopoff (Schwab, 1970), Abo-Zena method (Abo-Zena, 1979), Kennett reflection and transmission (R/T) matrix (Kennett, 1974; Kennett and Kerry, 1979) and the generalized R/T coefficient method (Kennett, 1983; Luco and Apsel, 1983) was remarkable progresses. The inversion has been performed and obtained geologic structure using the above methods. The present research is also motivated from the above discussions.

1.3 Motivation

The research work intended to be done here is motivated from the three factors as, (i) Bangladesh is susceptible to damaging earthquakes, and hence it needs the realistic

assessments of the crustal structure of the country, (ii) how can it be accomplished? and (iii) what should be done, which is economically viable. This is thought that geophysical techniques can perform such jobs particularly by the study of seismological activities. It seems that recorded seismic wave data can be obtained with a minimum cost, therefore analysis and modelling can be performed over recorded data in order to obtain regional geologic structure of the earth.

1.3.1 Problem statement

Earthquake is one of the catastrophic events of the natural disasters that are prone to cause great damage to life and property. The history of human civilization reveals that man has been combating with natural disasters from its origin but natural disasters have not only disturbed the normal life pattern in various times but also caused huge losses to life and property. Disasters also interrupted the development process. But unfortunately until now prediction at the present time is not an exact science, and forecasts of earthquake occurrences have not been very accurate. In order to decrease of life and property damage, it is essential to be gained knowledge for studying the crustal structure of the earth.

It is realistic to think that the analysis of earthquake seismic waves, which are propagated through the earth and recorded at the seismological stations, can provide valuable information regarding the interior of the earth. Geologic properties beneath a region have a major impact on the ground motion by modifying the amplitude, phase, duration, and shape of seismic waves. Thus research problem can be delineated as the study of crustal structure of the south-eastern part of Bangladesh using group velocity dispersion analysis of seismic surface wave of the local and regional earthquakes, which are also recorded at the nearby local and regional stations.

1.3.2 Objective of the thesis

The ultimate objective of the thesis is to study the crustal structure particularly major crustal boundaries and thicknesses of the south eastern region of Bangladesh. In order to obtain a meaningful crustal structure the following intentions are being introduced.

- To review the effectiveness of the existing techniques of the seismic surface wave analysis for studying the crustal structure.

- To select a useful technique that can be used for model development.

- To develop models and to justify the sensitivity of the models with crustal parameters.

- To select the best model based on statistical analysis and to estimate the crustal thicknesses of study area.

1.4 Study Area

The study area is covered Chittagong and a small part of Dhaka divisions of Bangladesh along with a part of Tripura and Mizoram state of India, north-west part of Myanmar and also small part of the Bay of Bengal (Fig. 1.1). The investigated area as in this thesis is the south-eastern region of Bangladesh. The area ranges with latitude $19^0 12'$ N to $23^0 44.10'$ N and longitude $89^0 52.5'$ E to 96^0 E.

1.4.1 Geologic setting

The south eastern region of Bangladesh is a complex tectonic area where major tectonic and subduction events have been identified from late Lower Cretacous to Mid-Miocene and Quaternary periods (Mitchell, 1993). This is a region of transition between the main Himalayan collision belt and the Andaman arc where the Indian plate is currently subducting under Asia. Structurally, the region consists of the Indo- Burman ranges (an accurate mountain belt), part of the Burmese basin (also called the Central Lowlands) and the Eastern Highlands. A magmatic arc divides the Burmese basin into back-arc and fore-arc troughs. A right-lateral strike-slip fault (the Sagaing Fault, SF) separates the eastern highlands from the Burmese basin. To the left of the Indo-Burma region is the Himalayan collision belt. To the north of the ranges are the northwest trending Mishmi thrust faults. The Indo-Burma boundary continues in a broadly NS accurate trend southward into the Bay of Bengal and joins the Andaman arc.
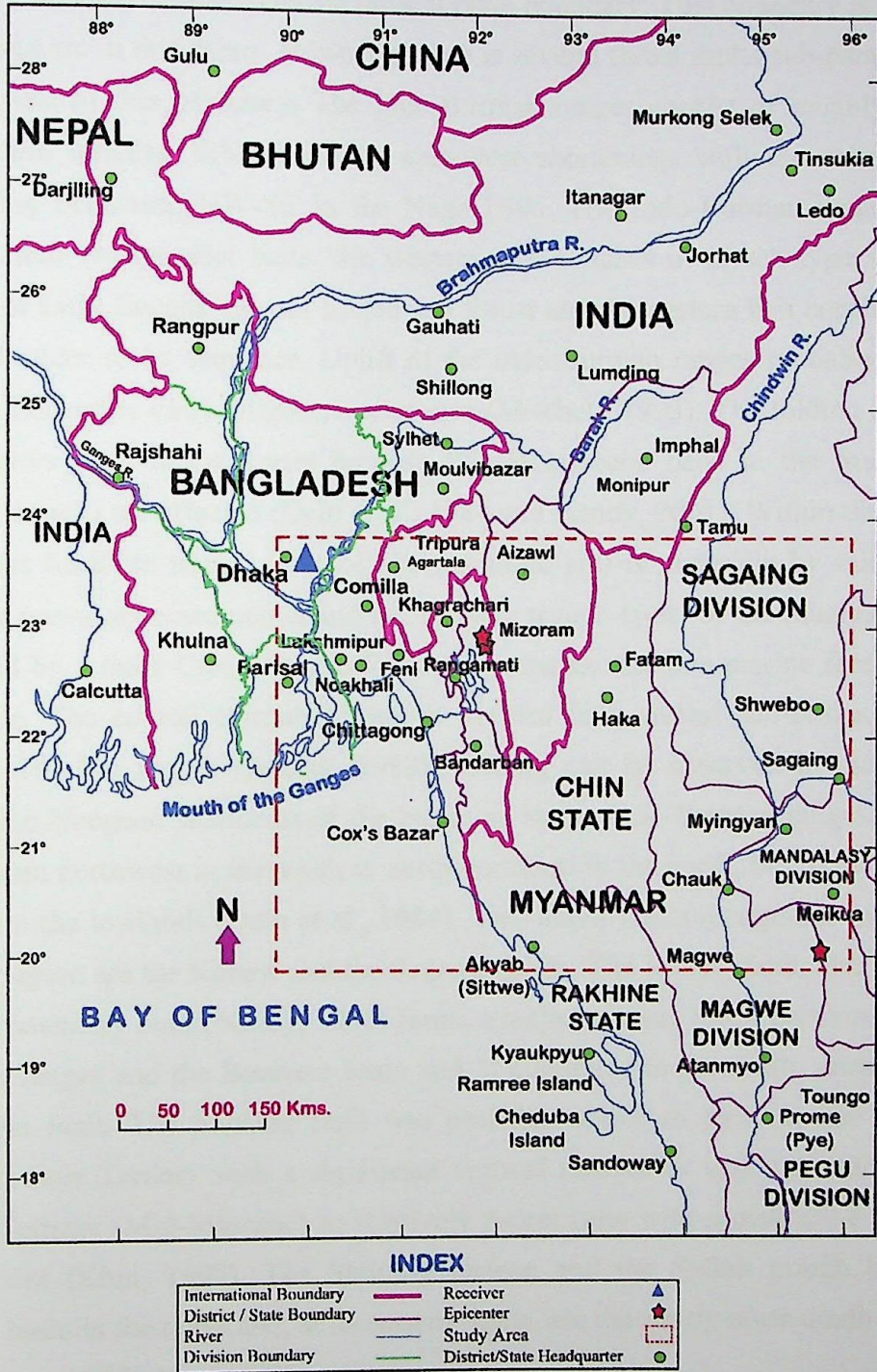
Fig. 1.1 Location map for study area.

The western edge of the Indo-Burman ranges, bounded by thrust faults along the Naga hills in the north and folds and thrusts in the Bengal basin (Dain et al., 1984 and Nandy, 2001), is considered as the present plate boundary. This boundary is termed as the Burma arc in this thesis. However, there is several thrust faults sub-parallel to the ranges west of this boundary. The Indo-Burman ranges consist of roughly parallel, north-south trending folds implying east-west shortening, with the orientation of shortening becoming NW-SE in the Naga Hills. The Indo-Burman ranges can be divided into two parallel belts: the western belt consists of flysch type sediments, largely of early Eocene age, all folded and thrust and the eastern belt consists largely of much older rocks sequence. Uplift of the Indo-Burman ranges probably began in the late Eocene or early Oligocene sequence (Mitchell, 1993). The folding must have been active until recent times because Plio-Pleistocene beds in the Surma basin (Sylhet trough) are affected (Dain et al., 1984 and Nandy, 2001). Within the Burmese basin, the back-arc trough (east of the magmatic arc) is underlain by mid- to late-Tertiary non-marine sediments and the fore-arc trough (west of the magmatic arc) is occupied by a thick Cretaceous to Quaternary marine and non-marine fore-arc basin sequence. The central Burmese basin is divided into several sub-basins along its nearly 1100 km length (Bender, 1983). Folding can be observed in many places within the Neogene sediments of the basin; as in the Indo-Burman ranges, the folds curve from northwest in the south to north-northeast in the north, but folding is much gentler in the lowlands (Dain et al., 1984). Two major faults recognized in the Indo-Burma region are the Kabaw and the Sagaing faults. The Kabaw fault, also called the eastern boundary fault (Nandy, 1980) forms a major tectonic break between the Indo-Burman ranges and the Burmese basin and, if continued to the south, joins the West Andaman fault. The Sagaing fault was probably active as early as the Mesozoic and/or Lower Tertiary with a significant vertical movement and was reactivated in Upper Tertiary (Mid-Miocene) to relatively recent time with a distinctive strike-slip component (Khin, 1990). The Shillong plateau and the Sylhet trough bound the Bengal basin in the north and, at its eastern limits, are the nearly north-south fold belts of Tripura and Chittagong hills.

The Shillong plateau has a maximum elevation of about 2 km and is bounded in the south by the Dauki fault. The Dauki fault forms the contact between the Shillong plateau and the Sylhet trough. The eastern and northern parts of the Bengal basin have

been subjected to more structural modification than have western and southern parts and a similar distribution applies to recorded seismicity (Morgan and Mcintire, 1959).
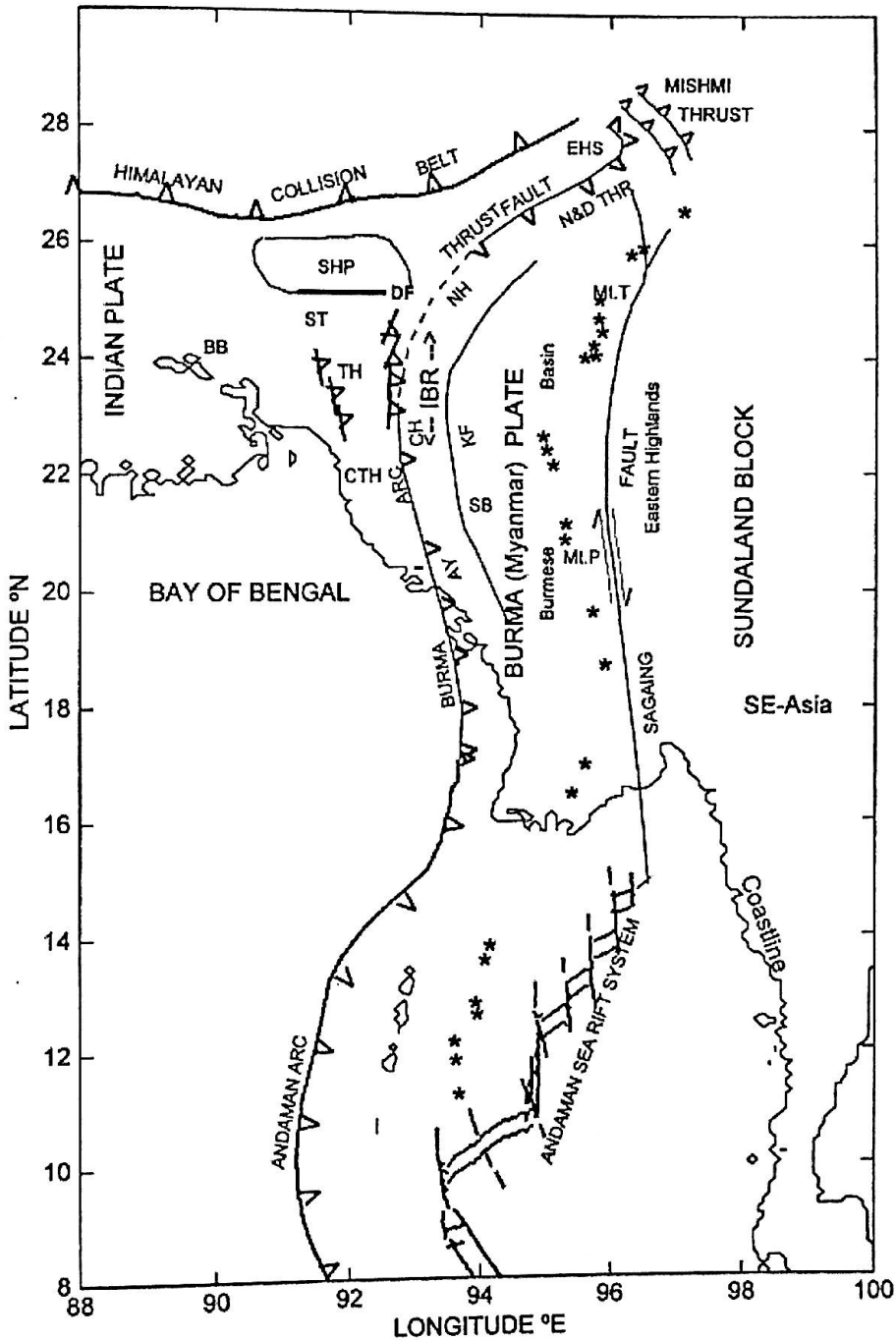
Fig. 1.2 Schematic map of the principal tectonic features in and around the Indo – Burma region. The Burma Arc and other thrust faults are shown by barbed lines and the Sagaing Fault by a line with half arrows representing dextral slip. Cenozoic volcanoes are shown by *. Abbreviations: BB – Bengal Basin, SHP – Shillong Plateau, DF – Dauki Fault, ST – Sylhet Trough, TH – Tripura Hills, CTH – Chittagong Hills, AY – Arakan Yoma ranges, CH – Chin Hills, NH – Naga Hills, IBR – Indo–Burman ranges, N&D THR – Naga and Disang Thrusts, KF – Kabaw Fault, SB – Salin Basin, Mt.P – Mount Popa volcano, Mt.T – Mount Taungthonton, THR – Thrust fault/s (after Mitchell, 1993).

7

A number of high angle thrust faults have been recognized across the Chittagong-Tripura hills (Khan, 1991). Folds and thrusts in the Bengal basin are also seen on the Land satimagery (Nandy, 1980 and Dain et al., 1984) and field investigations reveal that not only Early Tertiary rock but Pliocene and Pleistocene sediments have been involved in the folding and under thrusting. North-trending folds that are uplifted in the Chittagong-Tripura fold belt plunge northward into the Sylhet trough subsurface (Johnson and Alam, 1991) and the Sylhet trough merges with the main part of the Bengal basin. Within about 40 km south of the Dauki fault, the north-trending folds in the subsurface of the Sylhet trough are deflected to a northeast trend. Marine seismic surveys show that the beds close to the seafloor are deformed over anticlinal structures without any thinning or wedging of beds over the structures (Khan, 1991). The maximum thickness of the sedimentary section in the basin is more than 10 km and it thickens further to the east to 20 km or more (Ganguly, 1997).

1.4.2 Previous studies

The study area is a part of the Bengal basin, which is one of the largest geosynclinal basins in the world situated at the western foreland part of the Indo-Burma mobile belt and it contains thick deposit of Tertiary sediments under the cover of Ganga-Brahmaputra alluvium (Nandy, 2001). It is of interest to note that it contains nearly 15 km of sediments (Evans, 1964 and Talukdar, 1982). The geosynclinal basin in the southeast is characterized by the huge thickness of maximum of about 20 km near the basin centre of clastic sedimentary rocks, mostly sandstone shale of Tertiary age. It occupies areas of greater Dhaka, Faridpur, Noakhali, Sylhet, Comillah, and Chittagang and the Bay of Bengal (ASB, 2006). The Bengal basin covers an area of nearly 200,000 km^2 and contains a thick (up to 16 km) package of orogenic sediments derived from the Himalayas to the north and the Indo-Burma Ranges to the east (Uddin and Lundberg, 1998a).

The entire sedimentary column of the Tripura-Mizoram area is constituted of sandstone, siltstone, shale, mudstone, sand rock, silt and rarepockets of shell-limestone, which is divided into four major stratigraphic units based mostly on lithologic characteristics. Sequentially they are, (1) Barail (Oligocene; 3000 m) sandstone and shale, (2) Surma Group (Miocene) consisting mainly of (a) arenaceous

Lower Bhuban Formation (9000m), (b) argillaceous Middle Bhuban Formation (3000m), (c) arenaceous Upper Bhuban Formation (1100 m) and (d) argillaceous Bokabili Formation (1000 m), overlain by (3) Tipam Group (Pliocene; 1300 m) consisting of feldspathic sand with fossil wood and minor silt and the youngest (4) Dupi Tila Formation consisting of mottled clay, fine silt and laterite occupies the synclinal valleys to the west and overlies the Tipams over a pronounced unconformity. Older and older rocks crop out toward east across the strike. Sediments are characterised by various types of primary sedimentary structures indicating shallow marine to deltaic environment (Nandy et al., 1983). Scanty faunal and floral record indicates that the sediments were deposited in shallow paralic environment (Ganguly, 1997). Details of the faunal assemblages of the area are given by Das Gupta (1984) suggesting Mio-Plioceneage of these sediments.

The average shear-wave velocity of the upper crust is ~ 3.2 Km /s with a gradational velocity increase in the lower crust to ~ 4.0 km /s of the western Bengal basin (Mitra et al., 2008). Agartala in the eastern Bengal basin has a high-velocity lower crustal layer of ~ 6 Km thickness corresponding to the oceanic crust (Mitra et al., 2006) beneath the 22 km thick sediments in the Bangladesh trough (Hiller, 1988). For direct viewing of the crustal structure in Burma arc and adjacent areas the horizontal sections of the S wave velocities are 3.2 ~3.6 Km/s. The crust structures of Burma block are relatively stable with S wave velocities between 3.6 ~ 3.7 Km/s at the depths of 20 ~ 35 km (lower crust). The seismic sounding (Kan and Lin, 1986) verifies that the crust velocity of P wave is only 6.2 Km/s. The crust velocity of Yunnan-Burma-Thailand block is 3.1 ~ 3.5 Km/s with depth of 20 Km. The Burma block on the west side of the Sagain fault has followed the evolution of India Plate, and the crust velocity is higher than that of Yunnan-Burma-Thailand block, with little velocity variation with the increase of depth (JiaFu et al., 2008). The recent studies (Hu et al., 2002) have verified that the Poisson's ratio of the crust in west-Yunnan is 0.30 ~ 0.32, and the artificial seismic sounding (Kan and Lin, 1986) verified that the P wave velocity at the top of upper mantle in the area is only 7.60 ~ 7.80 km/s.

The Central basin in Myanmar accommodated a tremendous thickness (about 12 km) of Palaeogene sedimentary rock, in particular Eocene–Oligocene fluvio-deltaic to

shallow marine deposits, yet these sediments appear to have been deposited in a broad synformal basin, with little internal deformation. Adjacent areas to the west (Indo-Burma ranges) and the east (Shan Plateau) were undergoing considerable uplift and deformation during the Eocene–Oligocene, whereas the intervening Central basin shows virtually no compressional deformation until the Miocene (Pivnik et al., 1998).

1.5 Outline of the Thesis

This thesis describes the ways of seismic surface wave analysis, which covers seismogram measurements, velocity distributions in the crust and the determination of the crustal structure of the south-eastern region of Bangladesh. It includes theoretical background, analysis, modelling and interpretation of crustal structure as organized in the following manner.

Chapter 1 deals with an overview of seismic surface wave analysis, intended research problem and the general informations about the south-eastern region of Bangladesh.

Chapter 2 focuses on the seismological variables through which the structure of the earth can be studied.

Chapter 3 contains the seismological earthquake data; this section also explains data type, data format and conversion for analysis.

In Chapter 4 various techniques are discussed and analyzed the local earthquake data. Direct and indirect modellings are also introduced.

Chapter 5 illustrates the model development procedure along with the sensitivity of the model with crustal parameters.

Chapter 6 interprets crustal structure of the south-eastern region of Bangladesh from models as prepared in previous chapter.

Chapter 7 and 8 show respectively the results and conclusions of the whole research work.

A conceptual framework of the present research work to be done has also been brought here as shown in Fig. 1.3.
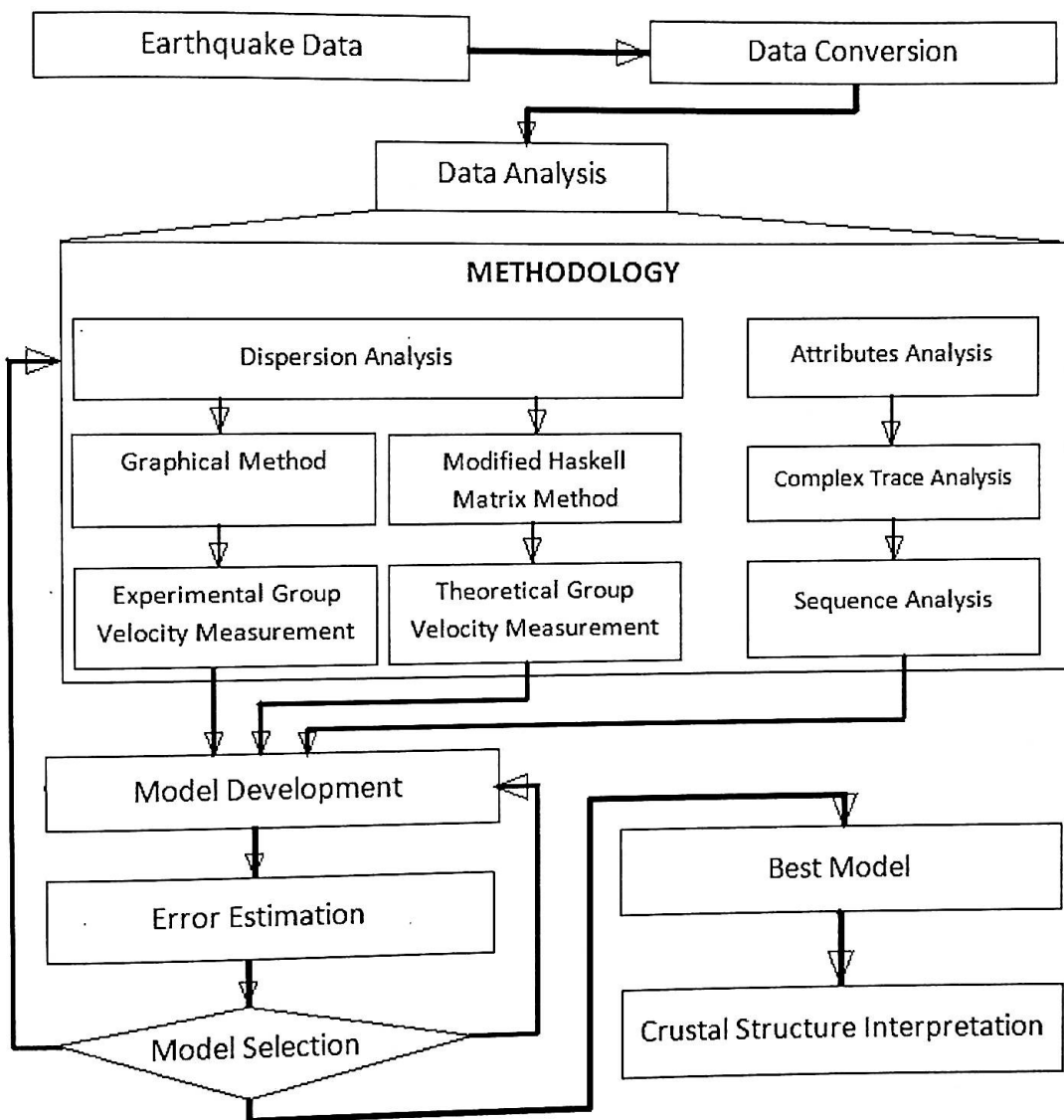
Fig. 1.3 Conceptual framework of the present research.

Chapter 2
Seismology and Earth's Structure

2.1 Introduction

An earthquake is known as a result of a sudden release of energy in the earth's crust that creates seismic waves. Seismic waves generated by an earthquake are usually considered to originate from a single source point within the earth. The place inside the earth where, earthquake occurred is called focus and the place on the surface vertically above is called the epicenter (Fig. 2.1). Every day there are about fifty earthquakes worldwide that are strong enough to be felt locally, and every few days an earthquake occurs that is capable of damaging structures. Each event radiates seismic waves that travel through out earth, and several earthquakes per day produce distant ground motions that, although too weak to be felt, are readily detected with modern instruments anywhere on the globe (Shearer, 1999). Seismology is the science that studies these waves and tells about the structure of earth as well as the physics of earthquakes. It is the primary means by which scientists learn about earth's deep interior, where direct observations are impossible, and has provided many of the most important discoveries regarding the nature of our planet.

Seismology is the study of elastic vibrations of earth. It is basically a geophysical discipline that has a remarkable diversity of applications to critical issues facing society and plays a major role in addressing key scientific frontiers involving earth's dynamics. Seismology is the integrated branch of geosciences and quantitative foundations of mechanics, elasticity, and applied mathematics. Modern seismological systems introduce state of the art digital ground motion recording sensors and real time communications systems so that anyone can openly access many seismological data archives (Lay, 2009).

Seismology occupies an interesting position within the more general fields of geophysics, and earth sciences. It presents fascinating theoretical problems involving analysis of elastic wave propagation in complex media, but it can also be applied simply as a tool to examine different areas of interest (IUGG, 2007; NRC, 2008; Lay, 2009 and NRC, 2001). Applications range from studies of earth's core, thousands of kilometers below the surface to detailed mapping of crustal structure of the earth. Much of the underlying physics is no more advanced than Newton's law $F=ma$, but the complications introduced by realistic sources and structures have motivated sophisticated mathematical treatments and extensive use of powerful computers (Shearer, 1999). Seismology is driven by observations, and improvements in instrumentation and data availability have often led to breakthroughs both in seismology theory and the understanding of earth structure.

Studying crustal structure using seismological information is a common phenomenon nowadays. Geoscientists or researchers are involved to learn more about the inner structure by the analysis and modelling of different type seismic waves detected by the sensors.
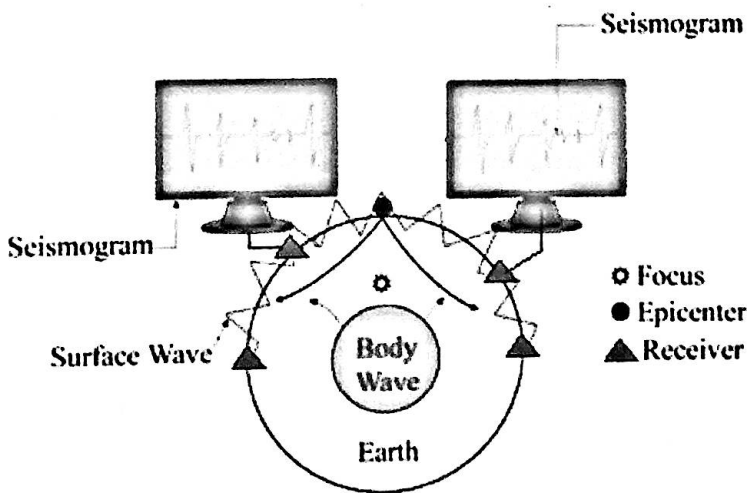
Fig. 2.1 Seismograms arrival at the receivers.

2.2 A Brief History of Seismology

Earth is suffering earthquakes for at least some hundreds of millions years. Geoscientists are trying to explain the better understanding of earthquake mechanism. It is worthy of note that eminent philosopher Aristotle also gave a classification of earthquakes into six types, according to the nature of the earth movement observed. Chinese philosopher Chang Heng devised an artistic instrument for indicating the direction of the first main impulse due to an earthquake in the year A.D. 132. This instrument was reputed to have detected some earthquakes not felt locally and Chang Heng was appointed as official earthquake observer (Dewey and Byerly, 1969; Zebrowski, 1997 and Fathom, 2002).

The role of rock fracturing in earthquake generation was not realized until the mid-nineteenth century. The great Lisbon earthquake and tsunami (tidal wave) of 1755 mark the beginning of the systematic study of earthquakes in western science (Reid, 1914 and Davison, 1927).

About the middle of the eighteenth century A.D., useful observations of earthquake effects began to accumulate. In 1760, John Michell in England published a notable memoir on earthquakes with wave motion in the earth. Most work on earthquakes during the late eighteenth and the early nineteenth century was concerned with appraisals of geological effects of earthquakes, and of effects on buildings. It was noted that the buildings on soft ground were more damaged by earthquakes than those on hard rock. Early in the nineteenth century, earthquakes lists were being regularly published, and in 1840 von Hoff published an earthquake catalogue for the whole world (Bullen, 1963). Beginning in 1841, James D. Forbes experimented with various pendulum arrangements, and he eventually built a "seismoscope" consisting of a pencil attached to an inverted pendulum, which successfully recorded two earthquakes. Unfortunately, it failed to respond to most of the several dozen other earthquakes that were felt in the area where it was set up (Davison, 1927 and Ben-Menahem, 1995).

About the middle of the nineteenth century, the foundations of instrumental seismology were laid when Robert Mallet suggested the setting up of a chain of observatories over the earth's surfaces, and Palmieri in Italy devised a seismograph capable of detecting distant earthquakes and of recording some features of the consequent local earth movements (Bullen, 1963; Ben-Menahem, 1995; Zebrowski, 1997 and Fathom, 2002). The history of seismology of period includes the names of Noggerath and Schmict, whom introduced the use of isoseismal lines to estimate the epicenter of an earthquake and the apparent speed of travel of the ensuing disturbance. Perrey and Montessus de Ballore of France compiled notable earthquake records; de Rossi of Italy and Forel of Switzerland produced the Rossi-Forel intensity scale together, the first well-known scale for estimation surface effects of earthquakes and determining isoseismal lines (Davison, 1927; Bullen, 1963 and Ben-Menahem, 1995).

In 1892, a major development had seen when John Milne in Japan developed a seismograph, which was sufficiently compact and simple in operation to enable it to be installed and used in many parts of the world (Bullen, 1963; Ben-Menahem, 1995 and Gregory, 2006). From that time and onwards precise instrumental data on earthquakes began to accumulate, and seismology began to develop from the qualitative towards the quantitative side.

Meanwhile a great deal of progress is being continued independently on the mathematical front. The study of wave motion was started to become fashionable among applied mathematicians throughout the nineteenth century, and much mathematical theory relevant to seismology was produced. Cauchy and Poisson determined the equations of motion of a disturbance in a perfectly elastic substance in 1882 and later Poisson showed that there could be two distinct types of wave (P and S waves) transmitted with different speeds through the interior of such a substance (Bullen, 1963; Ben-Menahem, 1995 and Novotny, 1999). Stokes showed that the waves were of dilatational and rotational types. Green studied the reflection and refraction of elastic waves. Later the contributions made by Kirchhoff, Kelvin and

Rayleigh introduced the theory of waves on the boundary of a homogeneous elastic substance (Todhunter and Pearson, 1893; Bullen, 1963 and Ben-Menahem, 1995). In 1897, Oldham identified the three main types of seismic wave (P, S and surface wave) on actual records from seismographs nearly 70 years after the mathematical theory of P and S waves had been formulated (Bullen, 1963 and Ben-Menahem, 1995).

In 1904 Lamb pointed out the problem of generation of seismic surface waves (Bullen, 1963 and Ben-Menahem, 1995). Mohorovicic in 1909, the overall thickness of layers down to the discontinuity that bears his name came to be well determined, and much information derived on the P and S velocities inside the layers. It was also well established that crustal thickness is much less under oceans than continents (Bullen, 1963 and Ben-Menahem, 1995) While Love (1911) explained the occurrence of a type of surface wave not included in the theory of Rayleigh and made a comprehensive study of the vibrations of compressible gravitating planet. Earth's internal structure to a quite remarkable degree was being started to realize by the use of seismological data since 1911.

In 1914, Gutenberg published his very accurate determination of the depth of the boundary of the central core one of the early results of a long and distinguished event.

Jeffreys became interested in seismology around this time and brought to bear elegant mathematical and statistical methods and a great knowledge of wider geodynamical problems. His attention to scientific method and statistical detail has been one of the main forces through which seismology has attained its present level of precision (Bullen, 1963 and Ben-Menahem, 1995).

From the 1920s on, seismology has been put to practical uses like the search for oil and gas in the subsurface by using artificial sources of elastic waves, primarily dynamite explosions (Davison, 1927 and Benjamin and Howell, 1990).

The first widely used measure of earthquake size was the magnitude scale developed for earthquakes (Shearer, 1999) in southern California by Charles Richter in 1935 (Appendix 1).

In 1936, Miss Lehmann produced the first evidence of the existence of the earth's inner core (Bullen, 1963 and Ben-Menahem, 1995). Herglotz and others contributed to enable P and S wave velocities to be deduced from the travel-time data, with the consequent furnishing of information on compressibility-density and rigidity-density ratios throughout much of the earth.

In 1940, there were notable instrumental developments in seismographs and international cooperation is becomeing higher than any other branch of research. There was the evolution of 'travel-time tables' from crudest beginnings through the 'Zeoppritz-Turnar tables' and 'Gutenberg-Richter tables', in which errors of the order of minutes had been reduced to errors of the order of seconds. By 1940, it had become possible to classify the earth's interior broadly into a number of regions occupying ranges of depth from the surface to the center (Bullen, 1963 and Ben-Menahem, 1995).

Following World War II, there was a remarkable increase of effort to put into seismological study. Most notable among the achievements which can as yet be assessed has been a great extension in the spectrum of recorded seismic waves. At one end, the methods of prospecting seismology have enabled periods in the order of 0.001 sec to be measured in ground movements. At the other end, new instruments have enabled not only surface waves with periods extending up to 10 min to be observed, but free oscillations of the whole earth with periods in excess of an hour. The spectral gap between surface wave oscillations of the order of 1 or 2 min and tidal oscillations of the order of hours has now been bridged (Bullen, 1963 and Ben-Menahem, 1995).

Beginning in the 1950s, seismology has been used for monitoring nuclear testing and for understanding other seismic events caused by humans such as those triggered by

pumping fluids such as water or oil into or out of the ground. Volcanic seismology has improved to the point that it can help predict volcanic eruptions. While seismologists still cannot predict earthquakes with accuracy, they have done much to explore their preconditions. As human population has increased, more funding has been devoted to earthquake preparedness, including the design of structures, the education of the public, and hazard analysis. In places where the historical record of earthquakes is too short to analyze earthquake probability, workers in the field of paleoseismology use geological evidence to document prehistoric earthquakes (Davison, 1927; Benjamin, 1990 and Bolt, 1993).

The second revolution occurred during 1950 to 1955 when digital computers were first introduced in seismology. The ability to perform fast calculations increased the dimensionality of seismology both in space and time: huge amounts of data could suddenly be processed in a relatively short time; integrals and sums could be evaluated quickly, and equations of all sorts could be solved most efficiently (Ben-Menahem, 1995).

The advent of computer in the 1960s changed the nature of terrestrial seismology, by enabling analysis of large data sets and more complicated problems, and led to the routine calculation of earthquake locations. The first complete theoretical seismograms for complicated velocity structures began to be computed at this time (Shearer, 1999). Earth's average radial velocity and density structures were well

established by 1970, including the existence of minor velocity discontinuities near 410 km and 660 km depth in the upper mantle. Attention then shifted to resolving lateral differences in velocity structure, first by producing different velocity versus depth profiles for different regions, and more recently by inverting seismic data directly for three-dimensional velocity structures. The latter methods have been given the name "tomography" by analogy to medical imaging techniques. During recent years, tomographic methods of increasing resolution have begun to provide spectacular images of the structure of earths crust and mantle. At shallower depths, reflection seismic experiments using controlled sources have led to detailed images of

crustal structure, both on land and beneath the oceans. The ability to image three-dimensional structures has greatly expanded the power of seismology to help resolve many outstanding problems in the earth sciences. These include the structure of fault zones at depth, the deep roots of continents, the fate of subducting slabs, the structure of oceanic spreading centers, the nature of convection within the mantle, the details of the core-mantle boundary region, and the structure of the inner core (Shearer, 1999). Beginning in 1976, data started to become available from global seismographs in digital form, greatly facilitating quantitative waveform comparisons. In recent years, many of the global seismic stations have been upgraded to broadband, high dynamic range seismometers, and new instruments have been deployed to fill in gaps in the global coverage. Large numbers of portable instruments have also become available for specialized experiments in particular regions. Seismic records are now far easier to obtain, with centralized archives providing online data access in standard formats (Shearer, 1999).

Now the modern seismology is at a mature state and developed from the knowledge of early history of seismology. Seismological information is being used today to help geoscientists for better understanding of the earth's structure. From the historical development of seismology it is revealed that the seismic waves are to be classified and analyzed in order to obtain the geology of the earth.

2.3 Seismic Wave Propagation

The fact that the waves travel at speeds which depend on the crustal properties, (e.g. elastic moduli and density) which are allowed to use seismic wave observations to investigate the interior structure of the planet. It can be looked at the travel times or the travel times along with the amplitudes or other characteristics of waves to infer the existence of features within the planet. In order to understand crustal properties or structure using vibrations, it must be studied how waves interact with the rocks that make up earth.

Seismic waves spread away from the source point and are being propagated vibrations that carry energy from the source of the shaking outward in all directions. The various

components of the wave field interact with crustal structure in a variety of ways which can lead to quite complex behavior in the distance range out to a few hundred kilometers from the source. Commonly observed interactions between waves and the subsurface geology are refraction, reflection, dispersion, diffraction and attenuation.

Refraction

As a wave travels through earth, the path it takes depends on the velocity. It is known that Snell's law is the mathematical expression which is allowed to determine the path a wave takes as it is transmitted from one rock layer into another. The change in direction depends on the ratio of the wave velocities of the two different rocks. When waves reach a boundary between different rock types, part of the energy is transmitted across the boundary. The transmitted wave travels in a different direction which depends on the ratio of velocities of the two rock types (Fig. 2.2). Part of the energy is also reflected backwards.
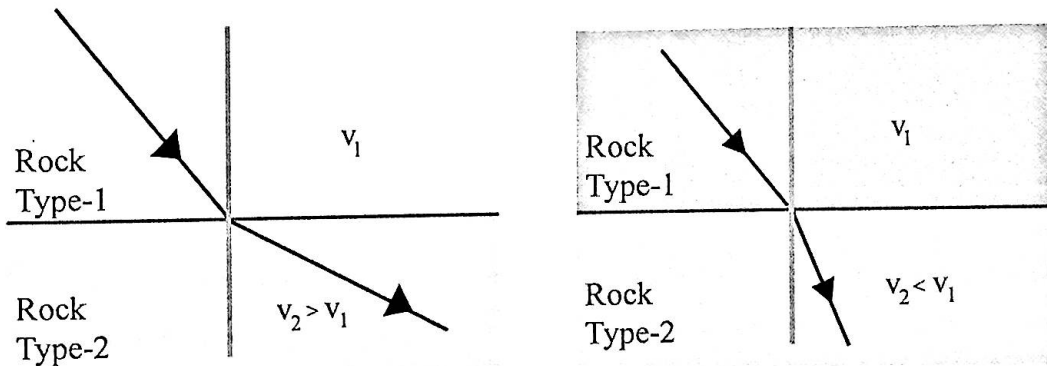
Fig. 2.2 Seismic refraction according to Snell's law.

Refraction has an important affect on waves that travel through earth. In general, the acoustic impedance for transmission of seismic waves in earth increases with depth and refraction of waves causes the path followed by body waves to curve upward. The overall increase in seismic wave speed with depth into earth produces an upward curvature to rays that pass through the mantle. A notable exception is caused by the decrease in acoustic impedance for transmission of seismic waves from the mantle to the core (Ammon, 2010). This speed decrease bends waves backwards (Fig. 2.3)

and creates a 'P wave Shadow Zone' between about 100° and 140° distance (1° = 111.19 km).
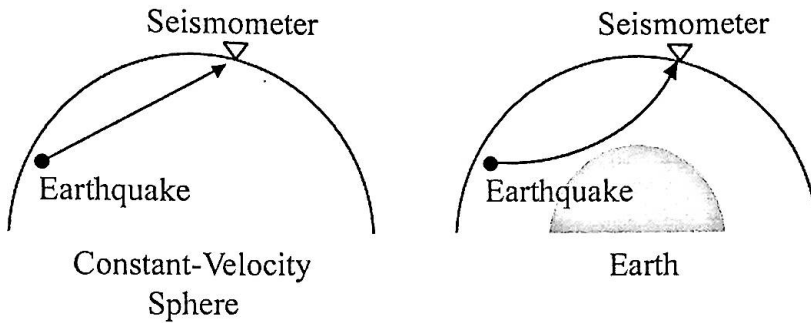
Fig. 2.3 Wave propagation within earth.

Reflection

The second wave interaction with variations in rock type is reflection. It is well known about reflected sound waves which are called echoes. And the reflection in a mirror or pool of water is composed of reflected light waves. In seismology, reflections are used to prospect for petroleum and investigate earth's internal structure. In some instances reflections from the boundary, Moho between the mantle and crust may induce strong shaking that causes damage about 100 km from an earthquake.

A seismic reflection occurs when a wave impinges on a change in rock type part of the energy carried by the incident wave is transmitted through the material and part is reflected back into the medium that contained the incident wave. When a wave encounters a change in crustal properties its energy is split into reflected and refracted waves (Fig. 2.4).

The amplitude of the reflection depends strongly on the angle of incidence that the wave makes, in few cases for greater than the critical angle all the energy can be returned back into the medium containing the incident wave.
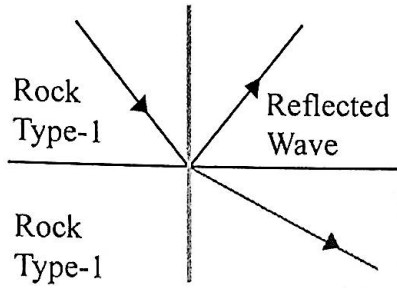
Fig. 2.4 Seismic reflection.

The actual interaction between a seismic wave and a contrast in rock properties is more complicated because an incident P wave generates transmitted and reflected P and S waves and so five waves are involved. Likewise, when an S wave interacts with a boundary in rock properties, it also generates reflected and refracted P and S waves.

Dispersion

It is known that the surface waves are dispersive, which means that different periods travel at different velocities (Fig.2.5). The effects of dispersion become more noticeable with increasing distance because the longer travel distance spreads the energy out. Usually, the long periods arrive first since they are sensitive to the speeds deeper in earth, and the deeper regions are generally faster.

The present research is intended to make dispersion analysis of the recorded seismic surface wave for studying crustal structure.
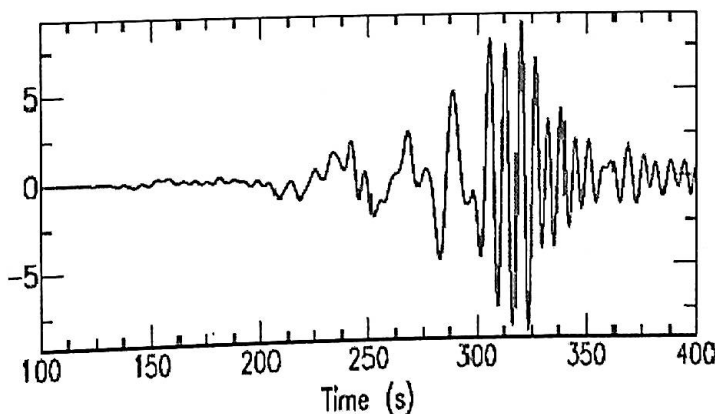
Fig. 2.5 A typical dispersed Rayleigh wave.

Attenuation

So far the changes in seismic wave amplitude have been considered that result from geometrical spreading of wave fronts, and the reflection and transmission coefficients that occur at discontinuities. A third factor that affects amplitudes is energy loss due to anelastic processes or intermal friction during wave propagation. This intrinsic attenuation may be distinguished from scattering attenuation in which amplitudes in the main seismic arrivals are reduced by scattering off small-scale heterogeneities, but the integrated energy in the total wavefield remains constant. The strength of intrinsic attenuation is given by the dimensionles quantity Q in terms of fractional energy loss per cycle (Shearer, 1999).

$$\frac{1}{Q(\omega)} = -\frac{\Delta E}{2\pi E} \qquad 2.1$$

Where, E is the peak strain energy and $-\Delta E$ is the energy loss per cycle. Q is sometimes called the quality factor, a term borrowed from the engineering literature. Note that Q is inversely related to the strength of the attenuation; low Q regions are more attenuationg than high Q regions. From this definition, one may derive an approximation, valid for $Q \gg 1$, that is better suited for seismic applications:

$$A(x) = A_0 e^{-\frac{\omega c}{2cQ}} \qquad 2.2$$

Where x is measured along the propagation direction and c is the velocity (e.g., $c=\alpha$ for P waves with attenuation Q_α, and $c=\beta$ for S waves with attenuation Q_β).

2.4 Type of Seismic Wave

Seismic waves are the elastic waves characterized by particle motion and wave motion. There are two major classes of seismic waves. Body waves move through the interior of the earth and are capable of penetrating the entire earth. Surface waves move up to the epicenter of the earthquake and spread out along the surface. It is the surface waves that provide the energy causes earthquake devastation. Each of these two major classes of seismic waves occurs in two forms. The two types of body waves are called P waves and the S waves. The two types of surface waves are called Love waves and Rayleigh waves. Each of these 4 types of seismic waves is distinct in the way they move through the ground (Fig. 2.6).

2.5 Wave Travel Times

Travel times are best conceptualized of with an analogy of an auto trip; the earthquake location as the starting point for the trip and the seismometer as the place where the trip concludes. Faster waves will travel the distance quicker and show up on the seismogram first.

Travel time = (Distance from earthquake to seismometer) / (Seismic wave speed)

Travel time is a relative time, it is the number of minutes, seconds, etc. that the wave took to complete its journey. The arrival time is the time when the arrival of a wave is recorded. It is an absolute time, usually referenced to Universal Coordinated Time, a 24 hour time system used in many sciences. Here's an example to illustrate the difference: if two earthquakes occurred at the same place but exactly 24 hours apart, the wave travel times would be the same but the arrival times would differ by one day.

2.6 Seismic Wave Speed

Seismic waves travel fast, on the order of kilometers per second (km/s). The precise speed that a seismic wave traveled depends on several factors and most important is the composition of the rock. It is pleaser that the speed depends on the rock type because it is allowed to use observations recorded on seismograms to infer the composition or range of compositions of the planet. But the process isn't always simple, because sometimes different rock types have the same seismic wave velocity, and other factors also affect the speed, particularly temperature and pressure.

Temperature tends to lower the speed of seismic waves and pressure tends to increase the speed. Pressure increases with depth in earth because the weight of the rocks above gets larger with increasing depth. Usually, the effect of pressure is the larger and in regions of uniform composition, the velocity generally increases with depth, despite the fact that the increase of temperature with depth works to lower the wave velocity.

When the different seismic wave types are described it will be quoted ranges of speed to indicate the range of values that observed in common terrestrial rocks. But it should

be kept in mind that the specific speed throughout earth will depend on composition, temperature, and pressure.
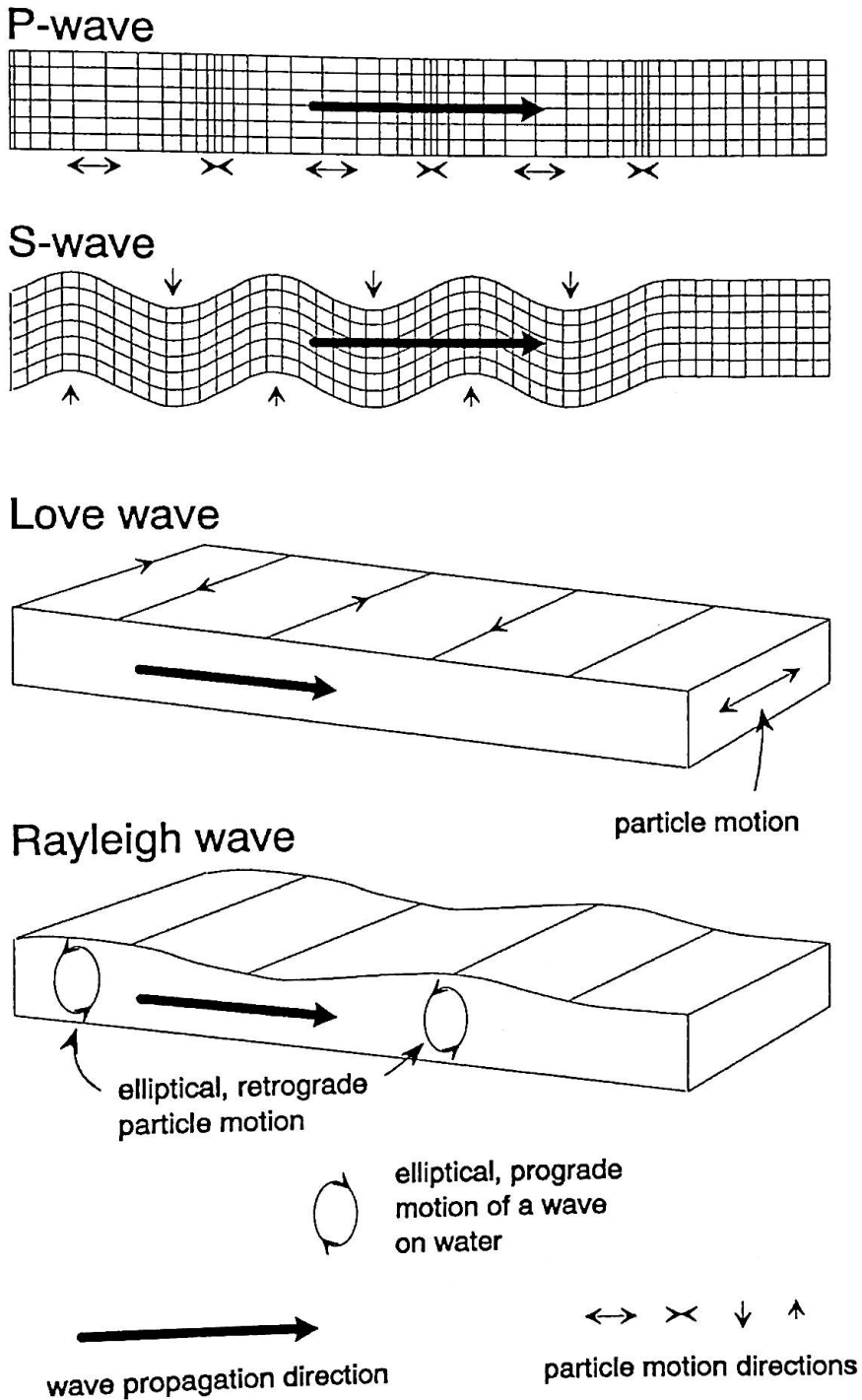
Particle motions for different kinds of seismic waves.

Fig. 2.6 The forms of ground motion near the ground surface in four types of seismic waves.

2.6.1 P waves

P waves are the first waves to arrive on a complete record of ground shaking because they travel faster (Fig 2.7). They typically travel at speed ranges from 1.00 km/s to 14.00 km/sec. The slower values correspond to a P wave traveling in water and the higher values to near the base of earth's mantle.

The velocity of a wave depends on the elastic properties and density of a material. If the elastic properties of a material represent κ, the bulk modulus, μ, the shear-modulus and ρ, the density, then the P wave velocity, α, is defined by:

$$\alpha = \sqrt{\frac{k + \frac{4}{3}\mu}{\rho}}$$ 2.3

A modulus is a measure of how easy or difficulty it is to deform a material. For example, the bulk modulus is a measure of how a material changes volume when pressure is applied and is a characteristic of a material. For example, foam rubber has a lower bulk modulus than steel.

P waves are sound waves but its frequencies are lower than humans' range of hearing (the speed of sound in air is about 0.3 km/sec). The vibration caused by P waves is a volume change, alternating from compression to expansion in the direction that the wave is traveling. P waves can travel through solid, liquid, or gas.
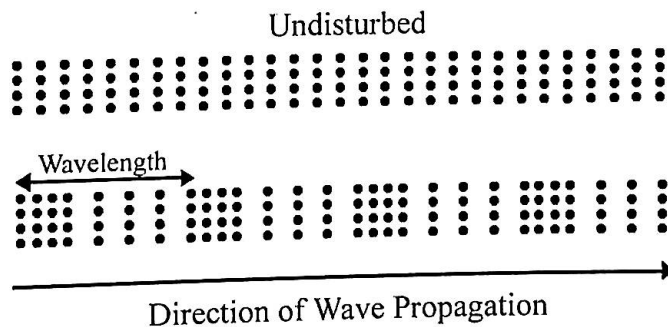
Fig. 2.7 P wave propagation.

2.6.2 S waves

Secondary or S waves travel slower than P waves and are also called shear waves because the S wave through which propagates, don't change the volume of the material but shear. S waves are transverse waves because they vibrate the ground in the direction transverse or perpendicular to the direction that the wave is traveling (Fig 2.8)

Undisturbed

Wavelength

Direction of Wave Propagation
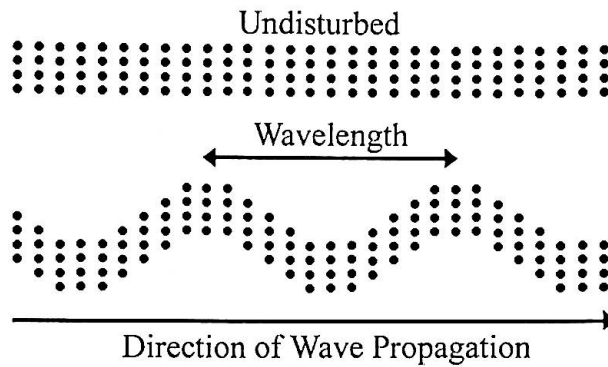
Fig. 2.8 S wave propagation.

The S wave speed, β depends on the shear modulus and the density of the material as shown below.

$$\beta = \sqrt{\frac{\mu}{\rho}}$$

2.4

Typical S wave propagation speeds are in the order of 1.00 km/s to 8.00 km/sec. The lower value corresponds to the wave speed in loose formation, unconsolidated sediment and the higher value is near the base of earth's mantle. An important distinguishing characteristic of an S wave is its inability to propagate through the fluid or gas because a fluids and gasses cannot transmit a shear stress and S waves are waves that shear the material. In general, earthquakes generate larger shear waves than compressional waves and much of the damage close to an earthquake is the result of strong shaking caused by shear waves.

2.6.3 Love waves

Love waves are transverse waves that vibrate the ground in the horizontal direction perpendicular to the direction that the waves are traveling (Fig. 2.9). They are formed by the interaction of S waves with earth's surface and shallow structure and are dispersive waves. The speed at which a dispersive wave travels depends on the wave's

period. In general, earthquakes generate Love waves over a range of periods from 1000 to a fraction of a second, and each period travels at a different velocity but the typical range of velocities is between 2.00 km/s and 6.00 km/s.

Fig. 2.9 Love wave propagation.

Another important characteristic of Love waves is that the amplitude of ground vibration caused by a Love wave decreases with depth, they are surface waves. Like the velocity the rate of amplitude decreases with depth and also depends on the period.

2.6.4 Rayleigh waves

Rayleigh waves are the slowest of all the seismic wave types and in some ways the most complicated. Like Love waves they are dispersive so the particular speed at which they travel depends on the wave period and the near-surface geologic structure, and they also decrease in amplitude with depth (Fig. 2.10). Typical speeds for Rayleigh waves are on the order of 1.00 km/s to 5.00 km/s.
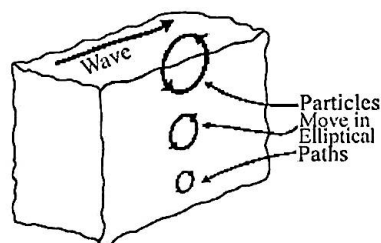
Fig. 2.10 Rayleigh wave propagation.

2.7 Waves on a Seismogram

The devises that used to record earthquake activity are called seismographs. Fig. 2.11 shows a typical seismogram recording taken from a seismograph during an earthquake event.
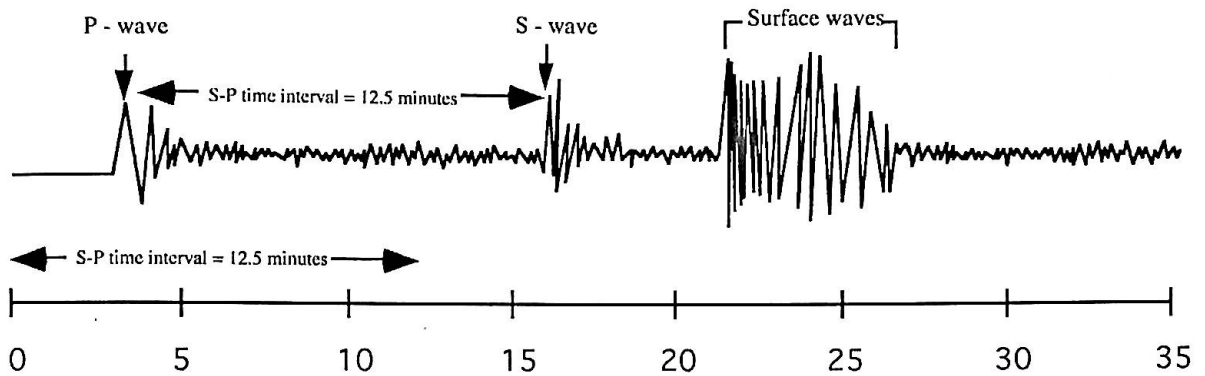
Fig. 2.11 A Typical seismogram during an earthquake event.

The first peak on a seismograph always corresponds to the P wave or primary body wave. It is a fast traveling compressional wave that can move through any type of matter (solid, liquid, or gas). The second major peak is the S wave or secondary body wave. The S wave always moves slower than the P wave, and can only move through solid matter. The high amplitude waves that follow behind the S wave are the Love and Rayleigh surface waves. These are seismic waves that only travel along the surface of the earth, and are responsible for the major ground shaking during an earthquake.

To determine the approximate distance from an earthquake epicenter to a seismograph, seismologists first measure from a seismogram the amount of time that has elapsed between the arrival of the P wave and the arrival of the S wave (called the SP time interval). The closer a seismograph is to the epicenter, the shorter this time interval because the faster P wave has had less change to move away from the slower S wave. Fig. 2.11 also illustrates how an SP time interval is measured from a seismogram using a time scale bar.

2.8 Earth's Structure by Seismological Research

Seismology is the study of earthquakes and earth, using seismic waves. There are mainly two sides or visions of seismological research. On one side, the seismic phenomenon study is targeted at understanding the mechanisms which directly oversee the earthquakes generation, and the following impact on man and the anthropic environment at the mitigating purpose. On the other side, focusing of the research is also connected to the comprehension of the large-scale, deep, structure and dynamics of the earth on apparently more fundamental issues. These two above aspects of seismological research are however intertwined. Significant advances in one of the two fields are not possible without advances in the other as well (INGV, 2009).

Information about the earthquake source may be derived, from recordings of earthquake-generated waves, including its magnitude, location, occurrence time, depth, and movement on the fault and its orientation. Seismic waves which are coming from the distant earthquakes are called teleseismic waves that provide information about the entire earth structure. A controlled source generated seismic waves which are used to image the earth's crustal structure. These images reveal the depth and area of basins fault networks, and the physical properties of rocks. Seismic imaging techniques have analogs in medical science. Therefore, wave transmitted directly through the earth produce a "catscan"-type image, while waves (reflected) back to the surface from layer boundaries or faults produce a "sonogram" type image. (USGS, 2009).

Traveltime observations and variations in amplitude, frequency, and waveform are combined to produce a model of the geologic structure. Also, surface wave dispersion analysis is used to determine the crustal structure of the earth.

A typical approximate layer from crust to core is shown in Fig. 2.12.

Layers from Crust to Core

Layer	Depth	Temperature
Rocky Crust	0 km	0°C
Upper Mantle	40	870°C
Mantle	150	
	400	Mohorovicic Discontinuity
	650	
Inner Mantle Semi-rigid		
	2,700	
	2,890	3700°C
		Gutenberg Discontinuit
Molten Outer Core Iron-Nickel		
	5,150	4300°C
Inner Core Iron-Nickel	6,378	7200°C

(Lithosphere: Rocky Crust and Upper Mantle)
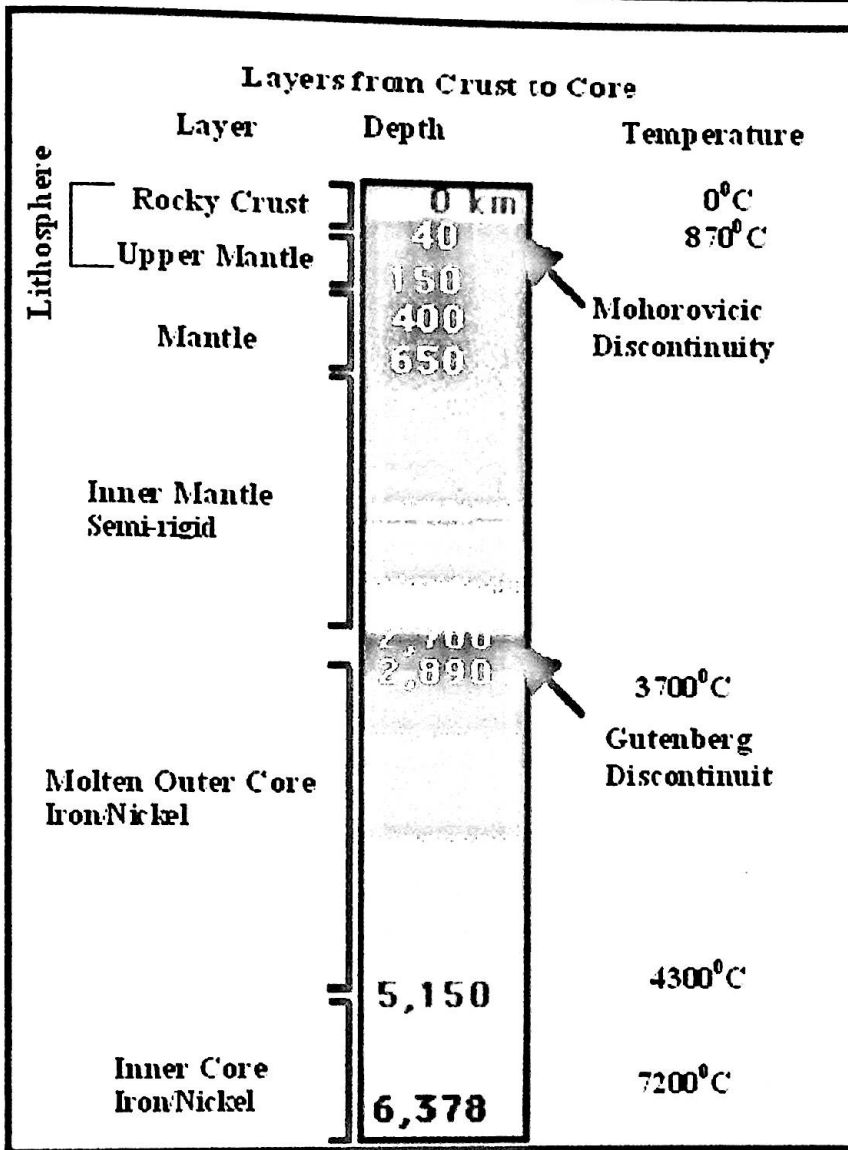
Fig. 2.12 Different Layers of the Earth.

Surface and crust

The earth's surface is composed mostly of water, basalt and granite. Oceans cover about 70% of earth's surface. These oceans are up to 3.7 km deep. The earth's thin, rocky crust is composed of silicon, aluminum, calcium, sodium and potassium.

The crust is divided as continental and oceanic crust. The crust is thinner under the oceans approximately from 6 to11 km thick. Continental crust is about 25 to 90 km thick. The lithosphere is defined as the crust and the upper mantle, a rigid layer about

100 to 200 km thick. The Mohorovicic discontinuity is the separation between the crust and the upper mantle. It can also be said the separation of lithosphere and aesthenosphere (Fig. 2.13).
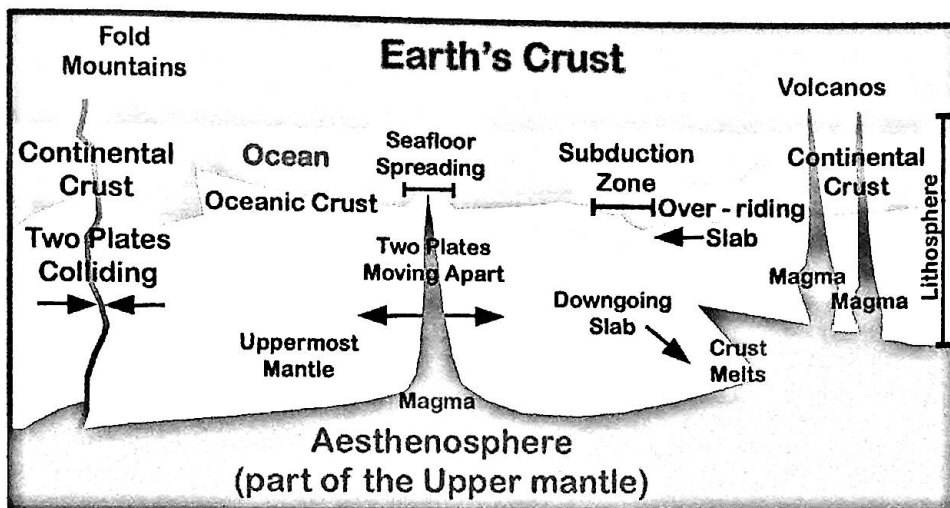
Fig. 2.13 Internal Structure of the Earth's Crust.

Mantle

Under the crust is the rocky mantle, which is composed of silicon, oxygen, magnesium, iron, aluminum, and calcium. The upper mantle is rigid and is part of the lithosphere. The lower mantle flows slowly, at a rate of a few centimeters per year. The asthenosphere is a part of the upper mantle that exhibits plastic properties. It is located below the lithosphere between about 100 and 250 kilometers deep. Convection (heat) currents carry heat from the hot inner mantle to the cooler outer mantle. The mantle is about 2,750 km thick. The mantle gets warmer with depth; the top of the mantle is about 870° C; towards the bottom of the mantle, the temperature is about 2,200-3,700° C. The mantle contains most of the mass of the earth. The Gutenberg discontinuity separates the outer core and the mantle.

Core

The earth has an iron-nickel core that is about 3380 km in radius. The inner core may have a temperature of about 7,200°C, which is hotter than the surface of the Sun. The

inner core has a radius of about 1,228 km is solid. The outer core is in a liquid state and is about 2,260 km thick (Bullen, 1963; Shearer, 1999 and Khan, 2010).

Most of the philosophy and logical approaches made to understand the structure of the earth is revealed from the seismological research or from seismic evidences. Because of power, seismology is the core branch to geosciences for further development. This research is also intended to study the crust of the earth making analyses and models from seismic evidences

Chapter 3
Earthquake Data

3.1 Introduction

International cooperation fully maintains seismology. Large sets of compatible high quality data only the accumulation in standardized formats from many stations and networks around the globe and over long periods of time will yield sufficiently reliable long term results in event localization, seismicity rate and hazard assessment, investigations into the structure and rheology of the Earth's interior and other priority tasks in seismological research and applications.

Only parameter readings taken from seismograms were exchanged with other stations and regularly transferred to national or international data centers for further processing due to almost a century. Because of the uniqueness of traditional paper seismograms and lacking opportunities for producing high quality copies at low cost, original analog waveform data, cumbersome to handle and prone to damage or even loss, were rarely exchanged. Willmore (1979) extensively described the procedure for carefully processing, handling, annotating and storing such records in the 1979 edition of the Manual of Seismological Observatory Practice. Also the traditional way of reporting parameter readings from seismograms to international data centers such as the U.S. Geological Survey, National Earthquake Information Center (NEIC), the International Seismological Centre (ISC) or the European Mediterranean Seismological Centre (EMSC) are outlined in the old Manual (Willmore, 1979). On the other hand, respective working groups on parameter formats of the International Association of Seismology and Physics of the Earth's Interior (IASPEI) and of its regional European Seismological Commission (ESC) have meanwhile debated for many years how to make these formats more homogeneous, consistent and flexible so as to better accommodate also other seismologically relevant parameter information.

Any data report must follow a format known to the recipient in order to be successfully parsed. Some of the goals for any format are: (i) concise avoiding unnecessary expense in transmission and storage, (ii) complete providing all of the information required to use the data, iii) transparent easily read by a person, perhaps without documentation and (iv) simple straightforward to write and parse with computer programs. For reporting parameter data, traditional formats sacrificed simplicity, transparency and even sometimes completeness in favor of the other goals. Modern formats more often sacrifice conciseness in favor of transparency and simplicity with the falling cost of data storage and exchange.

In addition, modern formats are usually extensible and include "metadata" which are information about the data, such as how and by whom the data were prepared. So it is an extensible format data which includes some way for new types of data to be introduced without either collection all the new information into unformatted comment strings or making messages with the new data types unreadable by old parsers. The Telegraphic Format (TF), as documented in the Manual of Seismic Observatory Practice (Willmore, 1979), is an extreme example of a traditional format for reporting and exchanging parameter data. The format was intended for use in an era when many stations were isolated and could report little more than their own phase readings, so event parameters such as hypocenter and magnitude were relegated to a secondary role. The TF incorporated further restrictions due to the special limitations of telex messages, such as no lowercase letters and sometimes no control over line breaks. A seismic network with modern, calibrated instruments can provide far more information than telegraphic format allows, while low cost email has eliminated the restrictions and high costs of telex messages. Consequently, since at least 1990 most seismic parameter data have been stored and exchanged in modern formats that are more complete, simpler and usually more transparent than the Telegraphic Format. Until recently, however, there was no generally accepted standard modern format. A major step forward in this direction was made by the Group of Scientific Experts (GSE) organized by the United Nations Conference on Disarmament. It developed GSE/IMS formats (described in later section) for exchanging parametric seismological data in tests of monitoring the Comprehensive Nuclear Test Ban Treaty (CTBT) which became popular also with other user groups.

Seismological research, however, has a broader scope than the International Monitoring System (IMS) for the CTBT. Therefore, a new IASPEI Seismic Format (ISF), compatible with the IMS format but with essential extensions, has been developed and adopted by the Commission on Seismological Observation and Interpretation of the International Association of Seismology and Physics of the Earth's Interior at its meeting in Hanoi, August 2001. It is the conclusion of a 16-year process seeking consensus on a new format and fully exploits the much greater flexibility and potential of email and Internet information exchange as compared to the older telegraphic reports.

Digital waveform data, however, are nowadays by far the largest volume of seismic data stored and exchanged world wide. The number of formats in existence and their complexity far exceeds the variability for parameter data. With the wide availability of continuous digital waveform data and unique communication technologies for world-wide transfer of such complete original data, their reliable exchange and archival has gained tremendous importance.

3.2 Seismic Data Type

There are three basic types of earthquake seismic data (IRIS, 2011) as:

Event data

Historical data

Seismogram data

3.2.1 Event data

When an earthquake is occurred and recorded the event at any seismograph, this event is compiled by seismologist. Earthquake event information is stored in the catalog that is maintained by many national and international agencies. Catalog of earthquake events contain earthquake records. Each record represents one event and contains the spatial location (hypocenter), event time and event magnitude. The data of the catalogs are complied by the seismological observatory given under 'Data Source'. Detailed information about the source data sets can be found on the provider's website listed under 'Data Source'.

3.2.2 Historical data

Historical data are collected from the historic earthquake catalog of www.iris.edu and USGS (http://neic.usgs.gov) wave site. The IRIS and / or USGS event search tool allows one to search the historical earthquake catalog (by area, time, period, magnitude range and depth of focus of earthquake) to create map of epicenters from the search and optionally, show user defined earthquake location information. For example, 1762 Bengale-Arakan, 1885 Manikganj and 1918 Srimongal historical earthquakes are of great importance and located inside Bangladesh.

3.2.3 Seismogram data

Earthquake wave data is a time-series continuous data sets which are recorded in Seismograph. Seismograms contain wave data which are the basic information about earthquakes, chemical and nuclear explosions, mining-induced earthquakes, rock bursts and other events generating seismic waves. Seismograms reflect the combined influence of the seismic source, the propagation path, the frequency response of the recording instrument and the ambient noise at the recording site. Accordingly, the knowledge of seismicity, Earth's structure, and the various types of seismic sources is mainly the result of analysis and interpretation of seismograms.

Seismic Waves on a Seismogram

When it is shown a seismogram, there will be wiggly lines all across it. These are all the seismic waves that the seismograph has recorded. Most of these waves were so small that nobody felt them. These tiny microseisms can be caused by heavy traffic near the seismograph, waves hitting a beach, the wind, and any number of other ordinary things that cause some shaking of the seismograph.

The P wave will be the first wiggle that is bigger than the rest of the little ones (the microseisms). Because P waves are the fastest seismic waves, they will usually be the first ones that recorded at seismograph. The next set of seismic waves on seismogram will be the S waves. These are usually bigger than the P waves (Fig. 3.1).
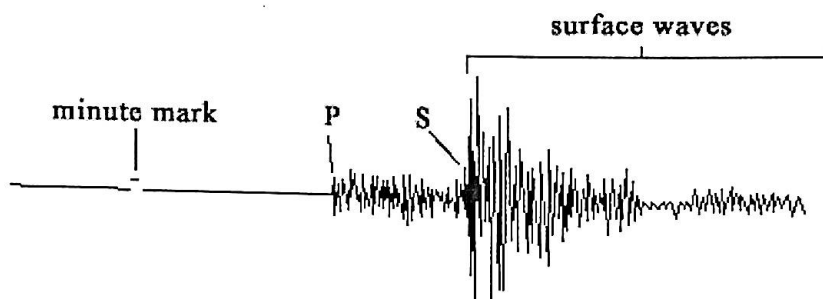
Fig. 3.1 A Typical Seismogram.

If there aren't any S waves marked on the seismogram, it probably means the earthquake happened on the other side of the planet. S waves can't travel through the liquid layers of the earth so these waves never made it to the seismograph.

The surface waves e.g. Love and Rayleigh waves are the other, often larger, waves marked on the seismogram. They have a lower frequency, which means that waves are more spread out. Surface waves travel a little slower than S waves, which, in turn, are slower than P waves, so they tend to arrive at the seismograph just after the S waves. For shallow earthquakes the surface waves may be the largest waves recorded by the seismograph. Often they are the only waves recorded a long distance from medium-sized earthquakes.

It has been used the vertical (Up-Down) component to measure the Rayleigh wave dispersion since there can be no interference between the Love and Rayleigh waves on the vertical. Therefore, on records of shallow seismic events, surface-wave amplitudes dominate over body-wave amplitudes (Fig. 3.2)

3.3 Formats of Seismological Earthquake Data

It has seen that the scientists are using seismological data, however, the formats of the data are not seemed to be unique. This is sometimes difficult for some researcher to work with different group or different region data. Conversion from one format to another is becoming very common.
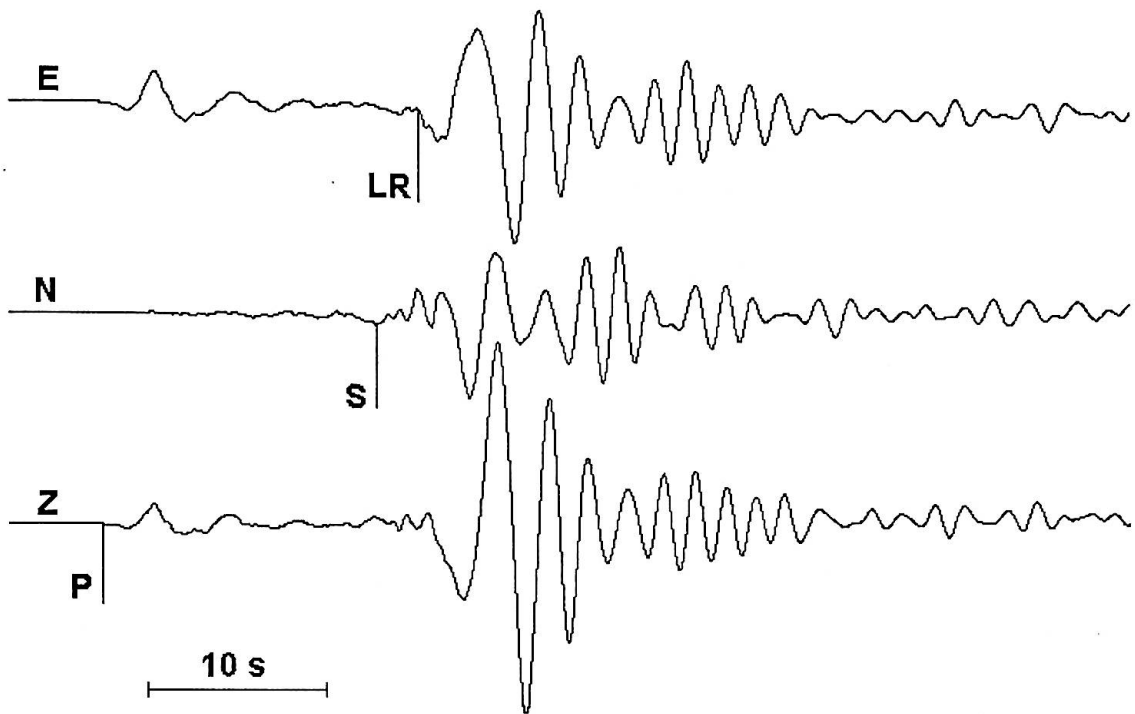
Fig. 3.2 Three-component BB-velocity record at station MOX of a mine collapse in Germany; (13 March 1989; Ml = 5.5) at a distance of 112 km and with a back azimuth of 273°. Note the Rayleigh surface-wave arrival LR with subsequent normal dispersion (after Peter, et al., 2009).

3.3.1 Parameter formats

All earthquake parameters like hypocenters, magnitudes, phase arrivals etc. are dealt parameter formats. There were no real standards, except the Telegraphic Format (TF) used for many years to report phase arrival data to international agencies (Willmore, 1979). The format is not used for processing. There have been attempts to modernize TF for many years through the IASPEI Commission on Seismological Observation and Interpretation and as already mentioned; the IASPEI Seismic Format (ISF) was approved as a standard in 2001. In practice, many different formats are used and the most dominant ones have come from popular processing systems.

HYPO71

HYPO71 (Lee and Lahr, 1972) is the very popular location program which has been most widely used for many years for local earthquakes. Only a few important parameters are available in this format which was limited to work

It is rather limited since only P or S phase names can be used and the S phase is referenced to the same hour-minute as the P phase; also, the format cannot be used with teleseismic data. However, it is probably one of the most popular formats ever for local earthquakes. The HYPO71 program has seen many modifications and the format exists in many forms with small changes.

HYPOINVERSE

For the popularity of HYPO71, several other popular location programs followed like Hypoinverse (Klein, 1978) and Hypoellipse (Lahr, 1989). The Hypoinverse input format just contains year, month, day, hour, min in the header and only one phase is given per line.

Nordic format

Nordic format was one of the first attempts to create a more complete for data exchange and processing in the 1980's. The format later became the standard format used in the SEISAN data base and processing system and is now widely used. The format tried to address some of the shortcomings in HYPO71 format by being able to store nearly all parameters used, having space for extensions and useful for both input and output.

The GSE/IMS formats

The Group of Scientific Experts (GSE) of the Conference on Disarmament in Geneva was originally developed the GSE format (versions GSE1.0 and GSE2.0) which was used for the global technical test GSETT-3 organized by the GSE. With the establishment of the International Monitoring System (IMS) for the Comprehensive Nuclear Test Ban Treaty (CTBT) monitoring a significantly revised version of this format, termed GSE 2.1, was renamed to IMS1.0. Many institutions around the globe have been widely used this format by particularly in AutoDRM data exchanges (Kradolfer, 1996) and for data transmission to international data centers, however less as a processing format than HYPO71 or the Nordic format. IMS1.0 is similar in structure to the Nordic format but more complete in some respects and lacking features in other. A major difference is that the line length can be more than 80 characters long, which is not the case for any of the previously described formats.

After SEISAN, IMS1.0 is the first major format for which completeness or readability has been recognized as a more important design goal than conciseness.

The official custodian of the IMS format is the Comprehensive Nuclear-Test-Ban Treaty Organization (CTBTO). As of December 2002, 166 States signed the CTBT and are participating in the development of the IMS system (Medalia, 2008). The IMS1.0 data format description can be obtained through National Data Centers (NDC) for CTBT which have been established in many countries on all continents.

The IASPEI Seismic Format (ISF)

The IASPEI Seismic Format (ISF) has been used for comprehensive seismological data exchange. ISF conforms to the IMS1.0 standard but has essential extensions for reporting additional types of data. This allows the contributor to include complementary data considered to be important for seismological research and applications by the IASPEI Commission on Seismological Observation and Interpretation.

This format is not as simple as some alternatives but it was reached by including many optional items. Despite this, the completeness, transparency, extensibility and metadata of ISF are expected to make it very widely used. Wide use of ISF will bring back the advantages of a generally accepted standard so that it becomes easier to exchange data, re-use data collected for past projects, and employ programs developed elsewhere.

3.3.2 Digital waveform data

Many different formats for digital data are used today in seismology; such as ESSTF, PDR-2, BDSN, GDSN, SEISAN, SAC, AH, BDSN, SEED, GSE, CSS, SUDS, etc. Some well known Digital Waveform Data formats are described below:

SAC

A Seismic Analysis Code (SAC) data file contains a single data component recorded at a single seismic station which is a general-purpose interactive program designed for the study of time sequential signals. Seismologists use this format in the research work as analysis tools. Each data file also contains a header record that describes the

contents of that file. Certain header entries must be present (e.g., the number of data points, the file type, etc.). Others are always present for certain file types (e.g., sampling interval, start time, etc. for evenly spaced time series). Other header variables are simply informational and are not used directly by the program. Although the SAC analysis software only runs on Unix platforms and the general format is binary, there is also an ASCII version that can be used on any platform.

SEED

The Standard for the Exchange of Earthquake Data (SEED) format was developed within the Federation of Digital Seismographic Networks (FDSN). The U.S. Geological Survey's National Earthquake Information Center (NEIC) and Albuquerque Seismic Laboratory (ASL) were designed the first set-up, primarily for the exchange of unprocessed waveform data. FDSN was adopted SEED in 1987 as its standard. IRIS has also adopted SEED, and uses it as the principal format for its datasets. SEED uses four types of control headers:

> Volume identifier headers
>
> Abbreviation dictionary headers
>
> Station headers
>
> Time-span headers

Each header can use several blockettes - individual portions of information that are header specific - that conform to the organization rules of their volume type. Some blockettes vary in length and can be longer than the logical record length. Data fields in control headers are formatted in ASCII, but data fields in data records are primarily formatted in binary. The full description can be found in the SEED reference Manual (SEED). It is worth pointing out that formats designed to handle the requirements of international data exchange are seldom suited to the needs of individual researchers. Thus, the wide availability of software tools to convert between SEED and a full suite of Class 2 formats is crucial for its success. A number of the present generation data acquisition systems (e.g., Quanterra, Nanometrics) produce data in SEED volumes only (miniSEED), without any of the associated control header information. Software packages have been developed to produce full SEED volumes from miniSEED

volumes (e.g., SeedStuff). At the ODC, a package has recently been developed and will be distributed as a general tool.

SUDS

The Seismic Unified Data System (SUDS) format was launched to be a more well thought out format useful for both recording and analysis and independent of any particular equipment manufacturer. The format has seen widespread use, but has lost some momentum, partly because it is not made platform-independent.

SeisGram ASCII and binary

Time series are contained in sequential, formatted ASCII files or sequential binary files. The SeisGram software (Lee, 1994) also reads fixed-record-length files using the BDSN Direct Access format. The following header informations is included in both the ASCII and the binary data files:

File type, Data format, Network, Station and instrument identifier, Type of recording, Date, Event number, Orientation of the Y component, Time unit per sample, Sample rate, Amplitude units, Amplitude units per digital count, Start time, Number of samples, Comment on event and data, Time series processing history. The ASCII files should be opened with "sequential access, formatted" format options. All header entries except start time are written with a single value on each line. The binary files are designed for compactness and fast access. Binary files should be opened with "sequential access, binary" format options. SeisGram's Direct Access data files are designed to store large sets of binary, direct access data from the BDSN (the network, not the format). The data in the file is identical to the data stream from the telemetry system, except for the addition of an eight-record header to identify uniquely the recording source, start time, and format. The Direct Access files should be opened with the "direct access, binary" format options.

3.3.3 Data archival

The storage of complete information on station, channel(s) and the structure of the data which is required Data Archival. Most existing formats are designed to provide part of the information. Presently most archival formats in use to include information on station and channel, but are not always complete in the description of the data.

Several features are following in the Standard for the Exchange of Earthquake Data (SEED) format:

- Data Description Language (DDL)
- Reference to byte order;
- Response information

The Data Description Language (DDL) is defined to enable the data itself to be stored in any data format (integer, binary, compressed). The language consists of a number of keys defining, for example, the applied compression scheme, number of bytes per sample, mantissa and gain length in bits and the use of the sign convention. For getting information how to deal with the data, it is necessary to interpret the DDL. There are both advantage and disadvantage of the DDL. The advantage of the DDL is that the original data structure can be maintained and is known. A disadvantage will be shown to interpret the DDL and have less performance in reading. However, the decoding information is available directly with the data and this is extremely important, since data are collected on platforms having different byte orders. In SEED the byte order of the original data is defined in the header, so the reader will be able to decide whether the data should be swapped. In most archival formats, response information can be supplied in terms of poles and zeroes. Fewer efforts are undertaken to give the FIR filter coefficients in the header, although they are accounted for in the definition of SEED and GSE2.X. A problem occurs when a description of the instrument response is given only in measured amplitude and phase data as a function of frequency, as is the case in the GSE1.0 format. Also, the GSE2.X does not specify and it is a minimum requirement. The main purpose of the response information is to correct for instrument response and thus the user will have to find the best fitting poles and zeroes to the given response. Although tools are available to calculate poles and zeroes from frequency, amplitude and phase data, results from the multiple inversion of the discrete frequency, amplitude and phase data will be different from the original data. The deployment of large mobile arrays consisting of heterogeneous instrumentation is an important research tool. Data archival of these data is important. Although there is a tendency to store the data in a common format, the responses of sensors and data acquisition systems are often poorly known. Finally, an issue in data archival is the responsibility of the data quality and the mechanism of

reporting data errors. The network/station operator is responsible for the quality of the original data. However, the data may be subjected to format conversion at a remote data center. This last stage could introduce errors and it is the originator of the data, which must be responsible for data quality and should agree on the final conversion, if such a conversion is done externally.

3.3.4 Data exchange formats

The data exchange formats are described separately when data is exchanged. Essentially, any format can be used for exchange, however, the idea of an exchange format is to make it easy to send electronically, have a minimum standard of content and be readable on all computer platforms.

There are many different techniques in use to exchange data, either between data users and data centers or between data centers. An overview of existing techniques is given Table 3.1.

Table 3.1: Different techniques for using data exchange

Exchange Type	Technique	Advantage	Disadvantage
Indirect on-line	autoDRM, NetDC	email based (no connection time)	small volume or download through ftp
Direct on-line	ftp, www, DRM (Spyder/Wilber/FARM)	direct access, enables easy data selection	slow for large data volumes
Off-line	CD-ROM (DVD)	direct access	no real-time data

Indirect on-line data exchange is arranged through (automated) Data Request Managers (DRMs) where the request mechanism is based on email traffic. There is work towards standardization on AutoDRM (Kradolfer, 1993) to prevent a situation where users will have to learn a multitude of data request mechanisms with each having its own specific request format. One step further is the implementation of a communication protocol for exchange between data centers in such a way that a user only has to send one request to a nearby data center node. His/her request is then automatically routed through the data centers that may contribute to the requested data set. Such a protocol is under development and is know as the NetDC initiative (Casey and Ahern, 1996). One basic problem in using email as the transport mechanism is the restricted data volume that can be exchanged. Also, the format

sometimes will have to be ASCII. The format issue is taken care of in the GSE format, although in the description of the AutoDRM protocol it is mentioned that also a format like SEED can be used. The only difference is that the user is requested to get the data through anonymous ftp (pull) or the data is pushed into an anonymous ftp area defined by the user. The AutoDRM system at the Orfeus Data Centre (ODC) supports the SEED format in data exchange.

Direct on-line access to data is arranged at the ODC, for example, mainly through a website (Dost, 1994). A distinction is made between near real-time data collection (Spyder) and complete data volumes (ODC-volumes, FARM). Spyder data are available within a few hours after a major event, while ODC volumes lag behind real-time. Internet speed is presently still limiting the usefulness of this direct on-line data exchange, especially since the volumes that are to be transferred may be large. One major advantage of direct on-line availability of the data is the capability to make a selection out of the vast amount of digital data. Procedures are presently under development to increase the power of these selection tools.

3.4 Format Conversions

Ideally, it should be all use the same format. Unfortunately, there are a large number of formats in use. With respect to parameter formats, one can get a long way with HYPO71, Nordic and GSE/ISF formats for which converters are available, such as in the SEISAN system. For waveform formats, the situation is much more difficult. First of all, there are many different formats and, since most are binary, there is the added complication that some will work on some computer platforms and not on others. This is a particular problem with binary files containing real numbers, e.g., the SeisGram format. Some formats have seen slight changes and exist in different versions; different formats have different contents so not all parameters can be transferred from one format to another; and conversion programs might not be fully tested for different combinations of data which are the additional problems.

It is required for many processing systems, a higher level format than the often primitive recording formats which is probably the most common reason for conversion; a similar reason is to move from one processing system to another. The

SEED format has become a success for archival and data exchange, but it is not very useful for processing purposes, and almost unreadable on PCs.

There are essentially two ways of converting. The first is to request data from a data center in a particular format or to log into a data center and use one of their conversion programs. The other more common way is to use a conversion program on the local computer. Such conversion programs are available both as free standing software and as part of processing systems. Equipment manufactures will often supply at least a program to convert recorder data to some ASCII format and often also to some more standard format as SUDS.

Conversion programs

Since conversion programs are often related to analysis programs, Table. 3.2 list some of the better-known analysis systems and the format they use directly.

Table 3.2: Examples of popular analysis programs

Program	Author(s)	Input format(s)	Output format(s)
CDLOOK	R.Sleeman	SEED	SAC, GSE
Geotool	J.Coyne	CSS, SAC, GSE	CSS, SAC, GSE
PITSA	F.Scherbaum, J.Johnson	ISAM, SEED, Pitsa binary, GSE, SUDS	ISAM, ASCII
SAC	Lawrence Livermore National Laboratory	SAC	SAC
SEISAN	J.Havskov, L. Ottemöller	SEISAN, GSE	SEISAN, GSE, SAC
SeismicHandler	K.Stammler	miniSEED, GSE, AH, ESSTF	GSE, miniSEED
SNAP	M.Baer	SED, GSE	SED, GSE
SUDS	P.Ward	SUDS	SUDS
Event	M.Musil	ESSTF, ASCII	ESSTF, ASCII
SeisBase	T.Fischer	ESSTF, Mars88, GSE	GSE

An overview of available format conversion programs can be found on the Orfeus Web pages under Orfeus Seismological Software Library. In this research PASSCAL package has been used (Orfeus, 2011 and IRIS, 2011)

PASSCAL package

The PASSCAL package made by P. Friberg, S. Hellman, and J.Webber, developed on SUN under SunOs4.1.4, compiled under Solaris 2.4 and higher and also under LINUX. It converts RefTek to SEGY and miniSEED. Program pql provides a quick

and easy way to view SEGY, SAC, miniSEED or AH seismic data. pql operates in the X11 window environment. The package is available from the PASSCAL instrument center (IRIS, 2011) at New Mexico Tech., Socorro.

This research has used the PASSCAL package to convert SEED data to convenient text data, as the present research is aimed to work with the earthquake wave data of Bangladesh recorded in SEED format.

3.5 Earthquake Wave Data of Bangladesh

Three events of the south eastern and nearby region of Bangladesh have been considered for the proposed research. The earthquake events are respectively of magnitude 5.6 occurred on 26 July 2003 at south west of Daluchari, Chittagong, Bangladesh, magnitude 5.1 occurred on 27 July 2003 at Kolabunia, Chittagong, Bangladesh and magnitude 5.6 occurred on 21 September 2003 at south of Meiktila, Myanmar nearer to the study area. Table 3.3 lists the source parameters of the selected events. The events were recorded at Dhaka University seismic station located at $23^0 44.10' N$ and $90^0 23.45' E$ and the station is equipped with a three component digital broadband sensor which can record up-down, north-south and east-west components. The recorded earthquake seismic waves are shown in Figs. 3.3-3.11.

Table 3.3: Earthquake Source parameters

Date	Origin Time	Location		Depth (Km)	Distance of epicenter	Magnitude (Mw)
		Latitude / Longitude	Region			
July 26 2003	23:18:17(UTC) 05:18:17(BST)	$22.892^0 N$ / $92.331^0 E$	South-West of Daluchari, Chittagong	2.6	219.02	5.6
July 27 2003	12:07:24(UTC) 18:17:26.8(BST)	$22.825^0 N$ / $92.343^0 E$	Kolabunia, Chittagong	10.0	224.22	5.1
September 21 2003	18:16:13(UTC) 00:16:13(BST)	$19.90^0 N$ / $95.73^0 E$	South of Meiktila, Myanmar	10.0	696.72	6.6
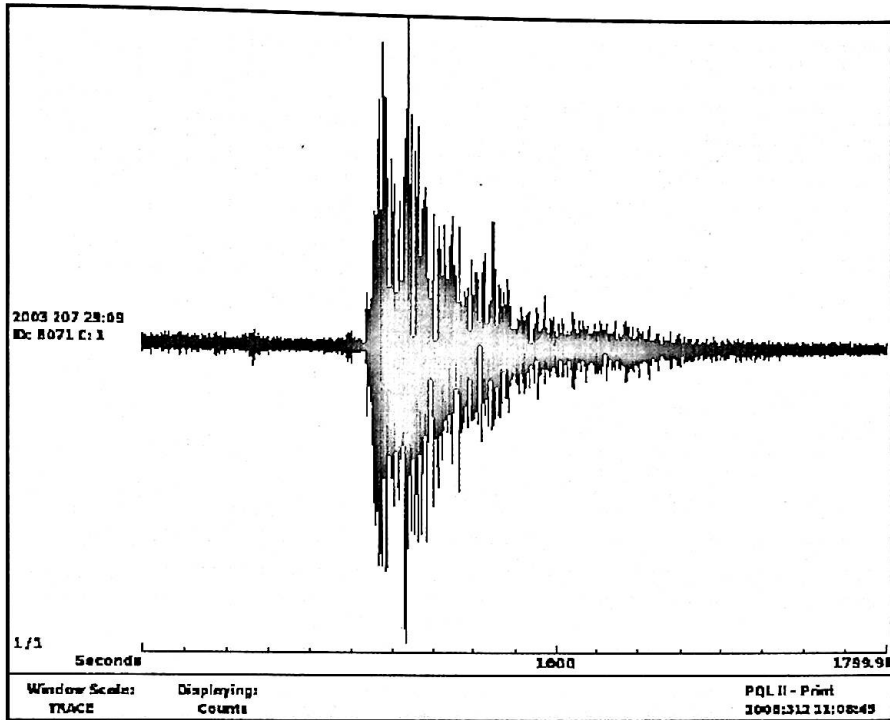
Fig. 3.3 Up-Down Ground accelerated seismic wave recorded at Dhaka University of M 5.6 earthquake on 26 July 2003 of 23:18:17 UTC time that occurred at the south-west of Daluchari, Chittagong.
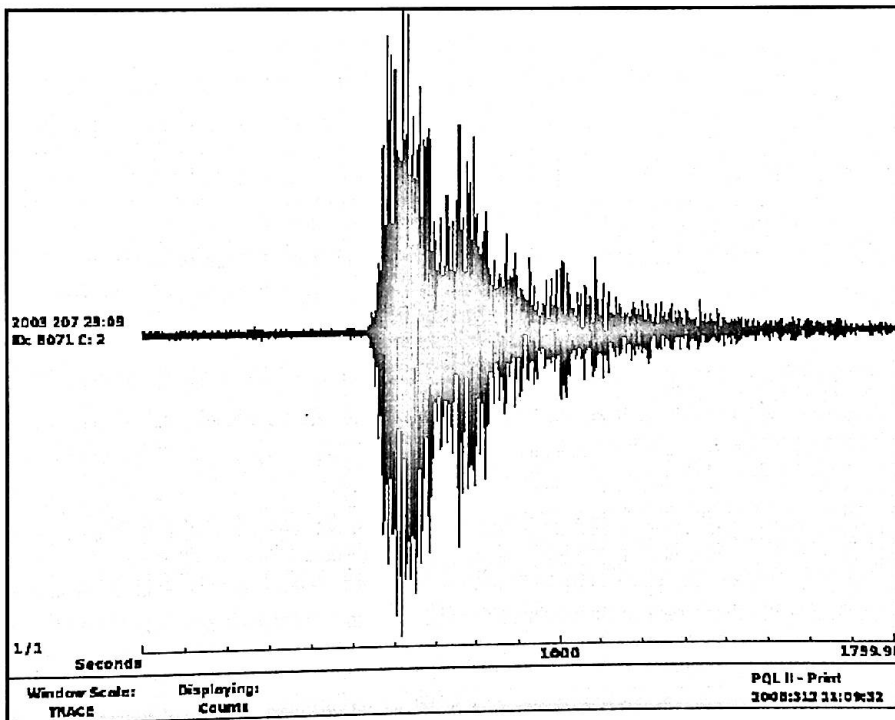
Fig. 3.4 North-South Ground accelerated seismic wave recorded at Dhaka University of M 5.6 earthquake on 26 July 2003 of 23:18:17 UTC time that occurred at the south-west of Daluchari, Chittagong.
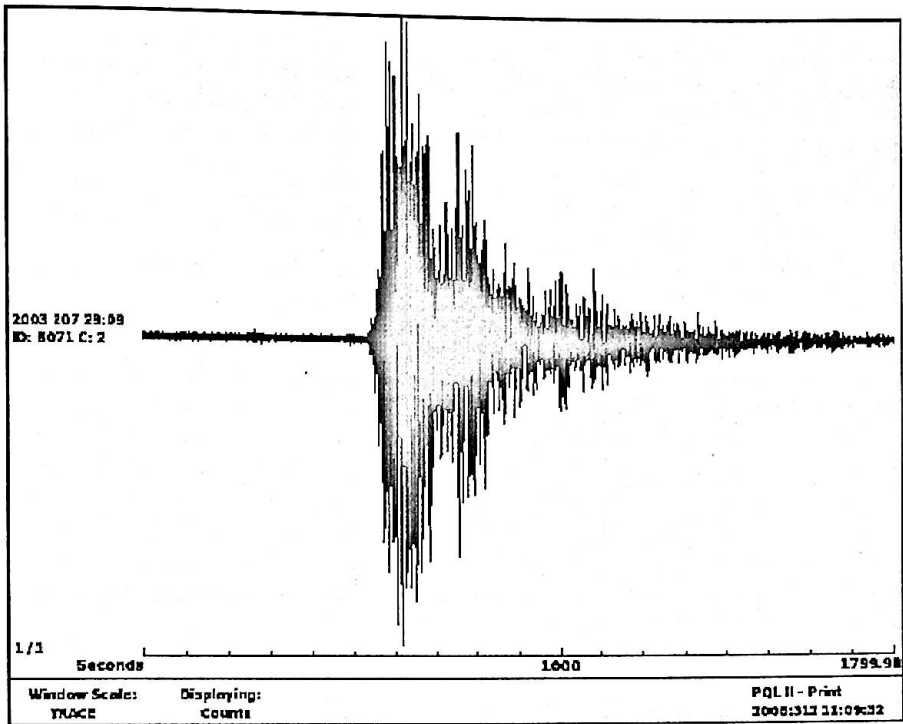
Fig. 3.5 East-West Ground accelerated seismic wave recorded at Dhaka University of M 5.6 earthquake on 26 July 2003 of 23:18:17 UTC time that occurred at the south-west of Daluchari, Chittagong
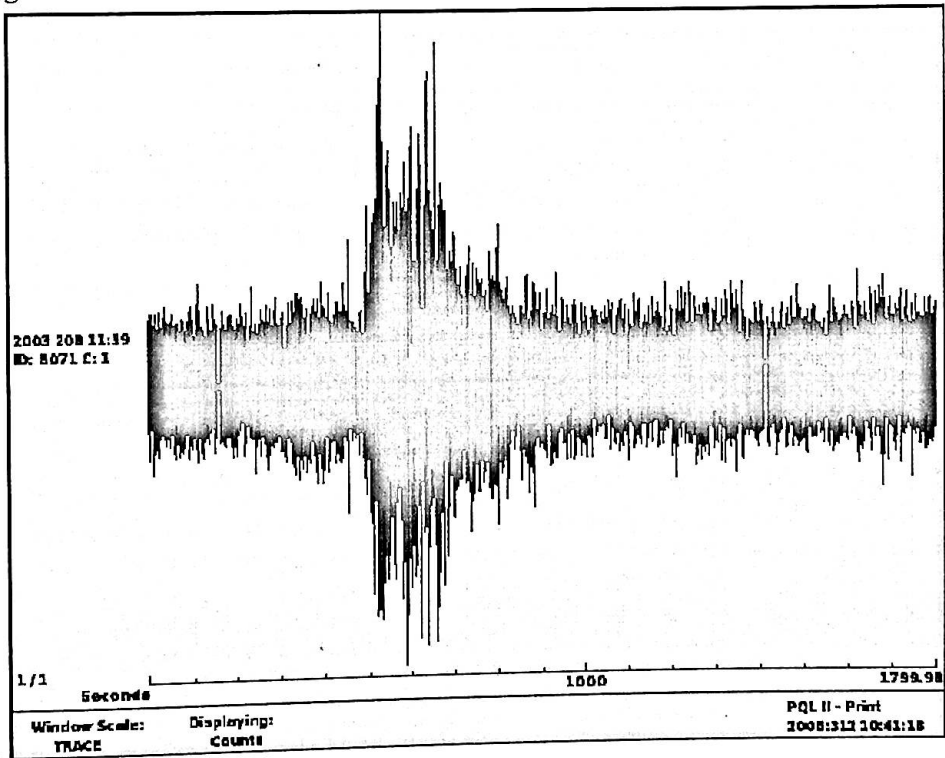
Fig. 3.6 Up-Down Ground accelerated seismic wave recorded at Dhaka University of M 5.1 earthquake on 27 July 2003 of 12:07:24 UTC time that occurred at Kolabunia, Chittagong.
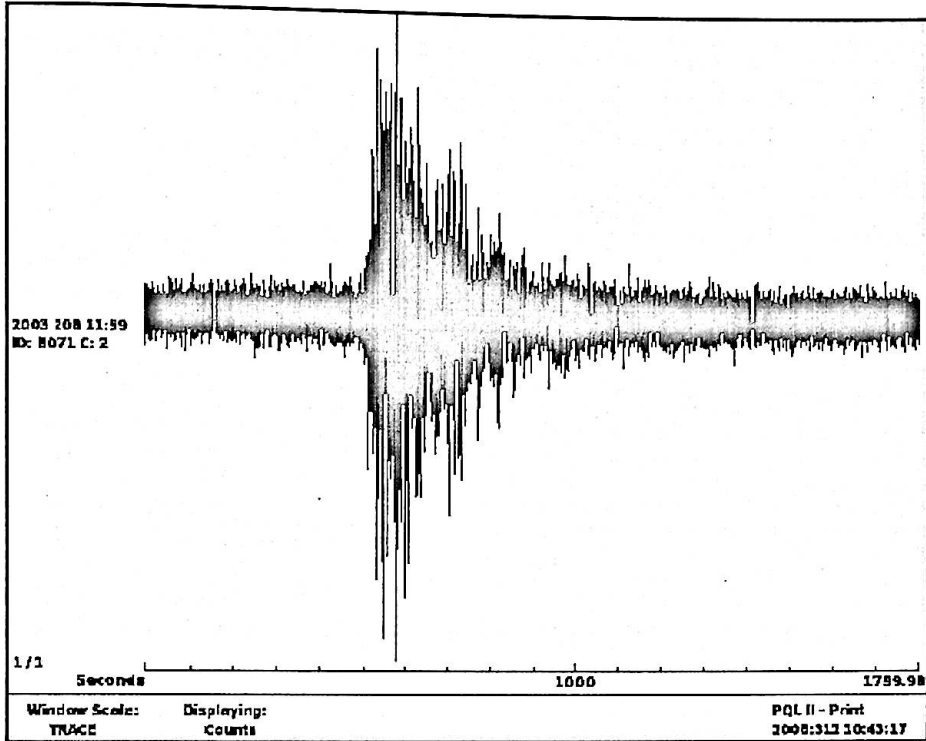
Fig. 3.7 North-South Ground accelerated seismic wave recorded at Dhaka University of M 5.1 earthquake on 27 July 2003 of 12:07:24 UTC time that occurred at Kolabunia, Chittagong.
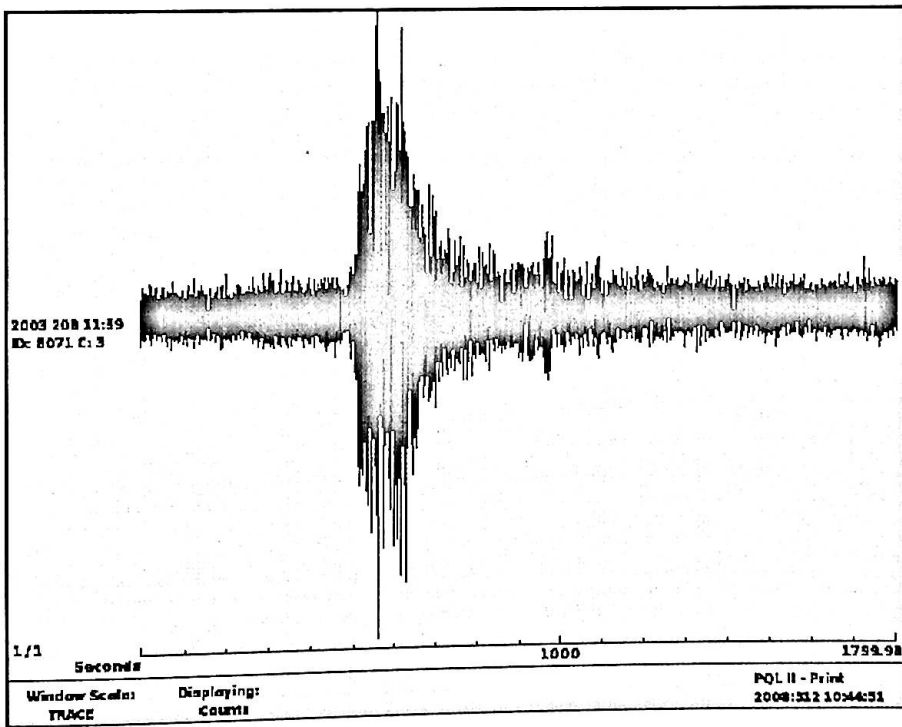
Fig. 3.8 East-West Ground accelerated seismic wave recorded at Dhaka University of M 5.1 earthquake on 27 July 2003 of 12:07:24 UTC time that occurred at Kolabunia, Chittagong.

51
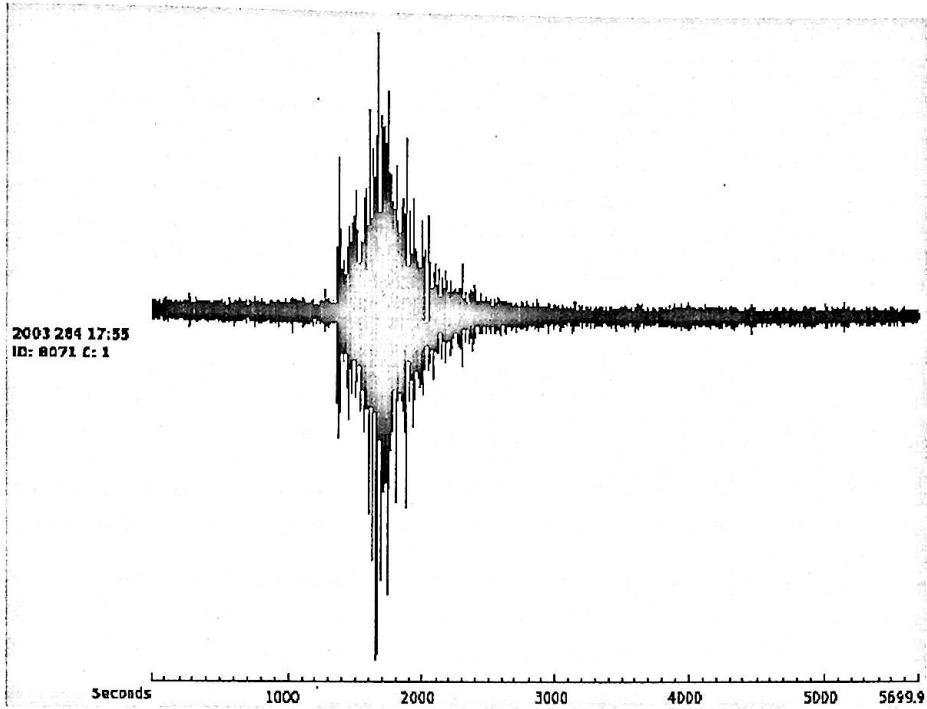
Fig. 3.9 Up-Down Ground accelerated seismic wave recorded at Dhaka University of M 6.6 earthquake on 21 September 2003 of 18:16:13 UTC time that occurred at the south of Meiktila, Myanmar.
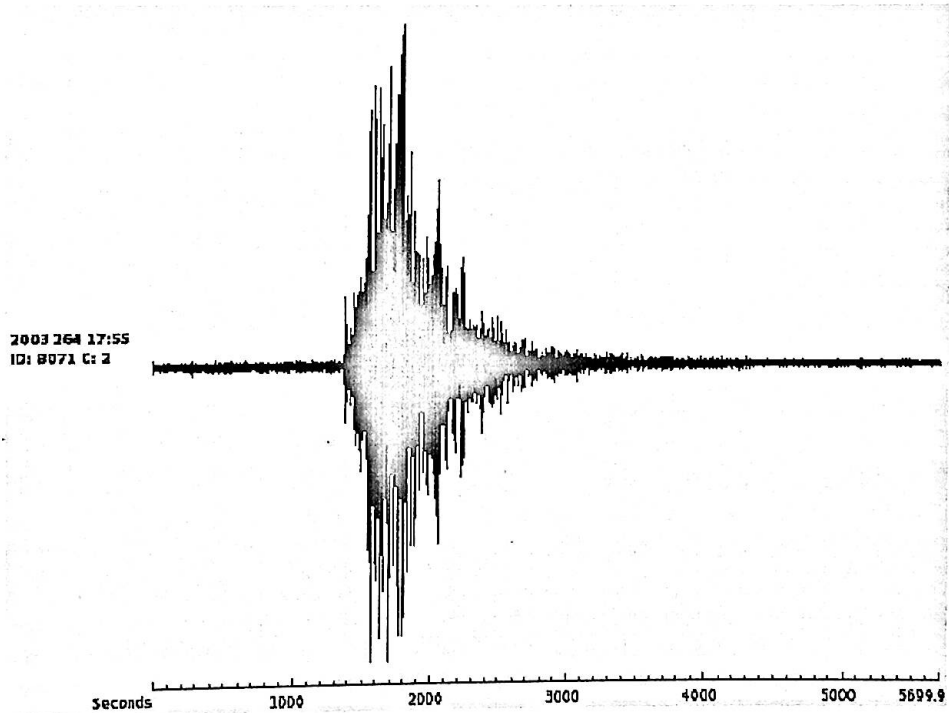
Fig. 3.10 North-South Ground accelerated seismic wave recorded at Dhaka University of M 6.6 earthquake on 21 September 2003 of 18:16:13 UTC time that occurred at the south of Meiktila, Myanmar.

2003 264 17:55
ID: B071 C: 3

Seconds   1000   2000   3000   4000   5000   5699.9
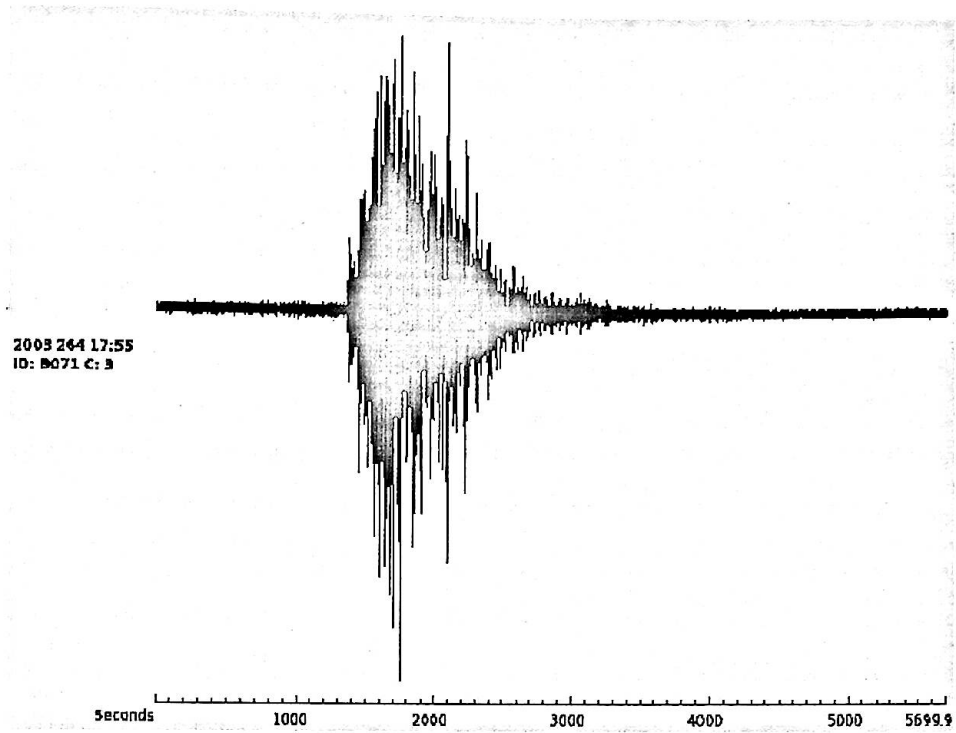
Fig. 3.11 East-West Ground accelerated seismic wave recorded at Dhaka University of M 6.6 earthquake on 21 September 2003 of 18:16:13 UTC time that occurred at the south of Meiktila, Myanmar.

Chapter 4
Analytical Techniques and Modelling for Seismological Earthquake Data

4.1 Introduction

There are different techniques which play the important role to perform the different analyses of earthquake event data. A number of researchers have been made various works to express seismicity in quantitative measures. Băth (1956), Ritsema (1954) and Amand (1956) have tried to define seismicity as the total energy release per unit area per unit of time. On the other hand, Riznichenko (1958) pointed out that integral energy values are quite attractive but their direct use for representing seismicity characteristics is irrational. Large earthquakes which generally occur in an area at great intervals of time are not only inaccessible for a study of mass phenomenon, but at the same time, they are responsible for most of the released seismic energy. As a consequence, the seismicity coefficients will change suddenly with the occurrence of each additional earthquake. More adequate in this respect is the use of quantities related to the number of earthquakes. The linear relation $Log\,N = a - bM$ has been observed to hold in any area over a wide range of magnitudes where ' a ' and ' b ' are constants and N is the cumulative number of earthquakes with magnitude M and above. The constant ' b ' hypothesis, as it may be termed, enabled Riznichenko (1958) to define the seismicity level or seismic activity of a region by a quantity equivalent to ' a '. Allen et al. (1965) have pointed out that the above method of Riznichenko (1958) has the advantage of reducing the effect of historic seismic events that may not be statistically representative, but a number of important assumptions are involved in his approach. In particular, small earthquakes are assumed to occur in association with large ones, and 'b' must be assumed to be constant throughout the region. Gubin (1964b) proposed a seismotectonic method of seismic zoning. This method is based on a combined use of qualitative and quantitative geological, geophysical, seismic and other data as against the quantitative seismic data on which is based the seismostatisticai method of Riznichenko (1959). Gubin (1966a and b) has further tried

to show the advantages of multiple-element seismic zoning maps in comparison to single-element seismic regionalization.

The Gutenberg-Richter relation and Largest-value theory has been described in this chapter for siesmicity and statistical analysis of the event data. Gutenberg-Richter formula is used to seismicity analysis in any region that describes the possibility of occurrence rate of each magnitude for larger and smaller earthquakes. The rate of larger and smaller earthquake is one of the parameters of seismicity (Aki, 1965). Gutenberg– Richter (GR) frequency–magnitude relation is very important to study the statistical properties of seismicity which states that earthquake magnitude, over a given area, follows an exponential distribution (Kanamori and Brodsky, 2004).

Statistical analysis is very important to make a successful model for sequence of large earthquake and it is performed by using Largest-value theory. The number of earthquakes in a year with mean, and the earthquake magnitude is random variables in this case. The values of the, magnitudes of the largest possible shallow earthquakes can be estimated from parameters of the magnitude-frequency relation and extreme-value statistics (Schnkova and Karnik, 1970; Schnkova and Prochazkova, 1976). Estimation of earthquake risks are made by different relations that are described by Gutenberg and Richter (1954, 1956c), Utsu, (1965) and Aki (1965). Longitude and latitude of epicenter, focal depth, origin time and magnitude are very necessary parameters for the statistical analysis.

Again, there are many analytical techniques are involved for the seismic wave data analysis. Spectral analysis and Time frequency analysis, both are made on the basis of Fourier transform (FT). Fourier transform is one of the key concepts of signal processing techniques. The Fourier transform decomposes a signal into its constituent frequency components. Looking at the Fourier spectrum it can be identified these frequencies, however, it cannot be identified their temporal localization. The goal of spectral estimation is to describe the distribution over frequency of the power contained in a signal, based on a finite set of data. Time frequency distributions map a one dimensional signal into a two-dimensional function of time and frequency, and

describe how the spectral content of the signal changes with time. From a strict mathematical point of view, it is wanted to have a joint distribution, which will be given the fraction of the total energy of the signal at time and frequency. Time frequency analysis are using as an effective tool by the observation of changes of frequency with time (Chakraborty and Okaya, 1995; Steeghs and Drijkoningen, 2001 and Rahman et al., 2007).

Wavelet analysis deals with expansion of functions in terms of a set of basis functions. It is not a new theory in the sense that many of the ideas and techniques involved in wavelets. This analysis expands functions not in terms of trigonometric polynomials but in terms of wavelets, that are generated in the form of translations and dilations of a fixed function called the mother wavelet. Special scaling properties are involved in the wavelets.

Modelling is a very effective technique for understanding and interpretation of the recorded data at any region. It is the cornerstone of seismic inversion and seismic data processing and interpretation. There are number of direct and indirect modelling techniques, which are commonly being used in determination of the earth's interior from seismic surface wave dispersion.

4.2 Event Data Analysis

When an earthquake occur, the broadband seismological stations are recorded this data and it is called the event data. Origin time, source location, magnitude, focal depth, epicentral distance is measured by the analysis of the event data. Different agencies such as IRIS, USGS are stored earthquake event data with necessary information. The most notable events are larger than a magnitude of 5.5. For this reason, the DMC routinely pre-assembles data from earthquakes that exceed magnitude 5.7 at any depth and for events down to magnitude 5.5 if the depth is greater than 100 km.

For accessing these data there are many internet tools are available. Using these tools one can obtain information about the most recent earthquakes; search historical

earthquake catalogs for earthquakes in a given region over a selected time period; and view, download or make maps of recent or historical earthquake activity of the world or of a selected region. To obtain historical earthquake data for a specific area to relate a recent event to the background seismicity; analyzing sequences of earthquake activity, performing statistical analysis of earthquakes such as the frequency of occurrence of earthquakes of various magnitudes, and obtaining earthquake data for studies of aftershock sequences or other event time series of interest (Braile, 2004).

4.2.1 Seismicity analysis

Seismicity is the study of the worldwide distribution of earthquakes over time and probability of an earthquake occurring in a specific location. It depends on the nature of the tectonic activities and fault mechanisms of that area.

The analysis of seismicity in any region is made by using Gutenberg – Richter empirical formula that describes the occurrence rate of each magnitude, larger earthquakes occur, rarely and smaller frequently. The rate of smaller and bigger earthquakes is one of the parameters of seismicity (Aki, 1965). The character of seismic activity within any region is described by frequency-magnitude relationship according to Gutenberg and Richter (1954).

$$Log\ N = a - bM \qquad\qquad 4.1$$

Where the parameter ' a ' describes the level of seismic activity and ' b ' indicates the proportion of larger to smaller earthquake which depend on the physical properties of the region and magnitude determinations. The reliable determination of the parameter ' a ' and ' b ' is of special importance during the zoning procedure. N is the number of events with a magnitude equal or larger than M .

The evaluation of parameters (a,b) in equation 4.1 and their relation to regional tectonics; the parameter ' b 'as a measure of regional seismicity has been most important for the estimation of seismic hazard. It has been extensively studied by several researchers (Bender, 1983; Lilwall and Douglas, 1984; Smith, 1986; Wang, 1988; Christova and Vanék, 1990). Kaila et al. (1974) prepared seismotectonic maps of southwest Asia, based on the ' a ' and ' b ' values for earthquakes with magnitude 6.0 and above. A similar approach has been used for the European area

(Kaila and Rao, 1975). From one region to another, ' b ' values vary. Variations in the ' b ' value may be due to the following situations:

(a) In the case of no occurrence of large events or if the rate of occurrence for small events is much higher than in the surrounding area, higher ' b ' values are observed,

(b) Lower ' b ' values are observed in the case of occurrence of large events or if the rate of occurrence of small events is much less than in the surrounding area,

(c) ' b ' value estimates depend on the magnitude interval used (Bender, 1983), e.g., large magnitude intervals result in higher ' b ' values,

(d) An increase in the number of events used in the analysis will result in more accurate ' b ' values (Bender, 1983; Lilwall and Douglas, 1984),

(e) A cut-off or threshold magnitude in the analysis will result in higher ' b ' values.

Gutenberg and Richter (1954) derived the values of ' b ' using all the earthquakes above magnitude 6 and found that, for shallow $(upto\,70\,km)$ earthquakes, $b = 0.90 \pm 0.02$, for intermediate $(70-300\,km)$ earthquakes $b = 1.2 \pm 0.2$ and for deep $(>300\,km)$ earthquakes $b = 1.2 \pm 0.2$ respectively. These values are further associated as very low b values $(0.4 - 0.6)$ are associated with old shield, low b values $(0.6 - 0.7)$ for continental rift zones, medium b values $(0.7 - 1.0)$ for Circum-Pacific and Alpine orogenic belts, and high b values $(1.0 - 1.8)$ for oceanic regions. It is clear from Equation 4.1 that the ' b ' value is directly related to the occurrence of events for a specified period of time. If the time coverage is long enough to cover all possible earthquakes that occur then the ' b ' value within each seismic source zone will reach a maximum. Equation 4.1 is not valid for all magnitudes and restricted to the range $M_{min} <= M <= M_{max}$. In general, an over estimation is expected for smaller events when all events are considered for the estimation of ' b '. This generalization cannot be made for larger earthquakes because their behavior is not simple. Therefore, the choice of the threshold magnitude and the maximum magnitude is of importance for the estimated ' b ' values in seismic hazard analysis.

4.2.2 Statistical Analysis

A sufficient amount of highly-quality data is necessary to obtain reliable results from statistical analysis. The data are taken usually from earthquake catalogs. In most statistical studies earthquakes represented mostly by longitude and latitude of epicenter, focal depth, origin time and magnitude.

Largest – value theory

Statistical models for sequences of large earthquakes are relatively easy to produce. A successful model consists of two assumptions: (a) the number of earthquakes in a year is a Poisson random variable with mean, λ; (b) M, the earthquake magnitude, is a random variable distributed with cumulative distribution function :

$$F(M) = 1 - e^{-\beta M} \quad (M \geq 0) \qquad 4.2$$

This model termed as the "Large-Earthquake Model", is especially useful when records of largest earthquakes in a region are available (Lomnitz, 1974). The values of the, magnitudes of the largest possible shallow earthquakes can be estimated from parameters of the magnitude-frequency relation and extreme-value statistics (Schnkova and Karnik, 1970; Schnkova and Prochazkova, 1976).

The central result of extreme-value theory found by Gumbel (1958) is:

$$G(y) = \exp\left(-\alpha e^{-\beta y}\right) \quad (y \geq 0) \qquad 4.3$$

There are only four major mathematically distinct distributions of y. Gumbel's result is explained by the fact that $G(y)$ depends only on the tail of the distribution of x. Let us consider the problem of predicting maximum earthquake magnitude applying the 'Large-Earthquake Model', (equation 4.2). Seismic region is defined by a main fault with its tributaries and assume a homogenous earthquake process with a cumulative magnitude distribution

$$F(x) = 1 - e^{-\beta x} \quad (x \geq 0) \qquad 4.4$$

Let α be the mean number of earthquakes per year above magnitude zero. Then y, the maximum annual earthquake magnitude will be distributed as in equation 4.3.

In order to estimate the parameters α and β one takes the largest yearly earthquake magnitudes $y_1, y_2, \ldots, y_n$ in a sample of n consecutive years. These magnitudes are

arranged in order of increasing size, so that $y_{(1)} \le y_{(2)} \le \ldots \le y_{(n)}$. Then one estimates the values of $G(y)$ by:

$$G(y_{(j)}) = \frac{j}{n+1}$$ 4.5

Finally, the values of α and β are estimated from a least-square fit to equation 4.3.

$$\ln[-\ln G(y)] = \ln \alpha - \beta y$$ 4.6

The following quantities are of frequent use in problems of earthquake risk estimation.

a) Mean magnitude of earthquakes in a region

If M_{min} is the magnitude threshold of an earthquake sample over the region, the mean magnitude is estimated by:

$$M = M_{min} + \beta^{-1}$$

b) Number of shocks above magnitude M_{min}

The yearly number of earthquakes above magnitude zero is α. Hence the expected number of shocks above magnitude M_{min} in D years is:

$$DN_y = D\alpha \exp(-\beta M_{min})$$

c) Mean return period

If N is the expected number of earthquakes per year, $T = \frac{1}{N}$ is the mean return period in years.

The mean return period for shocks exceeding magnitude y is:

$$T_y = \frac{1}{N_y} = \frac{\exp(\beta y)}{\alpha}$$

d) Estimation of Earthquake Risk

If an earthquake having mean return period of 150 years is expected as critical design earthquake, i.e., a large structure will be designed to withstand a seismic event of the save size. Thus, it may be estimated the earthquake risk for different design periods, using the 'Large-Earthquake Model'. If the structure is designed for an effective period of service of 50 years the earthquake risk is:

$R50^{'}(150)=1-\exp\left(-\dfrac{50}{150}\right)=0.28$ It means that there is a probability of 28% that the structure will be subjected to a design earthquake during its projected period of operation.

Frequency-Magnitude Relation

In general, smaller earthquakes are much more frequent than larger ones. If the magnitude M is related to energy E (erg) by the equation of Gutenberg and Richter (1956c) then,

$$\log E = 1.5M + 11.8 \qquad\qquad 4.7$$

On the other hand, the dependence of constants 'b' on 'a' of the Gutenberg-Richter's frequency-magnitude relation $\log N = a - bM$, seems to be linear (Chouhan, 1970). The general distribution of earthquakes over the observed range of magnitude for the whole world shows the frequency of shocks at any given magnitude level is roughly 8 to 10 times that about one magnitude higher. This is expressed by the Gutenberg-Richter relation (1954) as,

$$Log_{10}\, N = a - bM$$

$$\text{Or,}\ N = 10^{a}\, 10^{-bM} \qquad\qquad 4.8$$

Where N is the number of earthquakes with magnitude M or greater per unit time, and 'a' and 'b' are constants.

Under the assumption that the magnitude data are random samples from a population obeying the Gutenberg-Richter relation, the method of moments (Utsu, 1965) and the method of maximum likelihood (Aki, 1965) both yield solution

$$b = \dfrac{\log_{10} e}{\left(\bar{M} - M_z\right)} \qquad\qquad 4.9$$

Where $\bar{M}$ is the mean magnitude of earthquakes of $\bar{M} \geq M_z$ and $\log e = 0.434294$

M_z is the threshold (minimum) magnitude above which the data should be completed.

4.3 Seismic Wave Data Analysis

There are also many analytical techniques by which the seismic wave can be analyzed.

4.3.1 Spectral analysis

A signal can be decomposed into individual frequency components by using Fourier transform (FT), i.e. a set of infinite sinusoids of various period and amplitudes, which when summed back together exactly reproduce the original waveform. The goal of spectral estimation is to describe the distribution (over frequency) of the power contained in a signal, based on a finite set of data. The power spectrum of a stationary random process x_n is mathematically related to the correlation sequence by the discrete-time Fourier transform. In terms of normalized frequency, this is given by (Welch, 1967; Marple, 1987; Kay, 1988; Percival and Walden, 1993 and Hayes, 1996):

$$S_{xx}(\omega) = \sum_{m=-\infty}^{\infty} R_{xx}(m)e^{-j\omega m} \qquad 4.10$$

This can be written as a function of physical frequency f (e. g., in hertz) by using the relation $\omega = \dfrac{2\pi f}{f_s}$, where f_s is the sampling frequency. Then,

$$S_{ss}(f) = \sum_{m=-\infty}^{\infty} R_{xx}(m)e^{-\frac{2\pi j f m}{f_s}} \qquad 4.11$$

The correlation sequence can be derived from the power spectrum by use of the inverse discrete Fourier transform (Welch, 1967; Marple, 1987 and Hayes, 1996):

$$R_{xx}(m) = \int_{-\pi}^{\pi} \frac{S_{xx}(\omega)e^{j\omega m}}{2\pi} d\omega = \int_{-\frac{f_s}{2}}^{\frac{f_s}{2}} \frac{S_{xx}(f)e^{\frac{2\pi j f m}{f_s}}}{f_s} df \qquad 4.12$$

The average power of sequence x_n over the entire Nyquist interval is represented by

$$R_{xx}(0) = \int_{-\pi}^{\pi} \frac{S_{xx}(\omega)}{2\pi} d\omega = \int_{-\frac{f_s}{2}}^{\frac{f_s}{2}} \frac{S_{xx}(f)}{f_s} df \qquad 4.13$$

$$= \int_{-\pi}^{\pi} P_{xx}(\omega) d\omega = \int_{-\frac{f_s}{2}}^{\frac{f_s}{2}} P_{xx}(f) df$$

Where,

$$P_{xx}(\omega) = \frac{S_{xx}(\omega)}{2\pi} \quad and \quad P_{xx}(f) = \frac{S_{xx}(f)}{f_s} \qquad 4.14$$

from the above expression are defined as the power spectral density (PSD) of the stationary random signal x_n

The average power of a signal over a particular frequency band (ω_1, ω_2), $0 \leq \omega_1 < \omega_2 \leq \pi$, can be found by integrating the PSD over that band.

$$\bar{P}(\omega_1, \omega_2) = \int_{\omega_1}^{\omega_2} P_{xx}(\omega) d\omega + \int_{-\omega_2}^{-\omega_1} P_{xx}(\omega) d\omega \qquad 4.15$$

It can be seen from the expression that $P_{xx}(\omega)$ represents the power content of a signal in an infinitesimal frequency band, and it is called the power spectral density. The units of the PSD are power (e. g., watts) per unit of frequency. In the case of $P_{xx}(\omega)$, this is watts/radian/sample or simply watts/radian. In the case of $P_{xx}(f)$, the units are watts/hertz. Integration of the PSD with respect to frequency yields units of watts, as expected for the average power $\bar{P}(\omega_1, \omega_2)$.

4.3.2 Wavelet analysis

Wavelet analysis also called wavelet theory or just wavelets has attracted much attention recently in signal processing. It is not a new theory in the sense that many of the ideas and techniques involved in wavelets were developed independently in various signal processing applications and have been known for some time.

Like Fourier analysis, wavelet analysis deals with expansion of functions in terms of a set of basis functions. Unlike Fourier analysis, wavelet analysis expands functions not in terms of trigonometric polynomials but in terms of wavelets, which are generated in the form of translations and dilations of a fixed function called the mother wavelet. The wavelets obtained in this way have special scaling properties. They are localized in time and frequency, permitting a closer connection between the function being represented and their coefficients. Greater numerical stability in reconstruction and manipulation is ensured.

The objective of wavelet analysis is to define these powerful wavelet basis functions and find efficient methods for their computation. It can be shown that every application using the fast Fourier transform (FFT) can be formulated using wavelets to provide more localized temporal (or spatial) and frequency information. Thus, instead of a frequency spectrum, for example, one gets a wavelet spectrum. In signal processing, wavelets are very useful for processing non-stationary signals.

The Analyzing Wavelet

Consider a complex-valued function Ψ satisfying the following conditions (Mallat, 1989; Pesquet et al., 1996 and Cohen, et al., 1993):

$$\int_{-\infty}^{\infty} |\psi(t)|^2 \, dt \leq \infty \qquad \qquad 4.16$$

$$c_\psi = 2\pi \frac{|\psi(\omega)|^2}{|\omega|} \, d\omega < \infty, \qquad \qquad 4.17$$

Where ψ is the Fourier transform of ψ. The first condition implies finite energy of the function ψ, and the second condition, the admissibility condition, implies that if $\psi(\omega)$ is smooth then $\psi(0) = 0$. The function ψ is the mother wavelet.

Continuous Wavelet Transform

If ψ satisfies the conditions described above, then the wavelet transform of a real signal $s(t)$ with respect to the wavelet function $\psi(t)$ is defined as:

$$S(b,a) = \frac{1}{\sqrt{a}} \int_{-\infty}^{\infty} \psi'\left(\frac{t-b}{a}\right) s(t)\,dt \qquad\qquad 4.18$$

where ψ' denotes the complex conjugate of ψ, and this is defined on the open (b,a) half-plane $(b \in R, a > 0)$. The parameter 'b' corresponds to the time shift and the parameter 'a' corresponds to the scale of the analyzing wavelet.

If we define $\psi_{a,b}(t)$ as:

$$\psi_{a,b}(t) = a^{-\frac{1}{2}} \psi\left(\frac{t-b}{a}\right) \qquad\qquad 4.19$$

which means rescaling by 'a' and shifting by 'b', then equation 4.18 can be written as a scalar or inner product of the real signal $s(t)$ with the function $\psi_{a,b}(t)$:

$$S(b,a) = \int_{-\infty}^{\infty} \psi'_{a,b}(t) s(t)\,dt \qquad\qquad 4.20$$

When function $\psi(t)$ satisfies the admissibility condition, from equation 4.17, the original signal $s(t)$ can be obtained from the wavelet transform $S(b,a)$ by the following inverse formula:

$$s(t) = \frac{1}{c_\psi} \int_{-\infty}^{\infty} \int_{-\infty}^{\infty} S(b,a) \psi_{a,b}(t) \frac{da\,db}{a^2} \qquad\qquad 4.21$$

Discrete Wavelet Transform

In the discrete domain, the scale and shift parameters are discretized as $a = a_0^m$ and $b = nb_0$, and analyzing wavelets are also discretized as follows:

$$\psi_{m,n}(t) = a_0^{-\frac{m}{2}} \psi\left(\frac{t-nb_0}{a_0^m}\right) \qquad\qquad 4.22$$

where m and n are integer values. The discrete wavelet transform and its inverse transform are defined as follows:

$$S_{m,n} = \int_{-\infty}^{\infty} \psi'_{m,n}(t) s(t)\,dt \qquad\qquad 4.23$$

$$s(t) = k_\psi \sum_m \sum_n S_{m,n} \psi_{m,n}(t) \qquad\qquad 4.24$$

where k_ψ is a constant value for normalization.

The function $\psi_{m,n}(t)$ provides sampling points on the scale time plane; linear sampling in the time $(b-axis)$ direction but logarithmic in the scale $(a-axis)$ direction.

The most common situation is that a_0 is chosen as:

$$a_0 = 2^{\frac{1}{v}}$$
                                                                4.25

where v is an integer value, and that v pieces of $\psi_{m,n}(t)$ are processed as one group, which is called a voice. The integer v is the number of voices per octave; it defines a well-tempered scale in the sense of music. This is analogous to the use of a set of narrowband filters in conventional Fourier analysis.

Wavelet analysis is not limited to dyadic scale analysis. By using an appropriate number of voices per octave, wavelet analysis can effectively perform the $\frac{1}{3}$ octave, $\frac{1}{6}$ octave, or $\frac{1}{12}$ octave analyses that are used in acoustics.

The wavelet basis function can be implemented as a Finite Impulse Response (FIR) filter or an Infinite Impulse Response (IIR) filter depending on the particular properties needed. There are various wavelet functions such as Haar Wavelet, Meyer Wavelet, Morlet Wavelet, Daubechies Wavelet, etc.

4.3.3 Time frequency analysis

Time frequency distributions are sometimes saying the key tools for non-stationary signal analysis, synthesis, and processing. Different types of time frequency analysis have been developed. Recent time-frequency analyses are: the Short Time Fourier Transform, used to generate the spectrogram (Koeing et al, 1946; Allen and Rabiner, 1977), the Wigner-Ville distribution (Classen and Macklenbrauker, 1980) and Complex trace analysis (Taner, et al., 1979). The time-frequency distribution ideally describes how the energy is distributed, and allow to estimate the fraction of the total energy of the signal at time and frequency in Fourier based analysis. The above statement states that the energy should be positive. On other hand complex trace analysis produces instantaneous frequency. A real seismic trace, $u(t)$ can he

expressed in terms of a time-dependent amplitude $A(t)$ and a time dependent phase $\theta(t)$ as (Taner et al.,1979):

$$u(t) = A(t)\cos\theta(t) \qquad\qquad 4.26$$

The quadrature trace $u*(t)$ can be written as

$$u*(t) = A(t)\sin\theta(t) \qquad\qquad 4.27$$

and the complex trace $U(t)$ is

$$U(t) = u(t) + ju*(t)$$

$$= A(t)e^{j\theta(t)} \qquad\qquad 4.28$$

On other hand, quadrature trace $u*(t)$ can be obtained from real seismic trace $u(t)$ using Hilbert transform as:

$$u^{*}(t) = \frac{j}{\pi} \times \int \frac{s(\tau)}{t-\tau} d\tau \qquad\qquad 4.29$$

Now $u(t)$ and $u*(t)$ are known, therefore the solution for $A(t)$ and $\theta(t)$ can be given below as:

$$A(t) = \sqrt{u^2(t) + u^{*2}(t)} = |U(t)| \qquad\qquad 4.30$$

and

$$\theta(t) = \tan^{-1}\left(\frac{u^{*}(t)}{u(t)}\right) \qquad\qquad 4.31$$

$A(t)$ is called the reflection strength and $\theta(t)$ is called the instantaneous phase. The rate of change of time-dependent phase gives a time-dependent frequency

$$\frac{d\theta(t)}{dt} = \omega(t) = 2\pi f(t) \qquad\qquad 4.32$$

$$f(t) = \frac{d\theta(t)}{2\pi dt} \qquad\qquad 4.33$$

which is one of the relations of time-frequency analysis.

As amplitude is the main basis with time in earthquake ground motion seismic wave and in exponential nature, two sets of synthetic data have been implemented mainly in exponential nature with varying amplitude and frequency shown in Figs. 4.1-4.2. Fig. 4.1 shows three waves changing amplitude in an addition with exponential change with time. Fig 4.2 shows the waves abrupt changes of frequency with time.
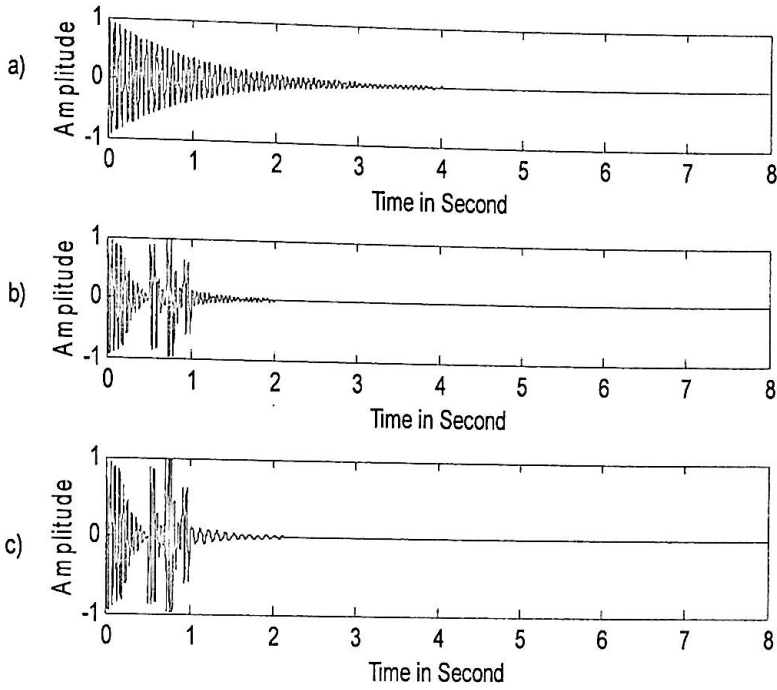
Fig. 4.1 Amplitude variation of synthetic earthquake seismic waveform at different frequencies a) 16 Hz, b) 20Hz and c) 10Hz, 20Hz, 25Hz and 30Hz.
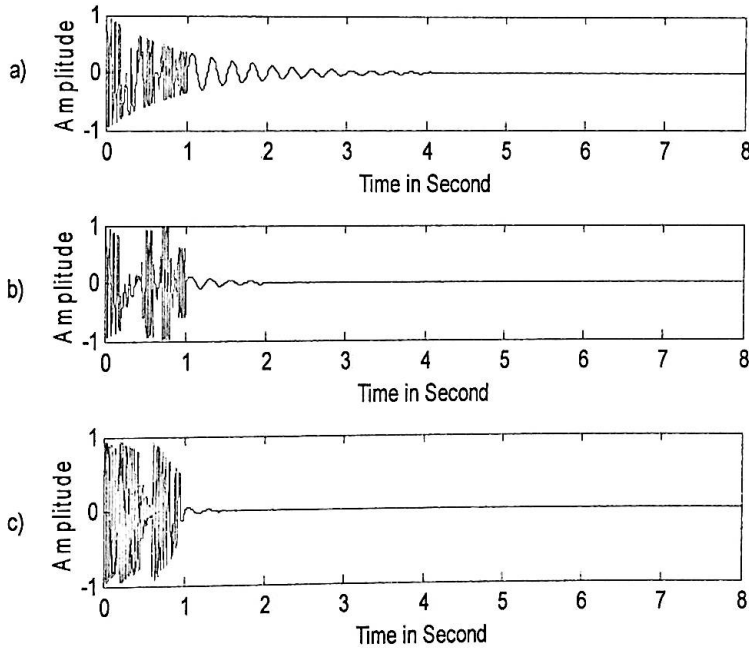
Fig. 4.2 Synthetic earthquake seismic wave, changing amplitude a) with varying frequency b) with varying both frequency and amplitude and c) with varying both frequency and amplitude in a more complicated way.

Using Equations 4.28-4.33, time frequency analyses of the synthetic earthquake

waves as shown in Figs. 4.1-4.2 are demonstrated. Figs. 4.3-4.4 respectively show the analyses.

Time frequency analyses of the recorded earthquake (Figs. 3.3-3.11) waves are also performed and shown in Figs. 4.5-4.13.
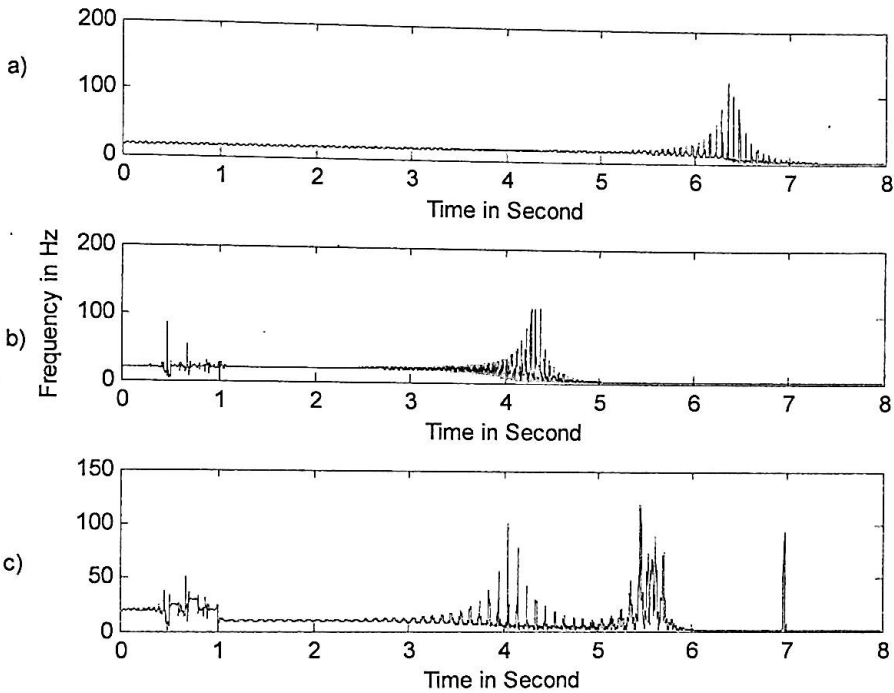
Fig. 4.3 Time frequency analysis of synthetic earthquake wave respectively of Fig. 4.1.
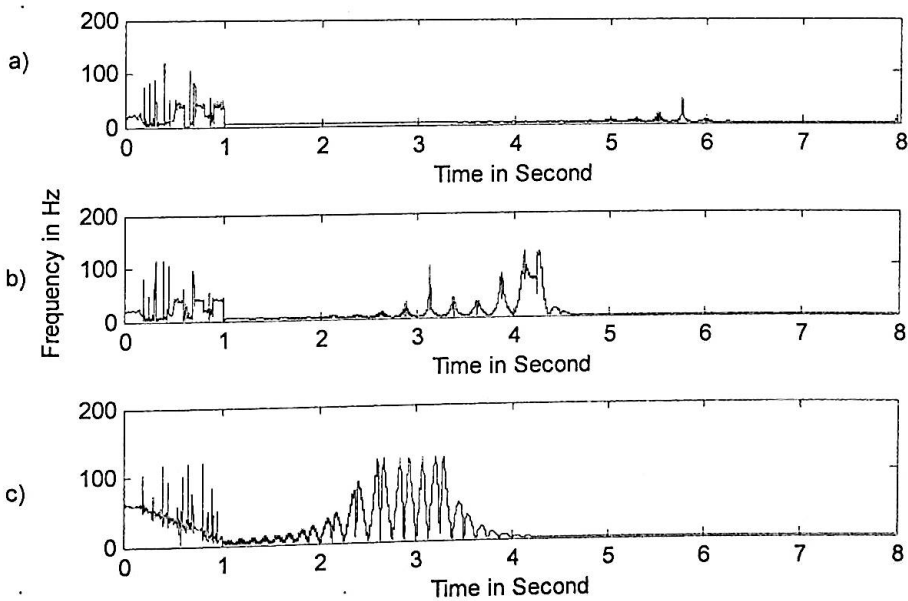
Fig. 4.4 Time frequency analysis of synthetic earthquake wave respectively of Fig. 4.2.
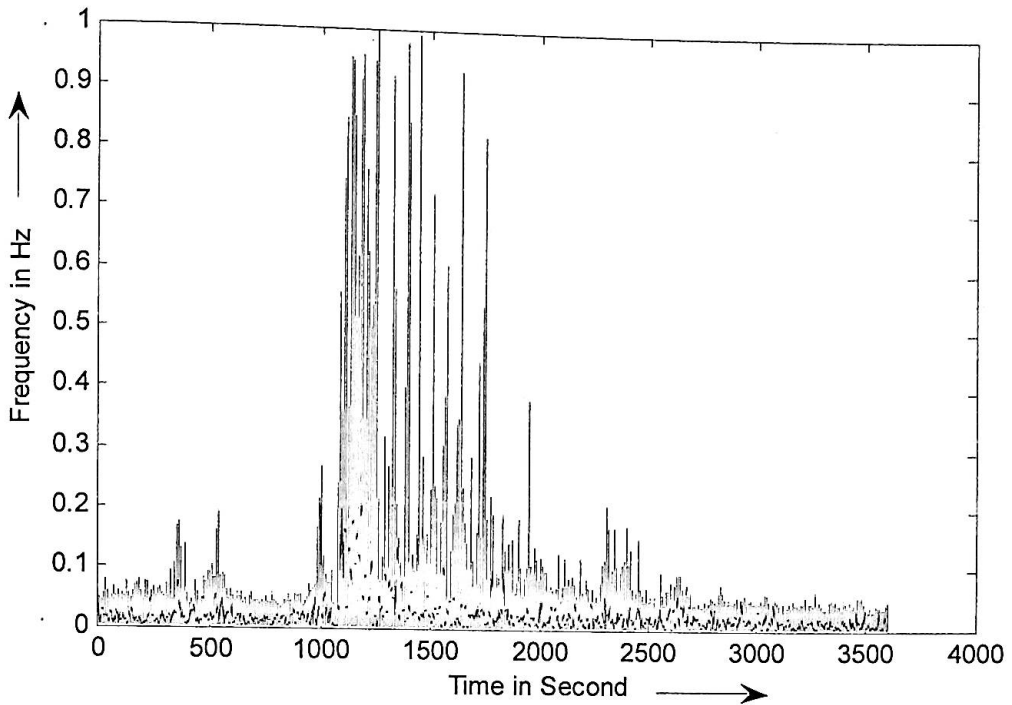
Fig. 4.5 Time frequency analysis recorded at station Dhaka University (up-down) of M 5.6 earthquake on 26 July 2003 of 23:18:17 UTC time occurred at the south-west of Daluchari, Chittagong.
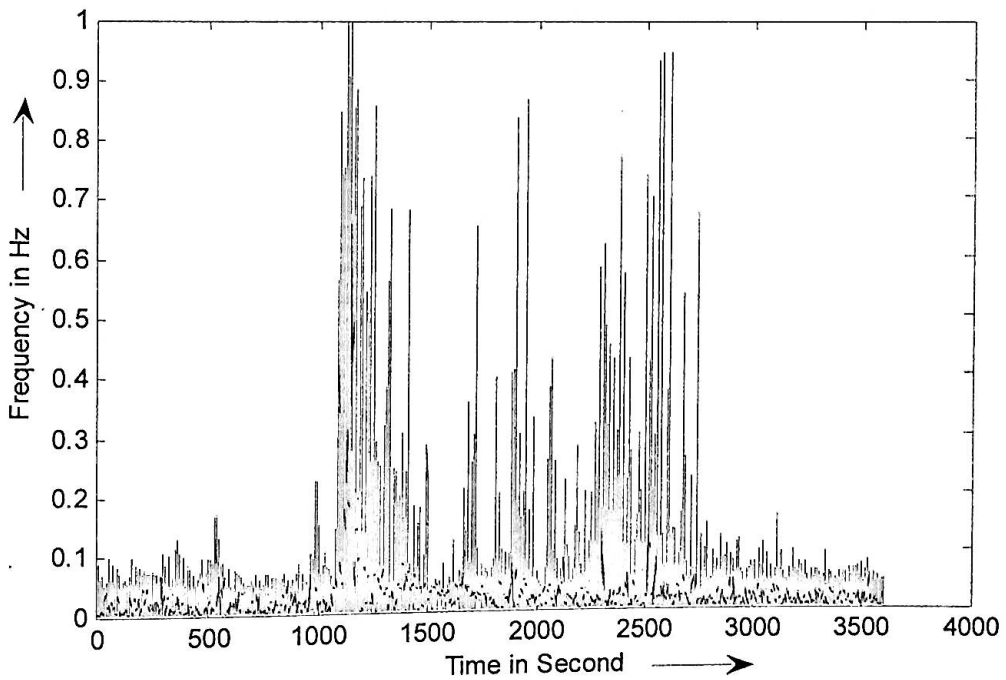
Fig. 4.6 Time frequency analysis recorded at station Dhaka University (north-south) of M 5.6 earthquake on 26 July 2003 of 23:18:17 UTC time occurred at the south-west of Daluchari, Chittagong.
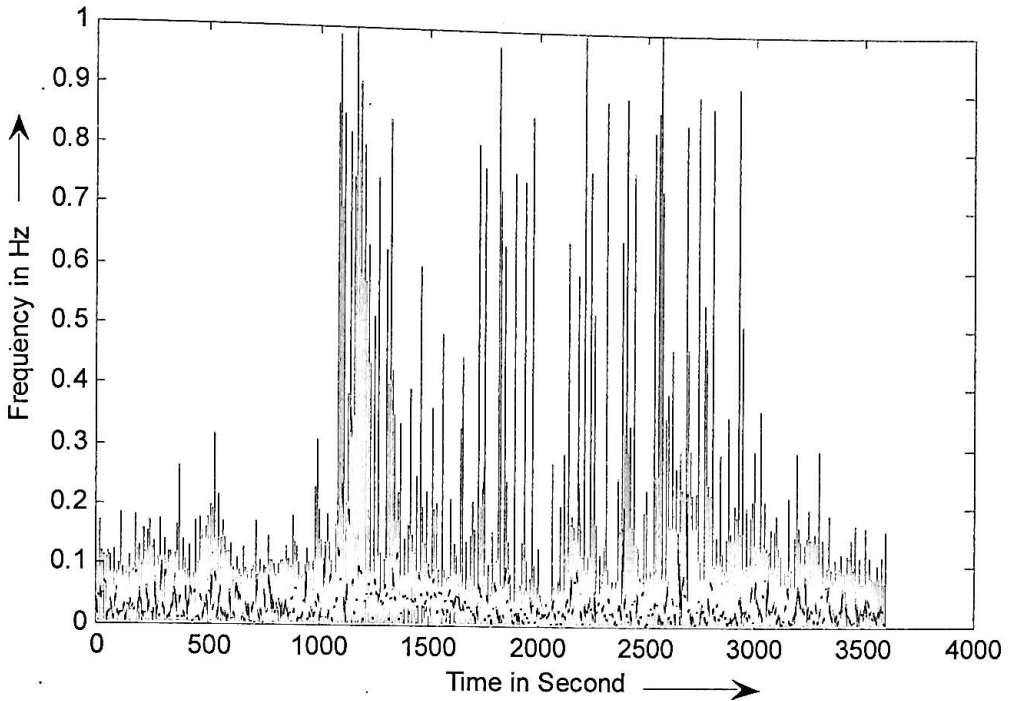
Fig. 4.7 Time frequency analysis recorded at station Dhaka University (east-west) of M 5.6 earthquake on 26 July 2003 of 23:18:17 UTC time occurred at the south-west of Daluchari, Chittagong.
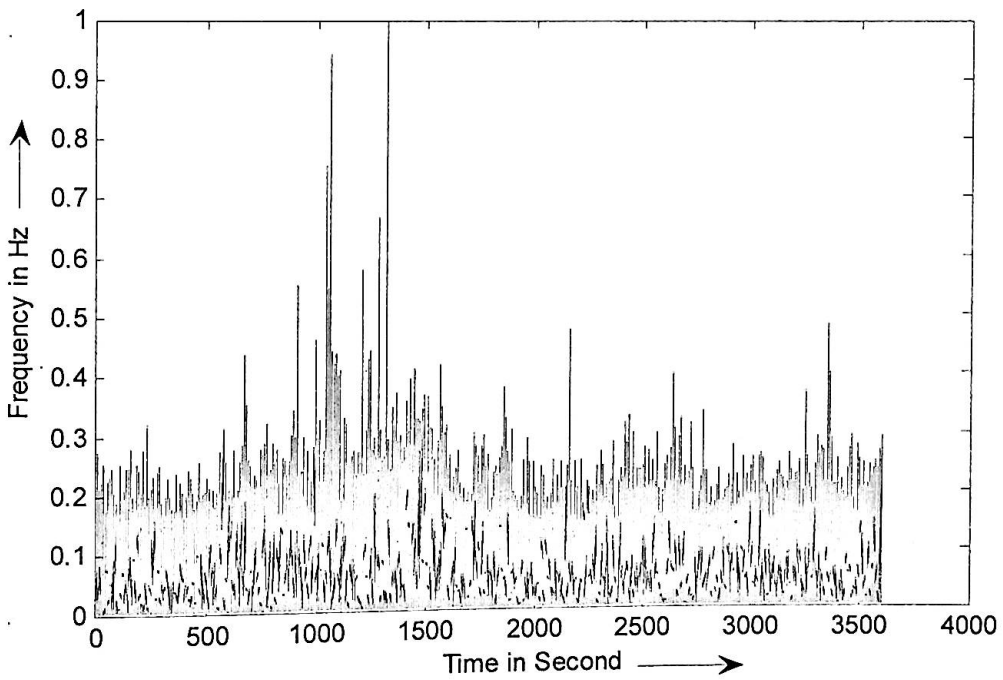
Fig. 4.8 Time frequency analysis recorded at station Dhaka University (up-down) of M 5.1 earthquake on 27 July 2003 of 12:07:24 UTC time occurred at Kolabunia, Chittagong.
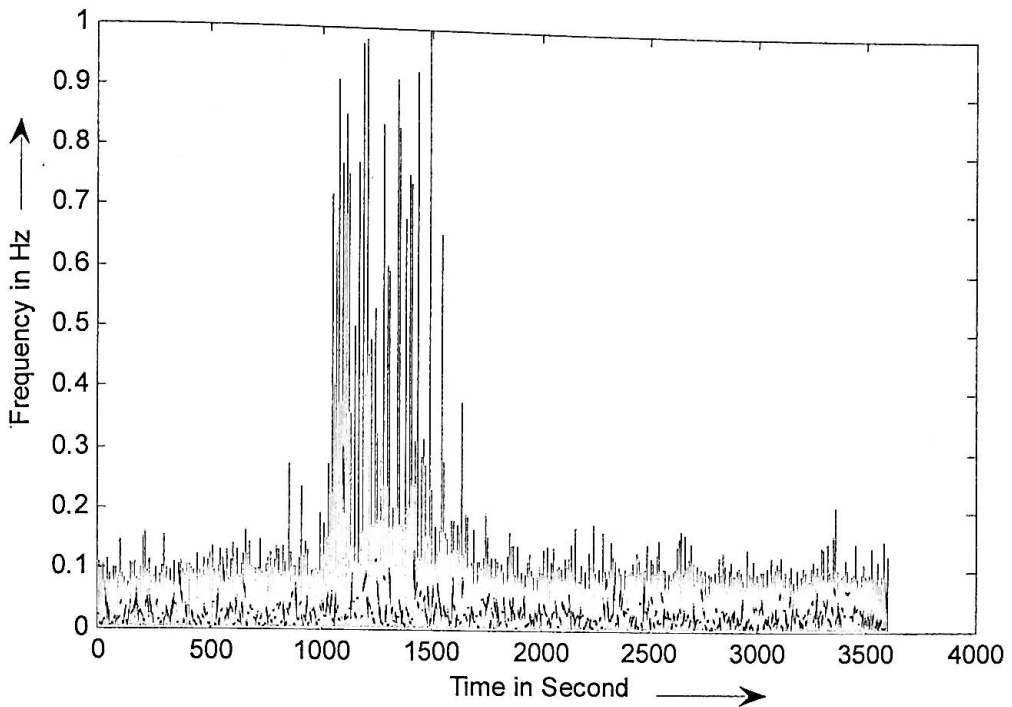
Fig. 4.9 Time frequency analysis recorded at station Dhaka University (north-south) of M 5.1 earthquake on 27 July 2003 of 12:07:24 UTC time occurred at Kolabunia, Chittagong.
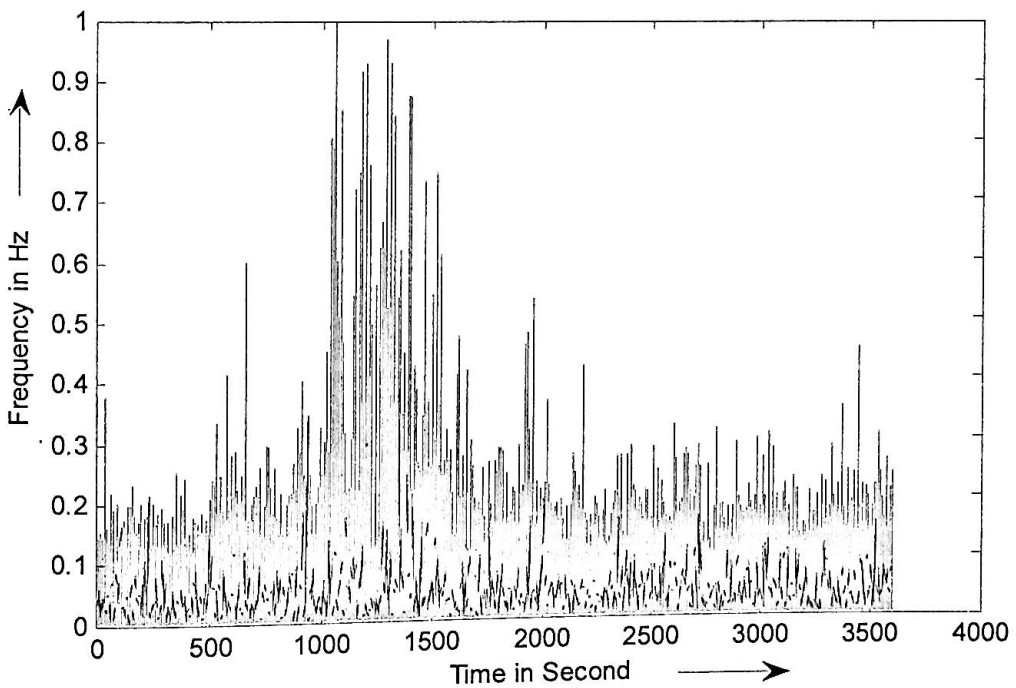
Fig. 4.10 Time frequency analysis recorded at station Dhaka University (east-west) of M 5.1 earthquake on 27 July 2003 of 12:07:24 UTC time occurred at Kolabunia, Chittagong.
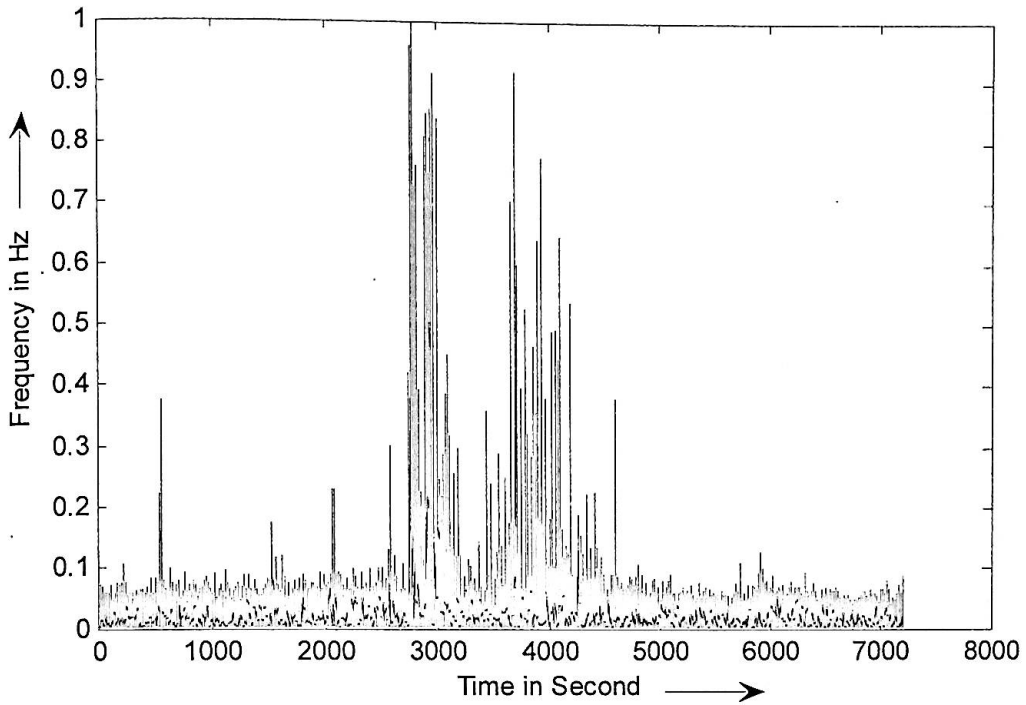
Fig. 4.11 Time frequency analysis recorded at station Dhaka University (up-down) of M 6.6 earthquake on 21 September 2003 of 18:16:13 UTC time occurred at the south of Meiktila, Myanmar.
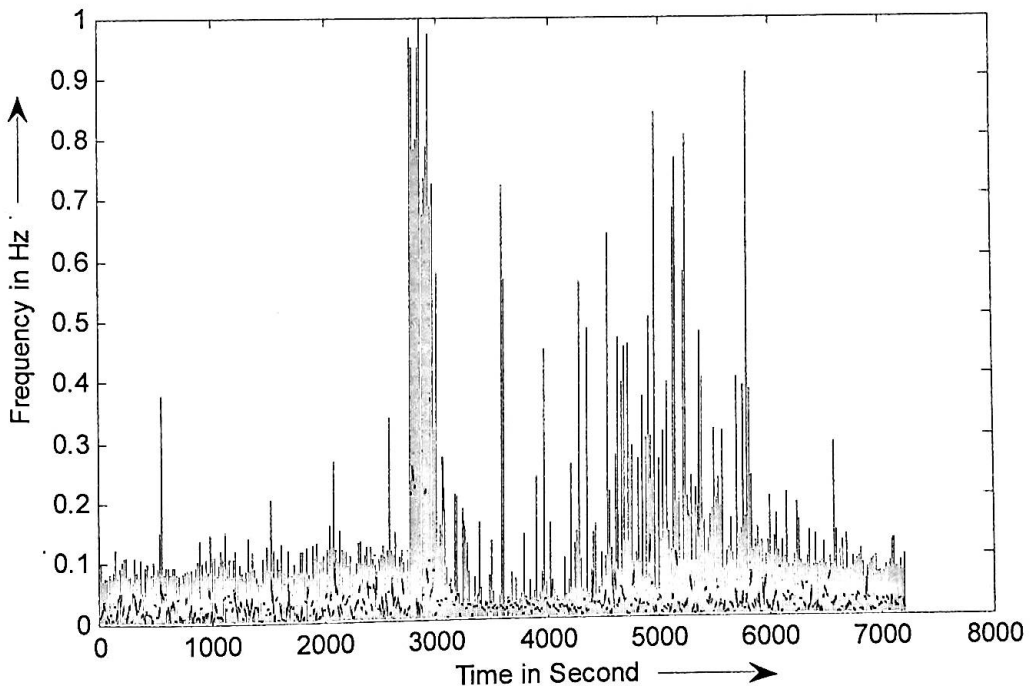
Fig. 4.12 Time frequency analysis recorded at station Dhaka University (north-south) of M 6.6 earthquake on 21 September 2003 of 18:16:13 UTC time occurred at the south of Meiktila, Myanmar.
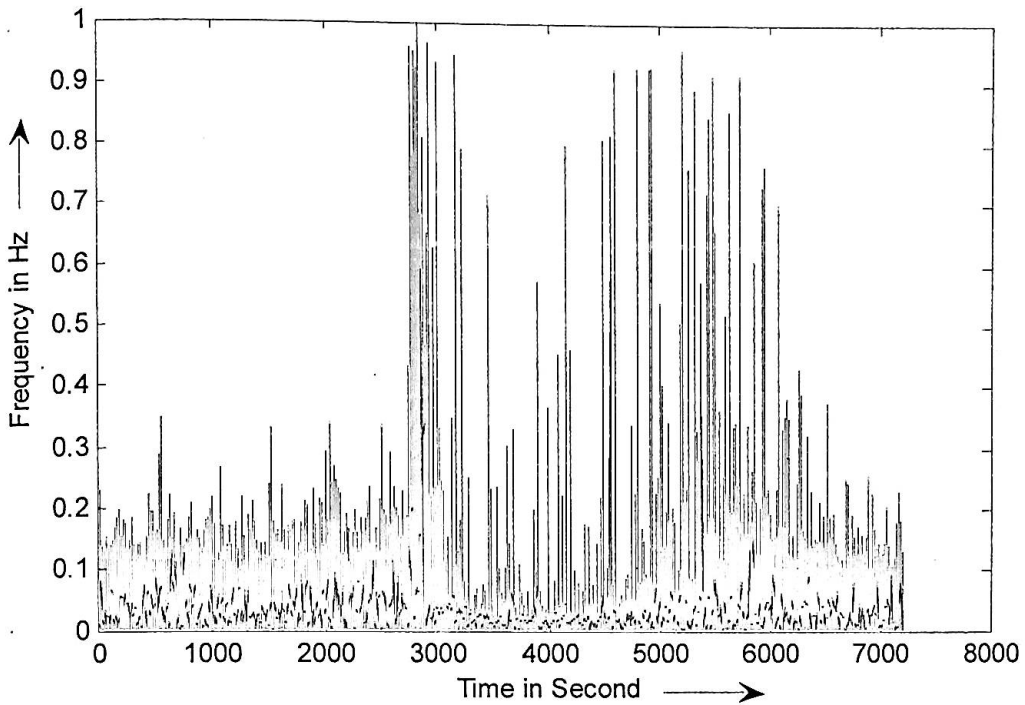
Fig. 4.13 Time frequency analysis recorded at station Dhaka University (east-west) of M 6.6 earthquake on 21 September 2003 of 18:16:13 UTC time occurred at the south of Meiktila, Myanmar.

4.3.4 Sequence analysis

Sequence is tried to derive from time frequency analysis to characterize the geologic sings over seismic wave. This is basically the extensions of time frequency analysis. The philosophy behind it is as the recorded waves might be affected from both amplitude and frequency. The ratio of instantaneous frequency to amplitude may provide the geologic sequences and it has been formulated as:

$$g(t) = \frac{f(t)}{A(t)} = \frac{d\theta(t)}{2\pi A(t)dt} \qquad 4.34$$

Therefore, equation (4.34) can provide instantaneous frequency to amplitude ratio of a wave. Instantaneous frequency to amplitude analysis has been made for synthetic and real earthquake data.

Using equations (4.28-4.34), Time frequency to amplitude analysis of the synthetic earthquake waves (Figs. 4.1-4.2) are also made and shown in Figs. 4.14-4.15 respectively. The time frequency to amplitude ratio as well as sequence for earthquake data are shown in Figs. 4.16-4.24 that are made from the seismological waves (Figs. 3.3-3.11)
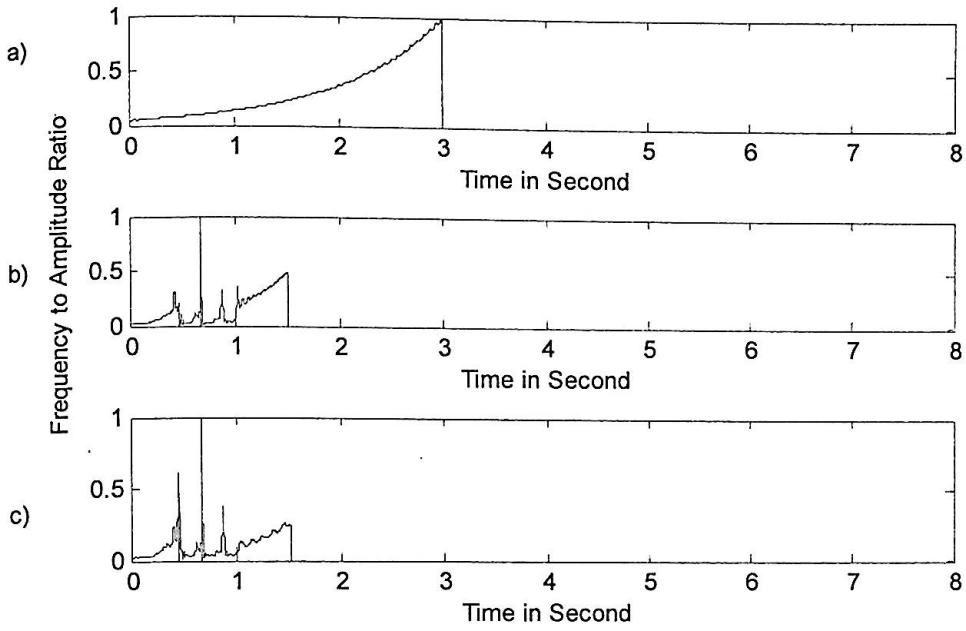
Fig. 4.14 Time frequency to amplitude analysis of synthetic earthquake wave respectively of Fig. 4.1.
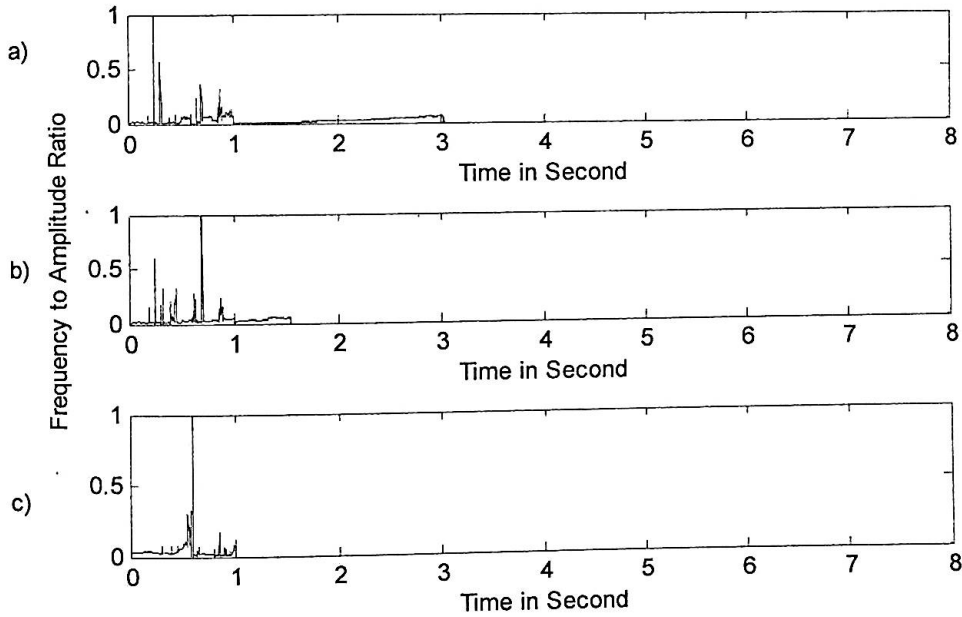
Fig. 4.15 Time frequency to amplitude analysis of synthetic earthquake wave respectively of Fig. 4.2.
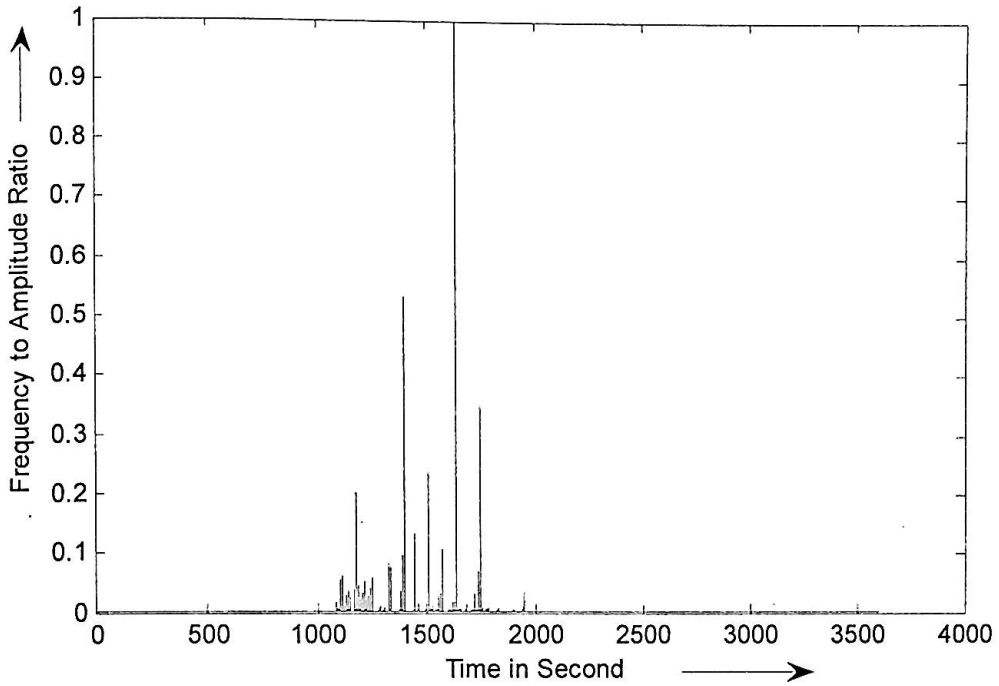
Fig. 4.16 Time frequency to amplitude analysis recorded at station Dhaka University (up-down) of M 5.6 earthquake on 26 July 2003 of 23:18:17 UTC time occurred at the south-west of Daluchari, Chittagong.
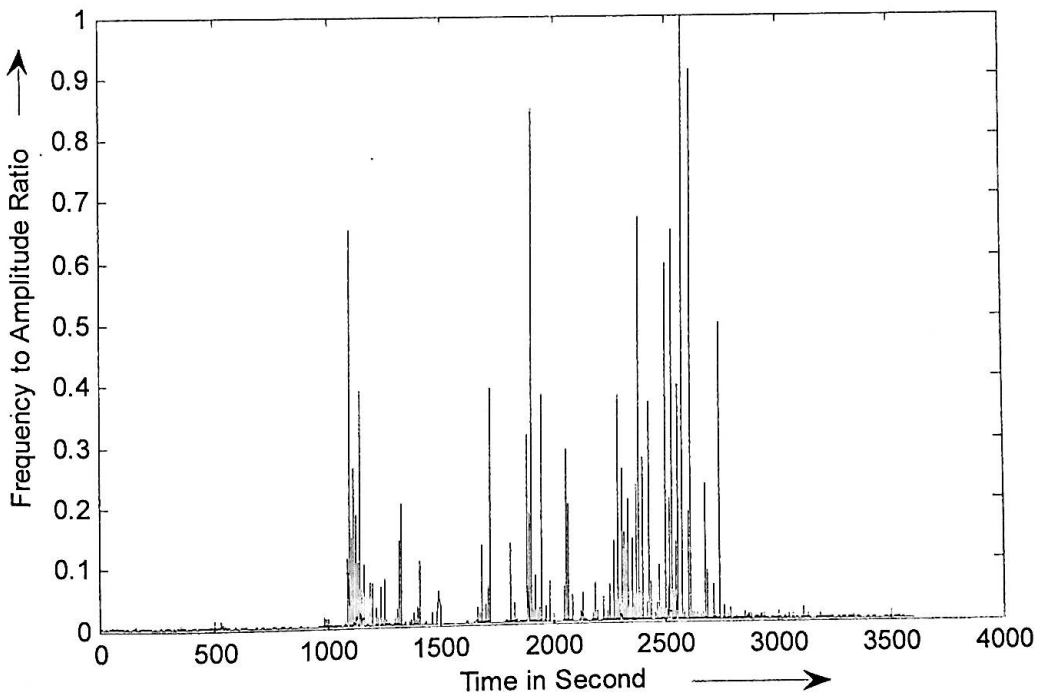
Fig. 4.17 Time frequency to amplitude analysis recorded at station Dhaka University (north-south) of M 5.6 earthquake on 26 July 2003 of 23:18:17 UTC time occurred at the south-west of Daluchari, Chittagong.
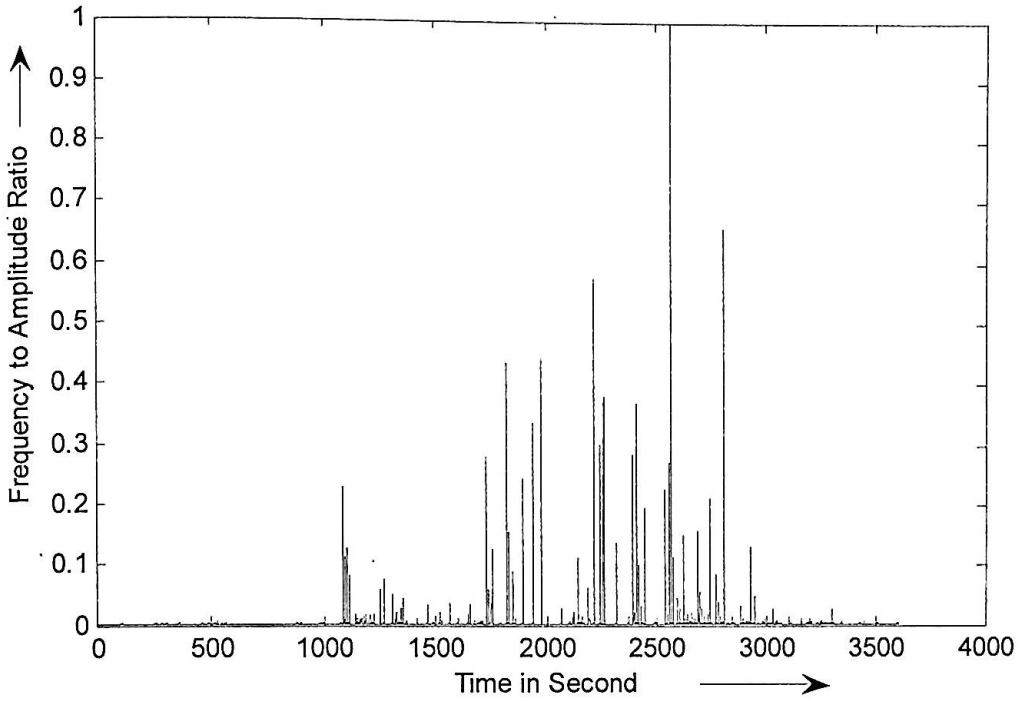
Fig. 4.18 Time frequency to amplitude analysis recorded at station Dhaka University (east-west) of M 5.6 earthquake on 26 July 2003 of 23:18:17 UTC time occurred at south-west of Daluchari, Chittagong.
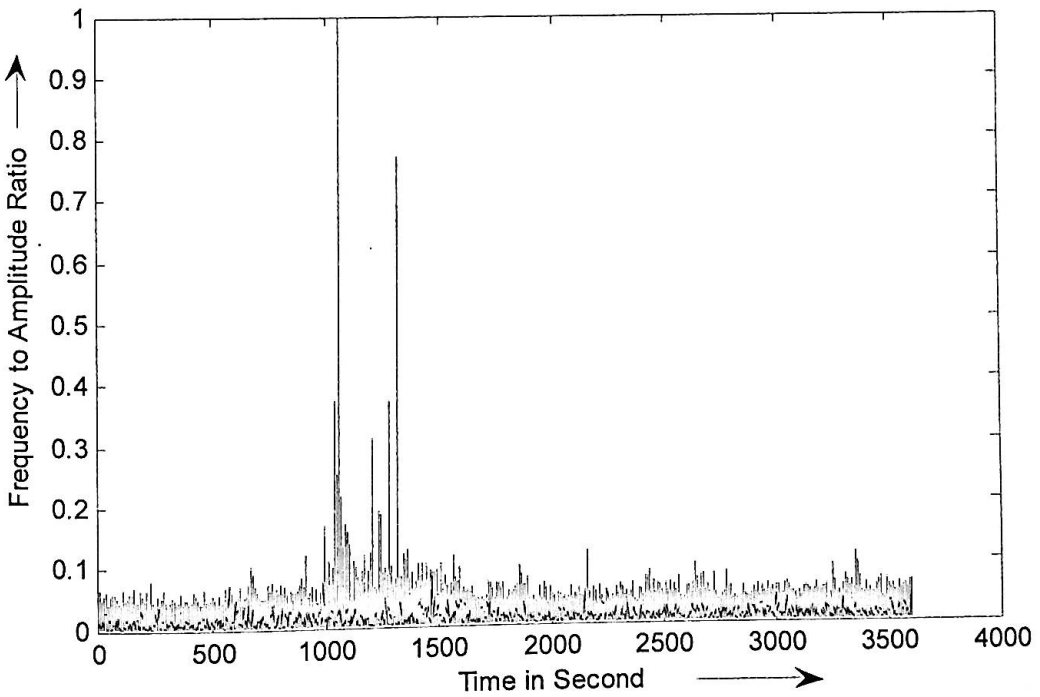
Fig. 4.19 Time frequency to amplitude analysis recorded at station Dhaka University (up-down) of M 5.1 earthquake on 27 July 2003 of 12:07:24 UTC time occurred at Kolabunia, Chittagong.
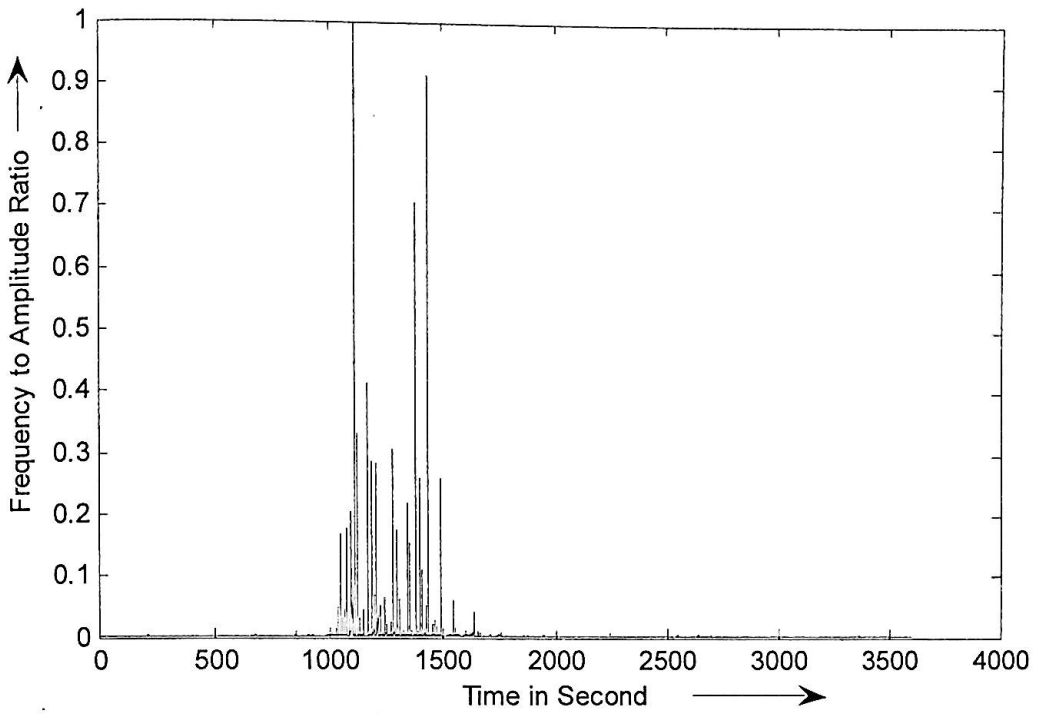
Fig. 4.20 Time frequency to amplitude analysis recorded at station Dhaka University (north-south) of M 5.1 earthquake on 27 July 2003 of 12:07:24 UTC time occurred at Kolabunia, Chittagong.
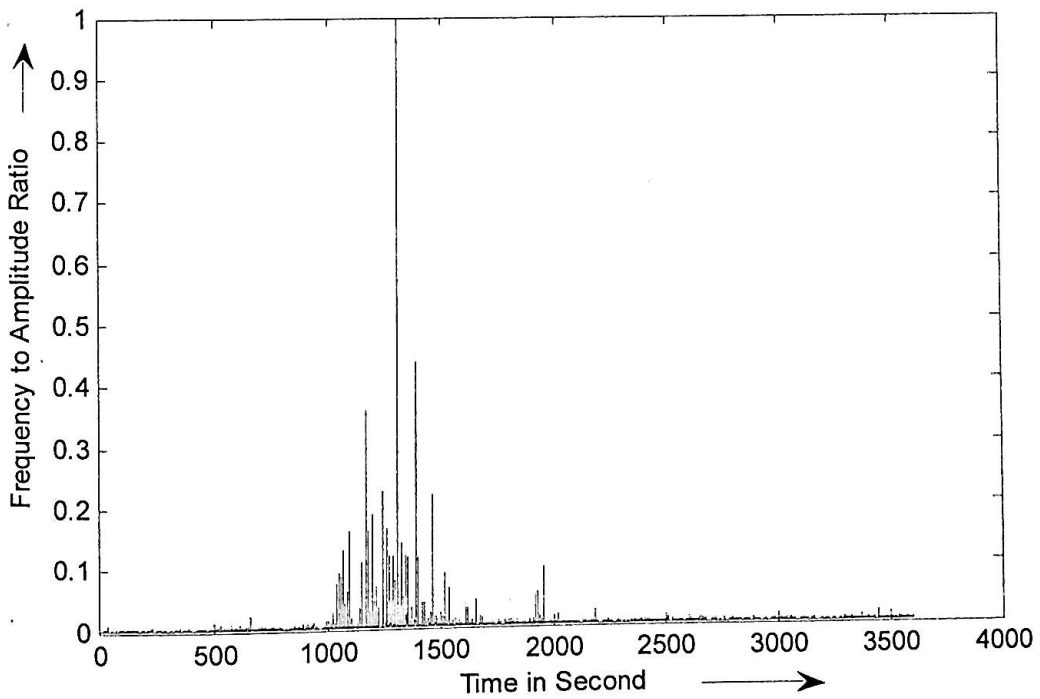
Fig. 4.21 Time frequency to amplitude analysis recorded at station Dhaka University (east-west) of M 5.1 earthquake on 27 July 2003 of 12:07:24 UTC time occurred at Kolabunia, Chittagong.
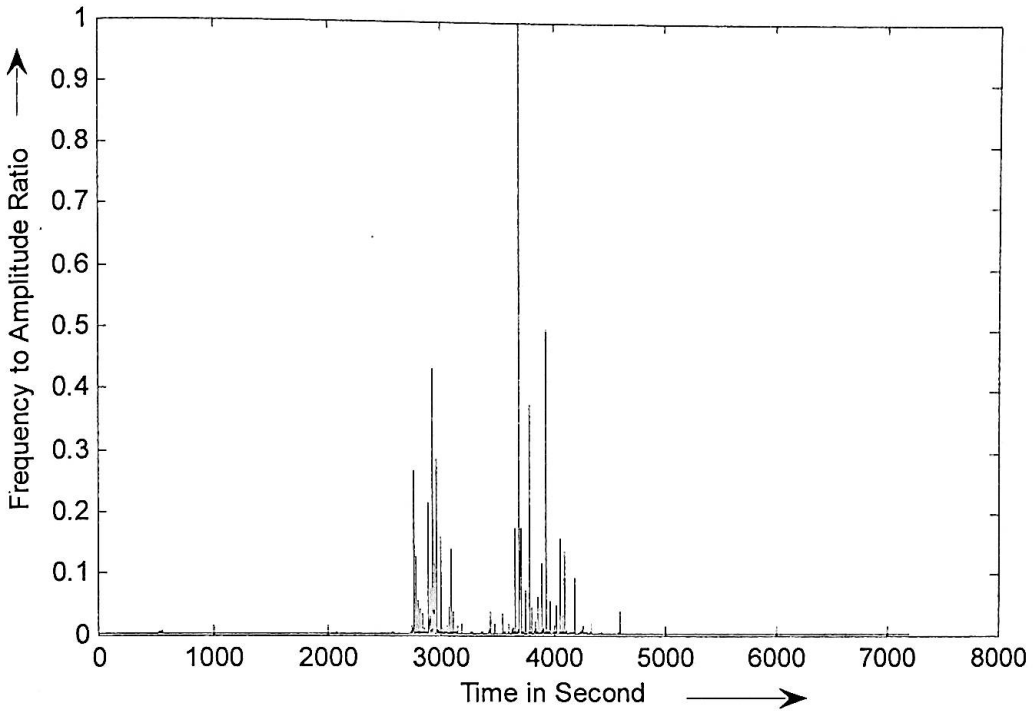
Fig. 4.22 Time frequency to amplitude analysis recorded at station Dhaka University (up-down) of M 6.6 earthquake on 21 September 2003 of 18:16:13 UTC time occurred at the south of Meiktila, Myanmar.
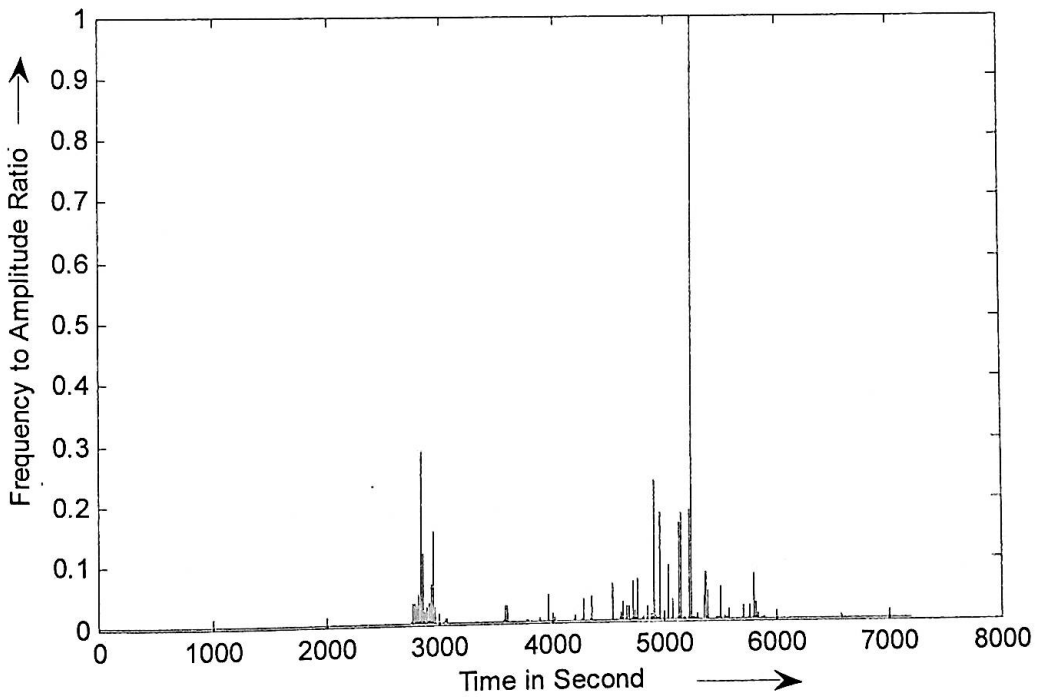
Fig. 4.23 Time frequency to amplitude analysis recorded at station Dhaka University (north-south) of M 6.6 earthquake on 21 September 2003 of 18:16:13 UTC time occurred at the south of Meiktila, Myanmar.
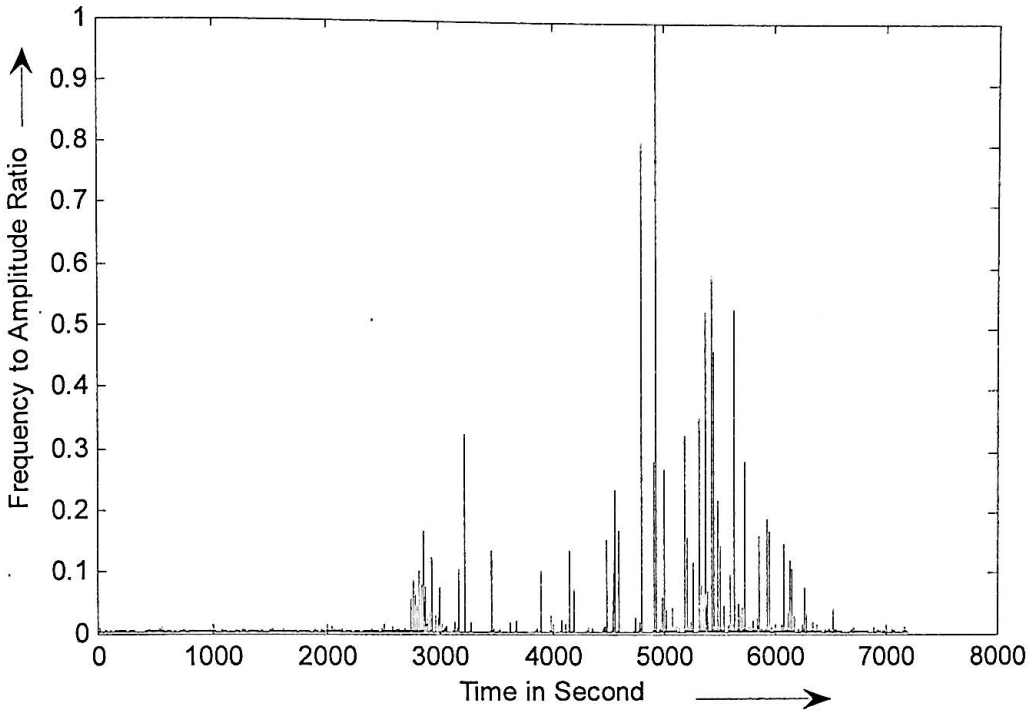
Fig. 4.24 Time frequency to amplitude analysis recorded at station Dhaka University (east-west) of M 6.6 earthquake on 21 September 2003 of 18:16:13 UTC time occurred at the south of Meiktila, Myanmar.

From the sequence analysis it is revealed that the frequency to amplitude ratio can be used to characterize the wave. However, it was not possible to make any useful relation for geologic variables.

4.4 Attenuation Analysis

Seismic wave attenuation is caused by two major factors such as scattering at heterogeneities in the earth and intrinsic absorption by anelasticity of the earth. This intrinsic attenuation may be distinguished from scattering attenuation, in which amplitudes in the main seismic arrivals are reduced by scattering off small-scale heterogeneities, but the integrated energy in the total wave field remains constant. The strength of intrinsic attenuation is given by the dimensionless quantity Q in terms of the fractional energy loss per cycle.

$$\frac{1}{Q(\omega)} = -\frac{\Delta E}{2\pi E} \qquad 4.35$$

Where E is the peak strain energy, ΔE is the energy loss per cycle and Q is the Quality factor; Q is inversely related to the strength of the attenuation; low- Q

regions are more attenuating than high -Q regions. From this definition, one may derive an approximation, valid for $Q \gg 1$, that is better suited for seismic approximation:

$$A(x) = A_0 e^{\frac{-\omega x}{2cQ}} \qquad 4.36$$

Where x is measured along the propagation direction and c is the velocity (e.g., $c = \alpha$ for P – waves with attenuation Q_α and $c = \beta$ for S – waves with attenuation Q_β). The amplitude of harmonic waves may be written as:

$$A(x,t) = A_0 e^{\frac{-\omega x}{2cQ}} e^{-i\omega\left(t-\frac{x}{c}\right)} \qquad 4.37$$

It is a product of a real exponential describing the amplitude decay due to attenuation and an imaginary exponential describing the oscillations.

Sometimes the exponentials in this equation are combined, and the effect of Q is included directly in $e^{-i\omega\left(t-\frac{x}{c}\right)}$ by adding a small imaginary part to the velocity c (Shearer, 1999). This provides an easy way to incorporate the effects of attenuation onto homogeneous layer techniques (e.g., reflectivity) for computing synthetic seismograms, since these methods typically operate in the frequency domain.

In ray theoretical methods, attenuation may be modeled through the use of t^*, defined as the integrated value of $\frac{1}{Q}$ along the ray path:

$$t^* = \int_{path} \frac{dt}{Q(r)} \qquad 4.38$$

Where r is the position vector, Equation 4.36 then becomes:

$$A(\omega) = A_0(\omega) e^{\frac{-\omega t^*}{2}} \qquad 4.39$$

The amplitude reduction at each frequency is obtained multiplying by $e^{\frac{-\omega t^*}{2}}$. The factor of ω means that the high frequencies are attenuated more than the low frequencies thus a pulse that travels through an attenuating region will gradually lose

its high frequencies. In the time domain, this can be modeled by convolving the original pulse by a t^* operator, defined as the inverse Fourier transform of the $t^*(\omega)$ function in the frequency domain. This convolution will cause the pulse broadening that is observed in the time domain.

A complication that we have neglected in these equations is that the existence of attenuation requires that velocity vary with frequency, even if Q itself is not frequency dependent over the same frequency band. This follows both from the necessity to maintain causality in the attenuated pulse and from considerations of physical mechanisms for attenuation. One of the most important results is that over a frequency interval in which $Q(\omega)$ is constant, the velocity c may be expressed as:

$$c(\omega) = c(\omega_0)\left(1 + \frac{1}{\pi Q}\ln\frac{\omega}{\omega_0}\right)$$
4.40

Where ω_0 is a reference frequency. The predicted velocity dispersion in the earth is fairly small at typically observed values of Q.

P wave attenuation Q_α and S wave attenuation Q_β are related to bulk attenuation Q_k and shear attenuation Q_μ by relationships (Shearer, 1999):

$$Q_\alpha^{-1} = LQ_\mu^{-1} + (1-L)Q_k^{-1}$$
4.41

and

$$Q_\beta = Q_\mu$$
4.42

Where $L = \left(\frac{4}{3}\right)\left(\frac{\beta}{\alpha}\right)^2$. Shear attenuation is observed to be much stronger than bulk attenuation in the Earth, and Q_k is generally assumed to be infinite except in the inner core.

4.5 Dispersion Analysis

Surface wave dispersion analysis is a method used to extract a subsurface structural model from records of earthquakes and mining explosions. Surface waves dispersion curves are commonly nonlinear functions with respect to the physical properties of

layers within the Earth, including shear and compressional wave velocities, the densities of the media and the thickness of the layers.

When different frequency components travel at different phase velocities, pulse shapes will not stay the same as they travel but will become dispersed as the frequencies separate. This leads to interference effects that cancel the wave energy except at particular times defined by the group velocity of the wave. This may be illustrated by considering the sum of two harmonic waves of slightly different frequency and wave number (Shearer, 1999):

$$u(x,t) = \cos(\omega_1 t - k_1 x) + \cos(\omega_2 t - k_2 x) \qquad 4.43$$

Relative to an average frequency ω and wave number k, we have

$$\omega_1 = \omega - \delta\omega, \qquad k_1 = k - \delta k,$$
$$\omega_2 = \omega + \delta\omega, \qquad k_2 = k + \delta k,$$

Substituting into $(4.43.)$, we obtain

$$
\begin{aligned}
u(x,t) &= \cos(\omega t - \delta\omega t - kx + \delta kx) + \cos(\omega t + \delta\omega t - kx\,\delta kx) \\
&= \cos[(\omega t - kx) - (\delta\omega t - \delta kx)] + \cos[(\omega t - kx) + (\delta\omega t - \delta kx)] \\
&= 2\cos(\omega t - kx)\cos(\delta kx - \delta\omega t) \qquad\qquad 4.44
\end{aligned}
$$

The resulting waveform consists of a signal with the average frequency ω whose amplitude is modulated by a longer period wave frequency $\delta\omega$. The short-period wave travels at velocity $\dfrac{\omega}{k}$ and the long period envelope travels at velocity $\dfrac{\partial\omega}{\partial k}$. The former is the phase velocity c and the later is the group velocity U. In the limit as $\delta\omega$ and δk approach zero, thus

$$U = \frac{d\omega}{dk} \qquad 4.45$$

The group velocity may be alternatively expressed as:

$$U = \frac{d\omega}{dk} c + k\frac{dc}{dk} = c\left(1 - k\frac{dc}{d\omega}\right)^{-1} \qquad 4.46$$

For earth, the phase velocity c of surface wave generally increases with period; thus $\dfrac{dc}{d\omega}$ is negative and from 4.46 it follows that the group velocity is less than the phase

velocity $(U < c)$. The graphical representation of the relation between period and phase and / or group velocity is called dispersion curve. Using dispersion curve geologic model can be implemented by which geology of an area may be known.

4.6 Modelling

Modelling is an essential tool of seismic data analysis in both exploration and earthquake seismology for understanding and interpretation of the recorded data at any region. It is the cornerstone of seismic inversion and seismic data processing and interpretation methods (Kelly and Marfurt, 1990; Carcione et al., 2002). In seismic modelling, the intend is to simulate seismic wave propagation through models corresponding to real geological targets or structures in the earth. Observed seismograms are a combination of source radiation, propagation path effects and recording instruments effects. Seismograms can be used to analyze the subsurface geology in two ways: direct and indirect modelling techniques, which are commonly used in the determination of the earth's interior from seismic surface wave dispersion.

4.6.1 Direct modelling

Direct modelling is used to determine the corresponding earth model from observed surface wave dispersion (Dorman and Ewing, 1962; McEvilly, 1964; Braile and Keller,1975; Bloch et al., 1969). Direct modelling utilizes the theoretical computations aspect of indirect modelling to make a direct determination of earth structure from surface wave dispersion. This technique place stringent requirements on data quality and these requirements sometime limit the application of direct modelling.

4.6.2 Indirect modelling

The most widely used modelling technique is an indirect trial-and-error procedure in which dispersion is computed for models in an effort to duplicate observed dispersion. Indirect modelling has been applied to surface wave phase and group velocity dispersion in the fundamental and higher mode operations (Dorman et al., 1960; Dorman and Ewing, 1962). Theoretically exact methods for the computation of dispersion have been presented by Haskell (1953) and Alterman et al., (1959). Since

the relationship between phase and / or group velocities at a given frequency and the properties of the propagation path is not simple, a numerical procedure is to be performed to compute one from another to invert for the earth model. An implicit theoretical relationship exits between wave type, mode, phase and group velocities, and structural earth parameters such as density ρ, layer thickness d, S wave velocity β and P wave velocity α. In the present research, indirect modelling technique has been used to determine the model for the crustal structure of the south-eastern region of Bangladesh.

Chapter 5
Seismic Surface Wave Analysis and Modelling

5.1 Introduction

The modern use of seismic surface waves for studying crustal and upper mantle structure started in the 1950s. Several studies on observations of surface waves are available for both global and regional models. Regional surface wave studies of the crust and upper mantle were reviewed by Ewing et al., (1957); Brune and Dorman, (1963); Knopoff et al., (1966) and Kovach, (1978); and surface wave dispersion for different tectonic provinces are presented by Ewing and Press, (1952); Haskell, (1953) Dziewonski et al., (1972) and Braile and Keller, (1975). Kovach, (1978) provided an overview of how surface-wave data from earthquakes are analyzed to infer details of the earth structure over particular propagation paths. Experimental methods for measuring surface wave dispersion, including the Fourier phase methods, the time correlation method, the band-pass filtering method, the group delay time method, graphical method and various digital moving window techniques, were also described by Kovach, (1978).

Surface wave dispersion analysis of the local earthquakes can be used to study the crustal structure of the earth using simple models of continental or oceanic crust. Ewing and Press, (1952) first introduced such model for the oceanic crust using Rayleigh wave dispersion and later Ewing et al., (1957) presented a theoretical dispersion relation for a two-layer model of continental crust. There are number of direct and indirect modelling techniques, which are commonly being used in determination of the earth's interior from seismic surface wave dispersion. Direct modelling determines the crustal structure from observed surface wave dispersion (Brune and Dorman, 1963; McEvilly, 1964; Bloch and Hales, 1968 and Bloch et al., 1969). On other hand, the most widely used indirect modelling techniques deal with trial-and-error procedures. Dispersion is computed for different

model parameters to see how the computed dispersion matches with the observed dispersion (Dorman et al., 1960 and Dorman and Ewing, 1962).

Hence, there are different techniques of seismic surface wave analysis which have been applied to determine the crustal structure of the earth. In this research, the group velocity dispersion has been computed and analyzed using graphical method (Ewing and Press, 1952) for the up-down component of the ground accelerated earthquake seismic wave and theoretical dispersion curves are estimated according to modified Haskell matrix method and finally an indirect model has been constructed based on surface wave analysis.

5.2 Seismic Surface Wave

The seismic waves originally described by Lord Rayleigh in 1885, now called Rayleigh waves, they are commonly known as surface waves. Surface waves generated by an earthquake or explosive source are generally recorded as low frequency normally dispersed wave trains.

Surface wave signals are generally the largest arrivals on the seismogram. It provides some of the best constraints on the Earth's crust structure. Waveforms of the surface wave are more complicated than body waves. They travel more slowly and decay less with distance than body waves and they are dispersed. Interpreting surface-wave dispersion measurements provides an important method for determining the shear-wave velocity variation in the Earth. Modern studies of surface waves and their application in structure interpretation were propelled by Haskell's matrix formulation of the multi-layered system period equation, which made possible rapid, accurate computation of dispersion curves for complex models (Knopoff et al., 1966).

5.3 Model Development

Group velocity dispersion is considered as the factor, which has relationship with crustal structure. Group velocity from recorded earthquake wave and multilayered crustal model can be studied respectively by graphical method and modified Haskell matrix method.

5.3.1 Graphical method

An interesting phenomenon that occurs when waves at close frequencies travel at slightly different velocities is that they mix together in a modulated trend whose frequency is the average of its constituents, and its envelope varies slower in amplitude with time. In such a case, the energy of the motion concentrates in packets that travel with a velocity known as the group velocity, which depends on the velocity of the individual waves and on how that velocity changes between them. This phenomenon is called dispersion. The curve showing the dependence of velocity on frequency or period is called the dispersion curve and it can be experimentally measured by graphical method.

Graphical method is basically a technique of group velocity dispersion determination. In this method the travel times (t) of some chosen phases along the surface wave train are measured and plotted on a graph versus the order number (n) of the chosen phases. Usually the travel times of the wave crests and troughs are read. The (n,t) curve built by these points is then approximated with linear segments. The period is determined by the slope of these lines and the corresponding travel times are read from the midpoints of the segments (Ewing and Press, 1952). The group velocity, U_g of seismic surface wave can be obtained as:

$$U_g = \frac{x}{t} \qquad\qquad 5.1$$

Where, x is the epicentral distance and t is the travel time.

The synthetic order number versus travel time curve is presented in Fig. 5.1
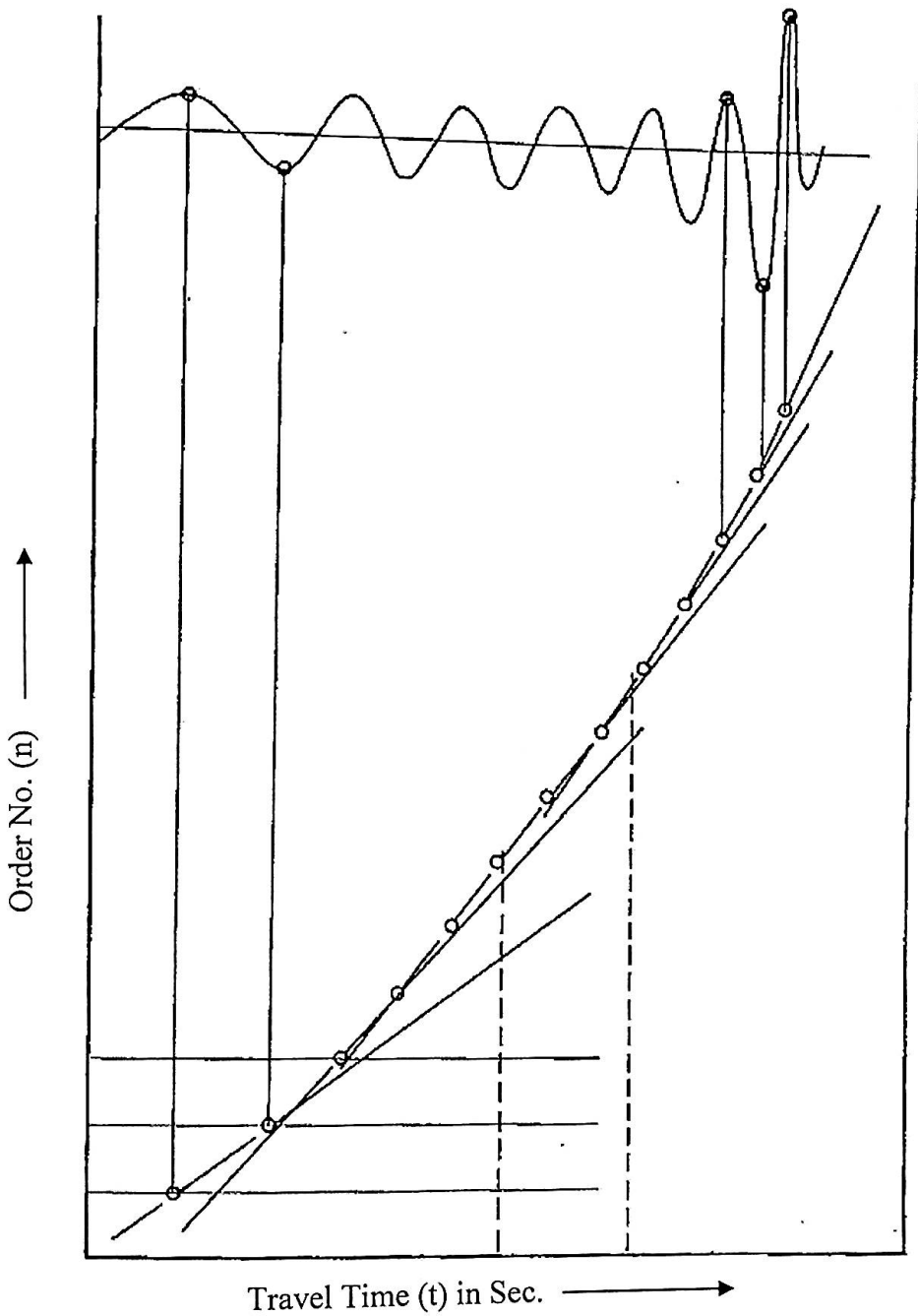
Fig. 5.1 Synthetic Order Number Vs Travel Time (n-t) Curve.

5.3.2 Modified Haskell matrix method

The multilayer dispersion computation of surface wave has been first performed by Haskell (1953). Since Rayleigh waves are composed of P and S-waves and Love waves are composed of only S waves, Haskell derived the elastic wave equations for both P and S-waves. These equations were modified to show Rayleigh wave motion.

After assuming a free surface boundary where no stresses or strains cross, the Rayleigh wave equation is simplified. For different values of layer thicknesses, densities, and elastic parameters in the form of P and S wave velocities, the Haskell matrix (equations 5.2-5.3) will yield a dispersion curve (Watson, 1970).

Notations employed in Haskell's matrix are:

ω = angular frequency

c = phase velocity

$k = \dfrac{\omega}{c}$ = angular-wave number.

For layer m:

ρ_m = density

d_m = thickness

α_m = compressional-wave velocity

β_m = shear-wave velocity

$$\gamma_m = 2\left(\frac{\beta_m}{c}\right)^2$$

$$r_{\alpha m} = +\left[\frac{c^2}{\alpha_m^2} - 1\right]^{1/2} \qquad\qquad c > \alpha_m$$

$$r_{\alpha m} = -i\left[\frac{c^2}{\alpha_m^2}\right]^{\frac{1}{2}} \qquad\qquad c < \alpha_m$$

$$r_{\beta m} = +\left[\frac{c^2}{\beta_m^2} - 1\right]^{1/2} \qquad\qquad c > \beta_m$$

$$r_{\beta m} = -i\left[1 - \frac{c^2}{\beta_m^2}\right]^{1/2} \qquad\qquad c < \beta_m$$

$$P_m = k r_{\alpha m}\, d_m$$

$$Q_m = k r \beta_m\, d_m$$

The Haskell matrix components for layer m are:

$$A_{11}^m = A_{44}^m = \gamma_m\, CP - (\gamma_m - 1)CQ$$

$$A_{12}^m = A_{34}^m = i\left[(\gamma_m - 1)r_{\alpha m}^{-1} SP + \gamma_m\, r_{\beta m}\, SQ\right]$$

$$A_{13}^m = A_{24}^m = -\left(\rho_m c^2\right)^{-1}(CP - CQ)$$

$$A_{14}^m = i\left(\rho_m c^2\right)^{-1}\left(r_{\alpha m}^{-1} SP + r_{\beta m} SQ\right)$$

$$A_{21}^m = A_{43}^m = -i\left[\gamma_m\, r_{\alpha m} SP + (\gamma_m - 1)r_{\beta m}^{-1} SQ\right]$$

$$A_{22}^m = A_{33}^m = -(\lambda_m - 1)CP + \lambda_m CQ$$

$$A_{23}^m = i\left(\rho_m c^2\right)^{-1}\left(r_{\alpha m} SP + r_{\beta m}^{-1} SQ\right)$$

$$A_{31}^m = A_{42}^m = \rho_m c^2 \gamma_m\,(\gamma_m - 1)(CP - CQ)$$

$$A_{32}^m = i\rho_m c^2\left[(\gamma_m - 1)^2 r_{\alpha m}^{-1} SP + \gamma_m^2 r_{\beta m} SQ\right]$$

$$A_{41}^m = i\rho_m c^2\left[\gamma_m^2\, r_{\alpha m} SP + (\gamma_m - 1)^2 r_{\beta m}^{-1} SQ\right]$$

Where

$$\text{SP} = \sin P_m \qquad\qquad \text{SQ} = \sin Q_m$$
$$\text{CP} = \cos P_m \qquad\qquad \text{CQ} = \cos Q_m$$

The Haskell matrix is

$$A^m = \begin{bmatrix} A_{11} & A_{12} & A_{13} & A_{14} \\ A_{21} & A_{22} & A_{23} & A_{24} \\ A_{31} & A_{32} & A_{33} & A_{34} \\ A_{41} & A_{42} & A_{43} & A_{44} \end{bmatrix} \qquad\qquad 5.2$$

The half space matrix is

$$\hat{E}^n = \begin{bmatrix} -2\left(\dfrac{\beta_n}{\alpha_n}\right)^2 & -c^2(\gamma_n - 1) & \dfrac{\alpha_n^2 r_{\alpha n}}{\left(\rho_n \alpha_n^2\right)^{-1}} & -\left(\rho_n \alpha_n^2 r_{\alpha n}\right)^{-1} \\ & & & \\ -\left(\gamma_n - \dfrac{1}{\gamma_n r_{\beta n}}\right) & 1 & \left(\rho_n c^2 \gamma_n r_{\beta n}\right)^{-1} & \left(\rho_n c^2 \gamma_n\right)^{-1} \end{bmatrix} \qquad 5.3$$

Modified Haskell matrix method for the case of $(n-1)$ homogeneous, isotopic elastic layers over a half-space matrix can be written as (Watson, 1970):

$$J = \hat{E}^n A^{n-1} .... A^m ... A^2 . A^1 \qquad\qquad 5.4$$

Where A^m is the 4X4 Haskell matrix for the m'th layer and $\hat{E}^n$ is the half-space inversion matrix. Then the dispersion relation is:

$$\Delta(T,c) = J\,|_{12}^{12} = J_{11}\,J_{22} - J_{12}\,J_{21} = 0 \qquad\qquad 5.5$$

Hence two columns or rows of J are necessary for this result and it requires a 2X4 matrix to store the product of each layer. It has been seen that Haskell matrix poses a loss of significant figures in the dispersion function (Knopoff, 1964; Dunkin, 1965 and Thrower, 1965). In order to minimize the losses, a 6X6 matrix is employed where the elements are second order sub-determinant of the Haskell matrix. The matrix can be written as:

$$R_i^m = \sum_{j=1}^{6} B_{ij}^m R_j^{m-1} \qquad\qquad 5.6$$

Where $B_{ij}^m = A^m\,|_{kl}^{ij}$

The 6X6 B_{pq}^m for the m'th layer is derived from the second order sub-determinants $A^m\,|_{pq}^{ij}$ of the Haskell matrix by the following convention:

$$ij\,(kl) \longrightarrow p\,(q)$$

ij (kl)	p (q)
12	1
13	2
14	3
23	4
24	5
34	6

Example: Let us consider a 4X4 matrix,

$$A^m = \begin{bmatrix} a_{11} & a_{12} & a_{13} & a_{14} \\ a_{21} & a_{22} & a_{23} & a_{24} \\ a_{31} & a_{32} & a_{33} & a_{34} \\ a_{41} & a_{42} & a_{43} & a_{44} \end{bmatrix}$$

According to the convention, second order sub-determinant matrix elements are:

$$A^m \big|_{12}^{12} = A_{11}^m A_{22}^m - A_{12}^m A_{21}^m = a_{11} a_{22} - a_{12} a_{21} = B_{11}^m$$

$$A^m \big|_{13}^{12} = A_{11}^m A_{23}^m - A_{13}^m A_{21}^m = a_{11} a_{23} - a_{13} a_{21} = B_{12}^m$$

$$\cdots\cdots\cdots\cdots\cdots\cdots\cdots\cdots\cdots\cdots\cdots\cdots\cdots\cdots\cdots$$

$$A^m \big|_{34}^{34} = A_{33}^m A_{44}^m - A_{34}^m A_{43}^m = a_{33} a_{44} - a_{34} a_{43} = B_{66}^m$$

Therefore, the 6X6 matrix,

$$B^m = \begin{bmatrix} B_{11} & B_{12} & B_{13} & B_{14} & B_{15} & B_{16} \\ B_{21} & B_{22} & B_{23} & B_{24} & B_{25} & B_{26} \\ B_{31} & B_{32} & B_{33} & B_{34} & B_{35} & B_{36} \\ B_{41} & B_{42} & B_{43} & B_{44} & B_{45} & B_{46} \\ B_{51} & B_{52} & B_{53} & B_{54} & B_{55} & B_{56} \\ B_{61} & B_{62} & B_{63} & B_{64} & B_{65} & B_{66} \end{bmatrix} \qquad 5.7$$

Hence the dispersion function, $\quad \Delta(T,c) = R^n B^n = 0$ \hfill 5.8

B^n is the matrix of sub-determinants of the half-space $\hat{E}^n$.

However, using Equation 5.6 B matrix shows that

$$R_i^1 = B_{i1}^1 \qquad\qquad 5.9$$

$$\text{and} \quad R_3^m = R_4^m$$

This phenomenon leads to define a 5X5 matrix $\hat{B}$ rather than 6X6 matrix and the modified $\hat{B}$ matrix can be expressed as:

$$\hat{B} = \begin{bmatrix} B_{11} & B_{12} & 2B_{13} & B_{15} & B_{16} \\ B_{21} & B_{22} & 2B_{23} & B_{25} & B_{26} \\ B_{31} & B_{32} & (2B_{33}-1) & B_{35} & B_{36} \\ B_{51} & B_{52} & 2B_{53} & B_{55} & B_{56} \\ B_{61} & B_{62} & 2B_{63} & B_{65} & B_{66} \end{bmatrix} \qquad 5.10$$

and similarly R_i^m is thus reduced from a six dimensional vector to five.

Dispersion relation (Eqn. 5.8) can be solved numerically according to the model parameters (α, β, ρ and d) in the form of group velocity versus time period plot. On other hand, same plot can also be obtained from the recorded earthquake data using graphical method. Hence crustal interpretations are now possible in an indirect way by matching both the dispersion relations.

5.4 Dispersion in Surface Waves

Ewing and Press, (1952) first utilized Rayleigh wave dispersion to develop simple models of oceanic crust by comparing observed phase velocity dispersion data with theoretical dispersion data, from the lengthy period equation for Rayleigh waves (Lee, 1932). Ewing et al., (1957) later calculated a theoretical dispersion curve for a two layer model of continental crust. These early studies developed only very simple layered models of earth structure because the manually calculated dispersion curves for detailed models could not be carried out in a reasonable time. Perhaps the greatest improvement in surface wave analysis came with the development of high speed digital computers. A matrix formulation for transmission of surface waves through a multilayered model (Haskell, 1953) was adapted for use on computers and permitted theoretical dispersion curves to be calculated for complex earth models. Besides providing an efficient way to model earth structure, the computers opened the way to other improvements in the analysis of surface wave data. For example, the study of the Canadian shield (Brune and Dorman, 1963) showed how a least-square fitting program developed by Dorman and Ewing (1962) could be used to minimize the error in comparing observed dispersion curves to theoretical curves. More recent improvements have included applying Fourier analysis to the determination of phase velocities (Knopoff et al., 1966; Bloch and Hales, 1968) using moving window and multi-filter techniques to extract group velocity data from seismograms (Bloch and Hales, 1968; Landisman et al., 1969), and cross-correlating observed seismograms with theoretical seismograms to obtain greater precision of dispersion measurements (Dziewonski et al., 1972). Computer programs are now in use to provide to calculate phase and group velocity due to propagation in a model of many layers.

Dispersion is observed in the frequency of dependent travel times of surface waves, resulting from the increase of velocity with depth. In general, short period surface

waves travel slower than long period waves. Long periods are more sensitive to the faster velocities found deeper in the earth. Both Love wave and Rayleigh wave exhibit dispersion and are used to estimate shear velocity in the crust and upper mantle. In a homogeneous elastic half-space with no damping, Rayleigh waves propagate along the surface of the body at a constant, frequency independent, phase velocity. In the layered or vertically heterogeneous half-space different frequency surface waves propagate with different phase velocities and different wave lengths. On the other hand, group velocity is a dispersive characteristic where constructive patterns travel along the surface as wave packets. Group velocity dispersion curves can be used to define velocity structure. In the 1960s, the development of numerical techniques has resulted in significant progress in making dispersion curves measurements (Dziewonski and Hales, 1972).

5.5 Determination of Group Velocity from Earthquake Data

Group velocity of real earthquake data (Figs. 3.3, 3.6 and 3.9) can be determined using equation 5.1 from earthquake source parameters (Table 3.3). Fig. 5.2 shows order number (n) versus travel time (t) plot and Fig. 5.3 shows group velocity variation with time period.
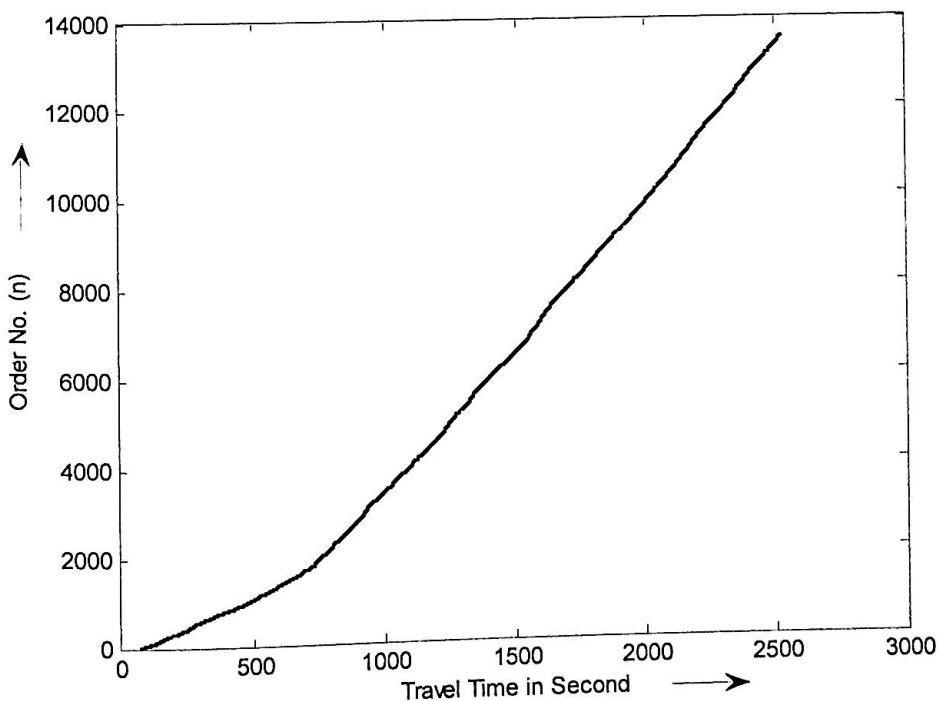
Fig. 5.2 Order number versus travel time curve for the south-west of Daluchari, Chittagong earthquake data (Fig. 3.3).

95
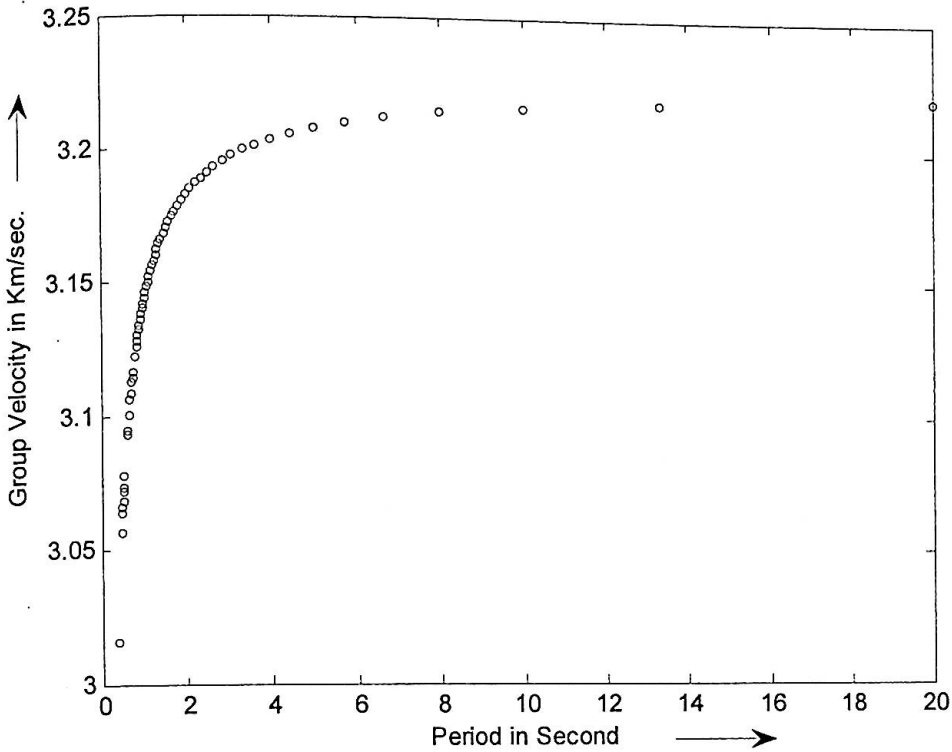
Fig. 5.3 Group velocity dispersion curve for the south-west of Daluchari, Chittagong earthquake data (Fig. 3.3).

5.6 Determination of Group Velocity from Model Parametric Data

Each layer of any model contains four parameters e.g. P-wave velocity, S-wave velocity, density and layer thickness. Group velocity can be determined using these four parameters which are given in the particular model with the help of modified Haskell matrix (eqn. 5.10). Two parameters S-wave velocity and thickness are changed freely but the other two parameters P-wave velocity and density of considered model are calculated by the following empirical equation (Ammon et al., 1990):

$$\alpha = 1.732\,\beta \qquad\qquad 5.11$$

$$\rho = .32\,\alpha + .77 \qquad\qquad 5.12$$

Three synthetic models with a half-space are considered in the following tables 5.1-5.3

Table 5.1: Synthetic model-1 with a half-space

Primary wave velocity (α) in km/sec.	Shear wave velocity (β) in km/sec.	Density (ρ) in gm/cc	Thickness (d) in Km
5.53	3.192	2.54	1.5
5.63	3.25	2.57	3.0
5.72	3.30	2.60	4.0
5.80	3.35	2.63	10.0
6.11	3.53	2.73	∞

Table 5.2: Synthetic model-2 with a half-space

Primary wave velocity (α) in km/sec.	Shear wave velocity (β) in km/sec.	Density (ρ) in gm/cc	Thickness (d) in Km
5.53	3.192	2.54	1.5
5.72	3.30	2.60	3.0
5.80	3.35	2.63	14.0
6.11	3.53	2.73	∞

Table 5.3: Synthetic model-3 with a half-space

Primary wave velocity (α) in km/sec.	Shear wave velocity (β) in km/sec.	Density (ρ) in gm/cc	Thickness (d) in Km
5.53	3.194	2.54	1.5
5.72	3.30	2.60	5.0
5.80	3.35	2.63	13.0
6.11	3.53	2.73	∞

According to above three models, phase velocity can be calculated by using equation 5.8 and group velocity can be determined by using the following relation:

$$U = \frac{c}{1 - \left(\frac{\omega}{c} \cdot \frac{dc}{d\omega} \right)} \qquad 5.13.$$

Therefore, if the phase velocity dispersion, $c(\omega)$ across some frequency range is known, the group velocity, $U(\omega)$ across that range can easily be determined (Larson and Ekstrom, 2001). The dispersion curves are shown in Figs. 5.4-5.6.
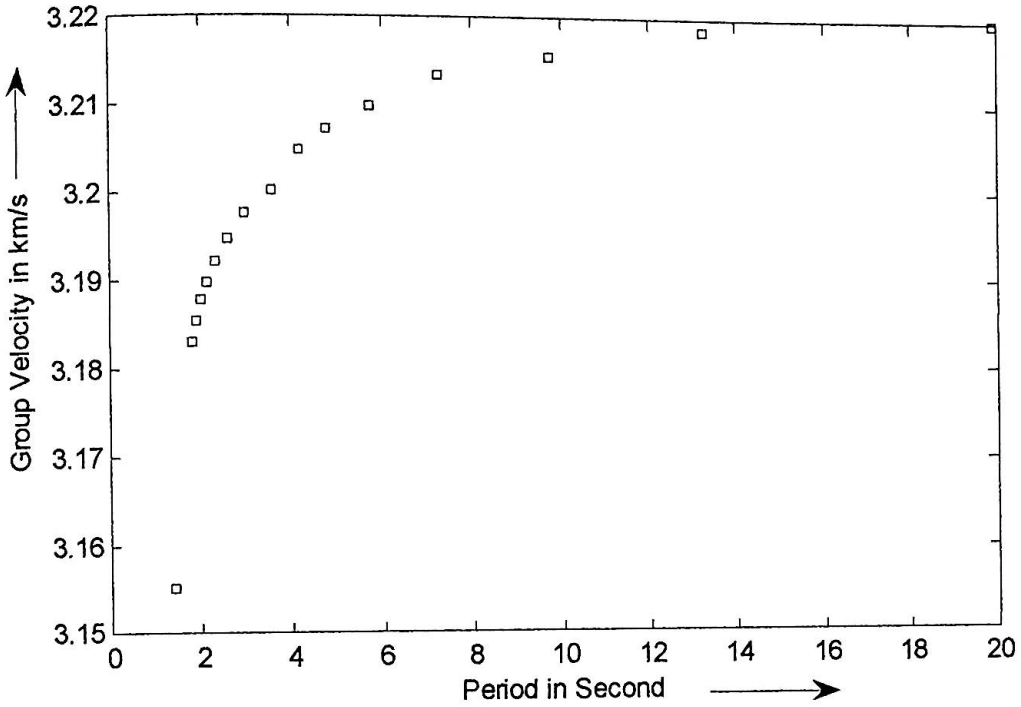
Fig. 5.4 Dispersion curve using the model parameters of table 5.1
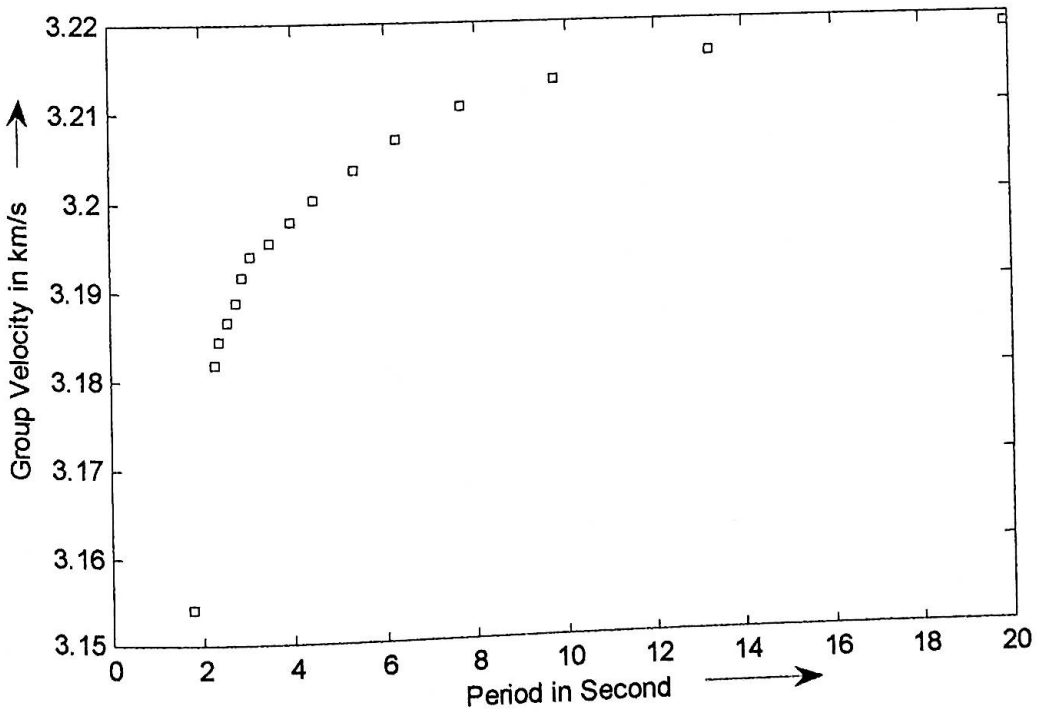
Fig. 5.5 Dispersion curve using the model parameters of table 5.2
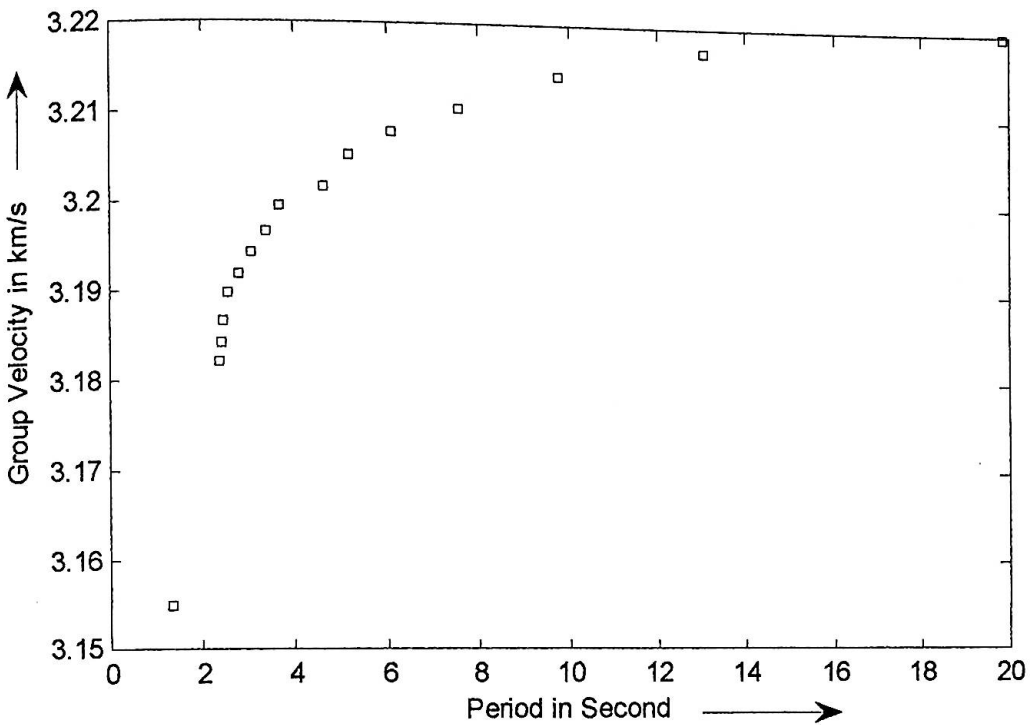
Fig. 5.6 Dispersion curve using the model parameters of table 5.3

5.7 Geological Interpretation from Dispersion Curves

. The dispersion curve can be prepared with in theoretically and experimentally and hence it is possible to interpret these curves in order to estimate the crustal structure. The structure of the earth's crust in any region is investigated using the dispersion properties of surface wave. Theoretical dispersion curves are computed for various crustal models by using the modified Haskell matrix method. The structure that fits the surface wave dispersion equally well is characterized by a particular thickness of the crust. In order to good fit between the experimental and theoretical dispersion curves indirect modelling technique is used. In this technique at first a model is selected abruptly with four parameters, they are P wave velocity (α), S wave velocity (β), density (ρ) and thickness (d) and the theoretical dispersion curve has been constructed. To improve the agreement between the theoretical and experimental dispersion curves, model parameters have been modified to generate a new theoretical dispersion curve. These parameters are varied until the best fit has obtained with the experimentally dispersion curves. For the geological interpretation from the theoretical dispersion curves, the sensitivity of the model parameters have also been studied.

5.8 Sensitivity of Model Parameters

The phase velocity and group velocity of the Surface wave are the function of four parameters which are P wave velocity (α), S wave velocity (β), density of geologic formations (ρ), and layer thickness (d) (Xia et al., 1999). Each of the parameters contributes to the dispersion curve. In order to show the sensitivity of the above four major earth's model parameters, an initial earth model has been considered as shown in Table 5.4. The group velocities have been computed with the change of individual layer parameters.

Table1 5.4: Initial Earth model parameters

Layer number	α (km/s)	β (km/s)	ρ (gm/cc)	d (km)
1	5.47	3.16	2.52	2.0
2	5.63	3.25	2.57	12.0
3	5.89	3.4	2.65	8.0
Half-space	6.1	3.53	2.72	Infinite

5.8.1 P wave velocity

When the P wave velocities are changed with respect to the initial earth's model, the group velocities have been also changed. A 4% increase in P wave velocities represents an average group velocities change of 1.82% .The initial and the changed group velocity dispersion curves are shown in Fig. 5.7.

5.8.2 S wave velocity

It is observed that the variations in S-wave velocities have a dramatic effect on surface wave group velocities. When the S-wave velocities are changed by 4% in the model (Table 5.4), an average change of 10.68% in group velocity is observed. The dispersion curve is presented in Fig. 5.8.
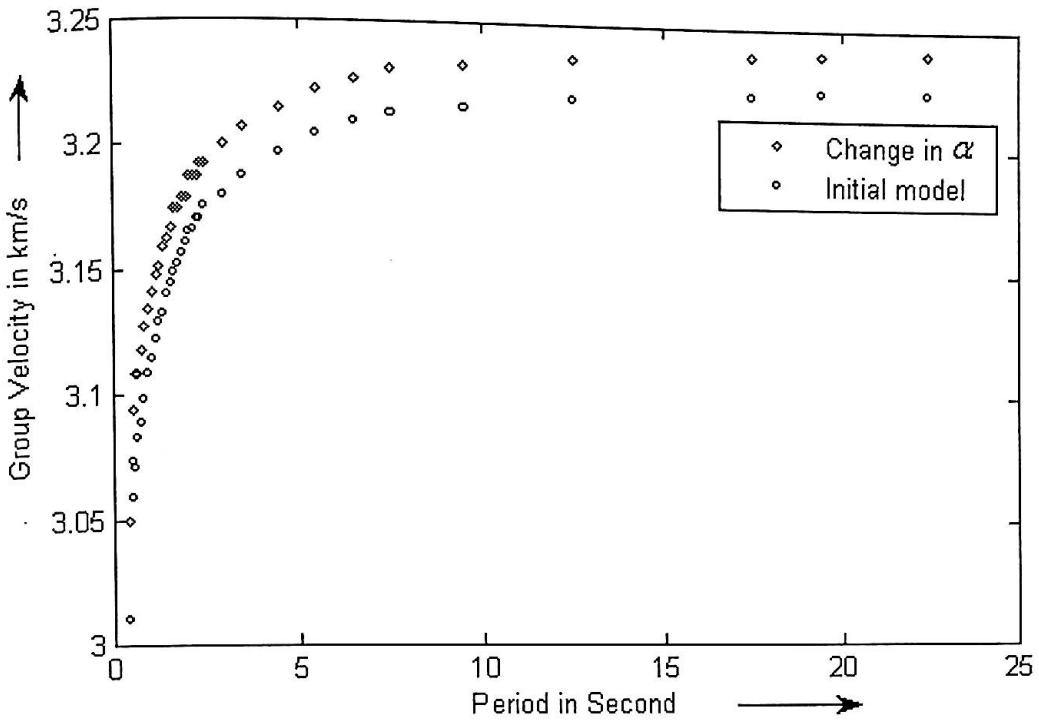
Fig. 5.7 Group velocity dispersion curve with 4% changes in P wave velocity (Table 5.4).
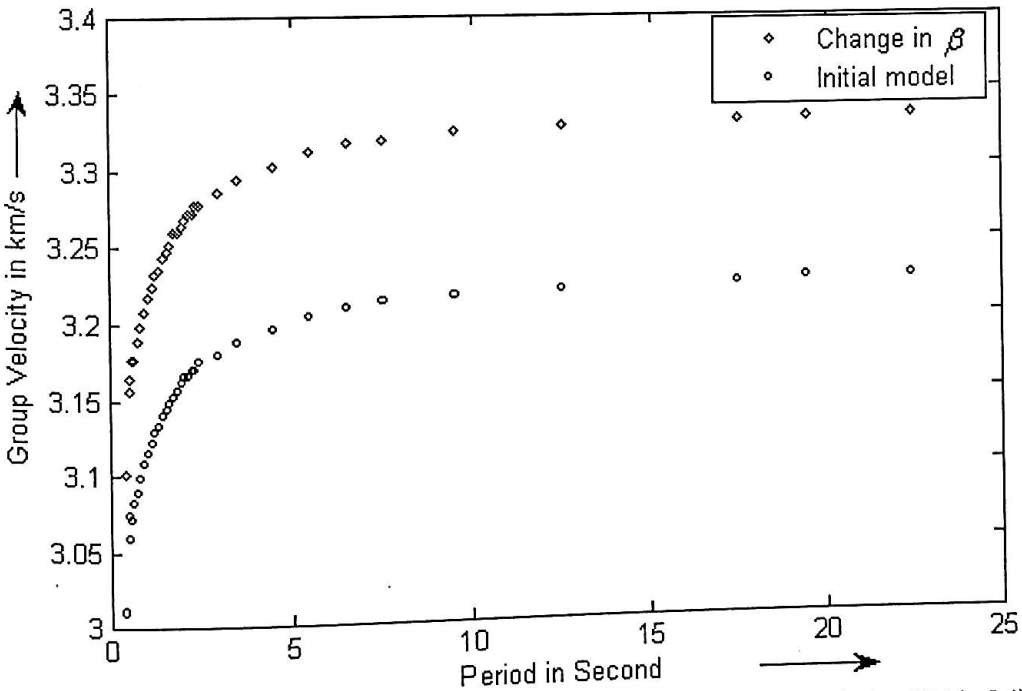
Fig. 5.8 Group velocity dispersion curve with 4% changes in S wave velocity (Table 5.4).

5.8.3 Density of geologic formation

Changes of density of geologic formations have less significant effect in the dispersion curve. A 4% increase in densities represents the average group velocity

changes only 0.11%. The dispersion curve with changing densities is depicted in Fig. 5.9.
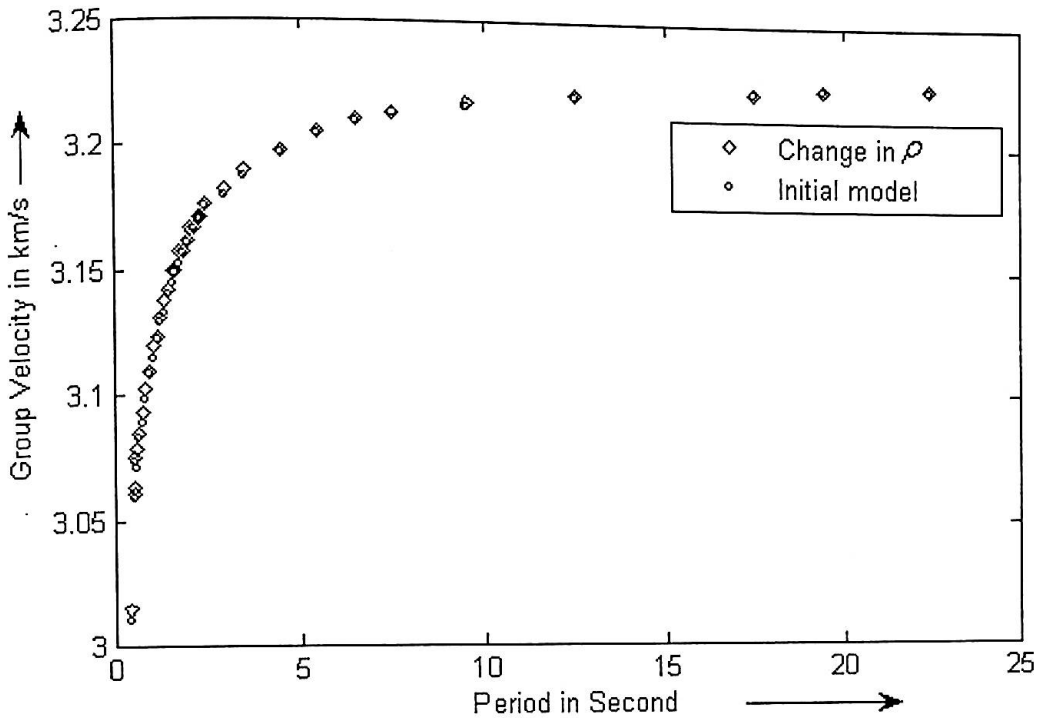
Fig. 5.9 Group velocity dispersion curve with 4% changes in density (Table5.4).

5.8.4 Thickness of crustal structure

When the layer thicknesses are changed from the initial earth's model, the group velocities have also been a little changed. Average group velocity is decreased in 0.1% due to an increase of 4% layer thicknesses. The dispersion curve is shown in Fig. 5.10.

Effects of the 4% change in S wave velocities are quite noticeable in comparison to similar changes in P wave velocity (Figs. 5.7-5.8). The significant change in density has very subtle effect on group velocity (Fig. 5.9).The effect of layer thicknesses on surface wave group velocities can be minimized by dividing the sub-surface into thinner layers within each unique and constant S wave interval velocity.

From the above analysis it can be said that the group velocity increases with the increase of S wave velocity, P wave velocity and density of geologic formations, but decreases with increasing layer thickness. The S wave velocity is the most effective parameter in the change of group velocity for this particular type model.
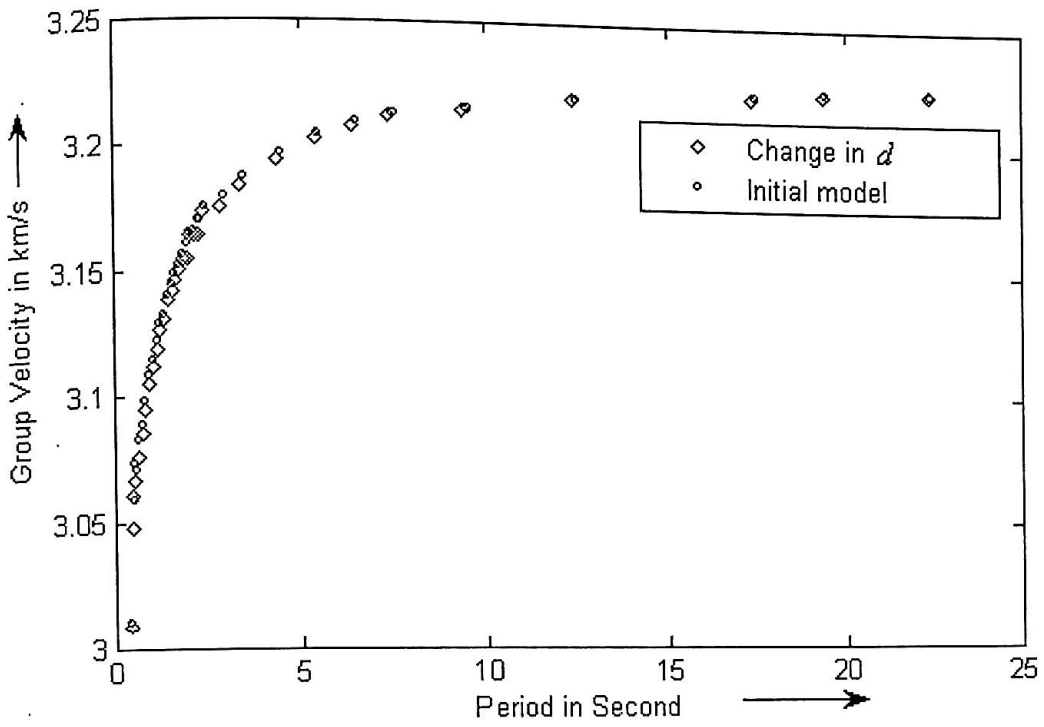
Fig. 5.10 Group velocity dispersion curve with 4% changes in thickness (Table 5.4).

Fig. 5.11 represents the change of group velocity with the change of four layers parameter.
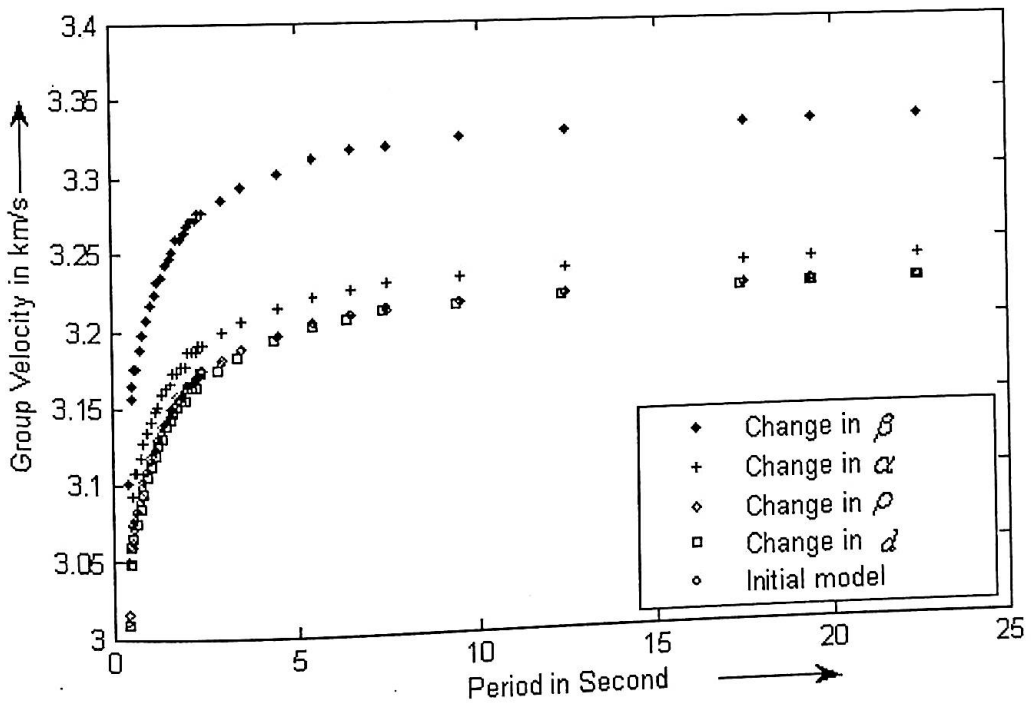
Fig. 5.11 Dispersion curves with change four layer parameters (Table 5.4).

5.9 Suitable Model for Crustal Structure

The earth model which predicts theoretical dispersion in best agreement with the experimental dispersion is assumed to represent actual earth structure. Dispersion measurements are compiled in the form of a dispersion curves. This curve is compared with the theoretical dispersion curves calculated for layered earth models. The model of the theoretical dispersion agrees closely with the experimental dispersion curve is assumed to represent actual earth structure.

To determine the suitable model for crustal structure, a statistical comparison is performed between experimental and theoretical dispersion curves. Comparisons of experimental and theoretical curves in this study are expressed in terms of some statistical calculation.

Chapter 6
Crustal Structure from Models

6.1 Introduction

The crust of the earth is composed of a great variety of igneous, metamorphic and sedimentary rocks. There exist different layers with different physical properties. When an earthquake occurred within the crust, seismograms are created and recorded at seismograph. Observed seismograms are a combination of source radiation, propagation path effects and recording instruments effects. Seismograms can be used to analyze the subsurface geology in two ways: by direct and indirect modelling techniques, which are commonly used in the determination of the earth's interior from seismic surface wave dispersion. The most widely used modelling technique is an indirect trial-and-error procedure in which dispersion is computed for models in an effort to duplicate experimental dispersion. Theoretically exact methods for the computation of dispersion have been presented by Haskell (1953) and Alterman et al. (1959). Since the relationship between phase and / or group velocities at a given frequency and the properties of the propagation path is not simple, a numerical procedure is supposed to be performed to compute one from the other to invert for the earth model. An implicit theoretical relationship exits between wave-type, mode, phase and group velocities and structural earth parameters such as P wave velocity (α), S wave velocity (β), density (ρ) and layer thickness (d).

Seismic surface wave modelling has been performed to observe the crustal structure. In order to do so, group velocity of surface wave has been computed and dispersion curve has also been drawn. Dispersion curves have been made one after another until the signal power fit (SPF) close to the 100%. This process has been performed by the trial and error basis. Many models are produced but few of the models were found statistically close to the real condition. In order to select the best model some statistical calculations and data fit criterion have been performed. Three types of

crustal structure are selected from the error estimations. Finally, crustal structure of the study area the south-eastern region of Bangladesh has been determined.

6.2 Estimation of Group Velocity form Earthquake Data of the Study Area

According to earthquake data (Figs. 3.3, 3.6 and 3.9) and earthquake source parameters (Table 3.3) deferent group velocities are computed and group velocity versus period curves are constructed. The dispersion curves are shown in the Figs. 6.1-6.3 which are made by graphical method.
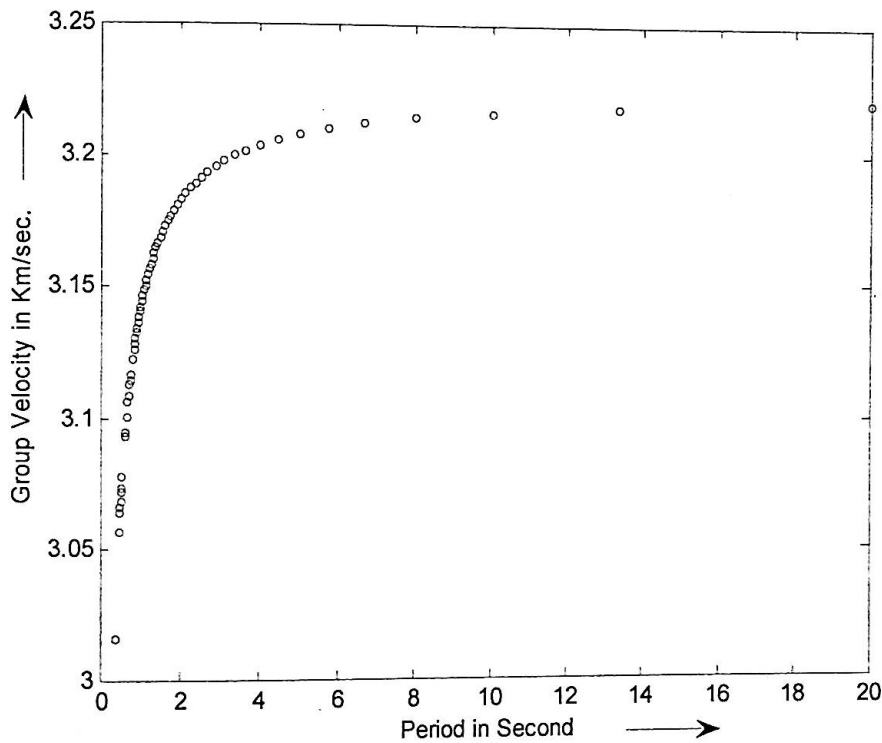
Fig. 6.1 Group velocity dispersion curve for the south-west of Daluchari, Chittagong earthquake data.

6.3 Estimation of Group Velocity from Crustal Models

In order to estimate the group velocity from crustal model, sixteen models are considered Model based group velocity has been computed using modified Haskell matrix method (Eqns. 5.4-5.10) with phase and group velocity relation (Eqn. 5.13). The experimental and theoretical dispersion curves and corresponding model parameters are presented for different data set.
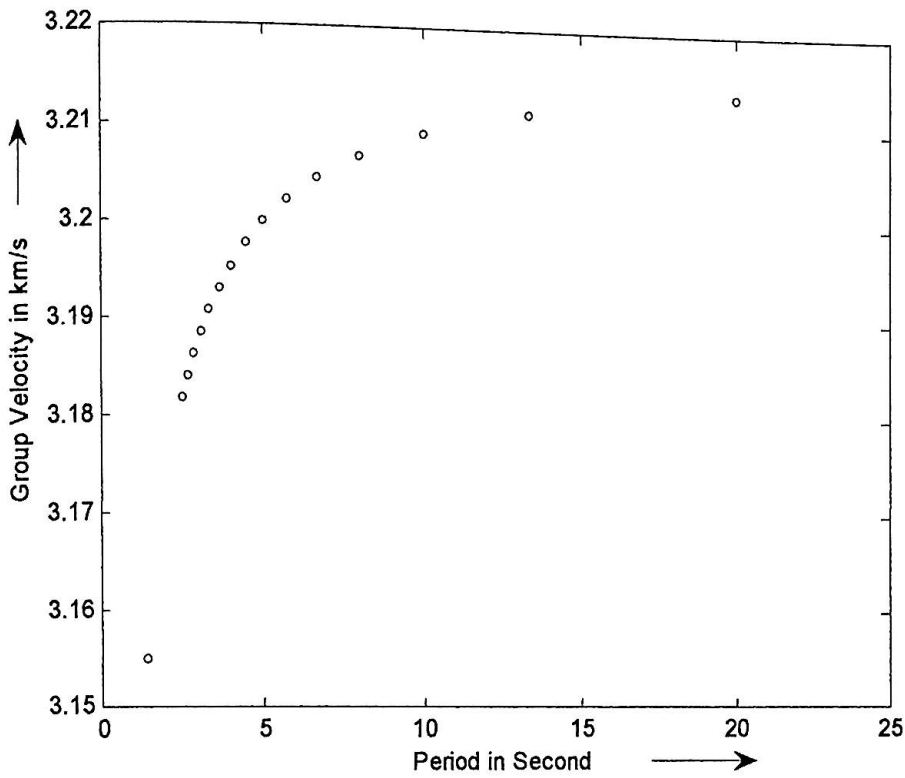
Fig. 6.2 Group velocity dispersion curve for Kolabunia, Chittagong earthquake data.
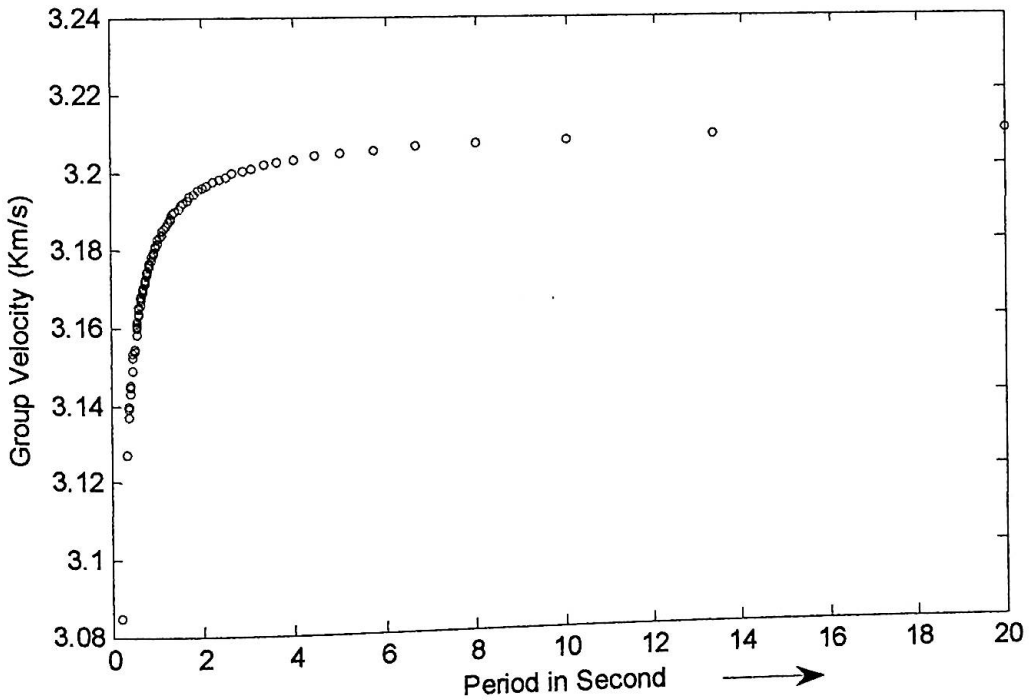
Fig. 6.3 Group velocity dispersion curve for the south of Meiktila, Myanmar earthquake data.

For estimation of group velocity dispersion curve of Daluchari earthquake data, four different models are considered. Statistical analyses have been performed to

determine the approximate actual crustal structure. Group velocity estimation of Daluchari, Chittagong earthquake data are presented in Figs. 6.4-6.7.
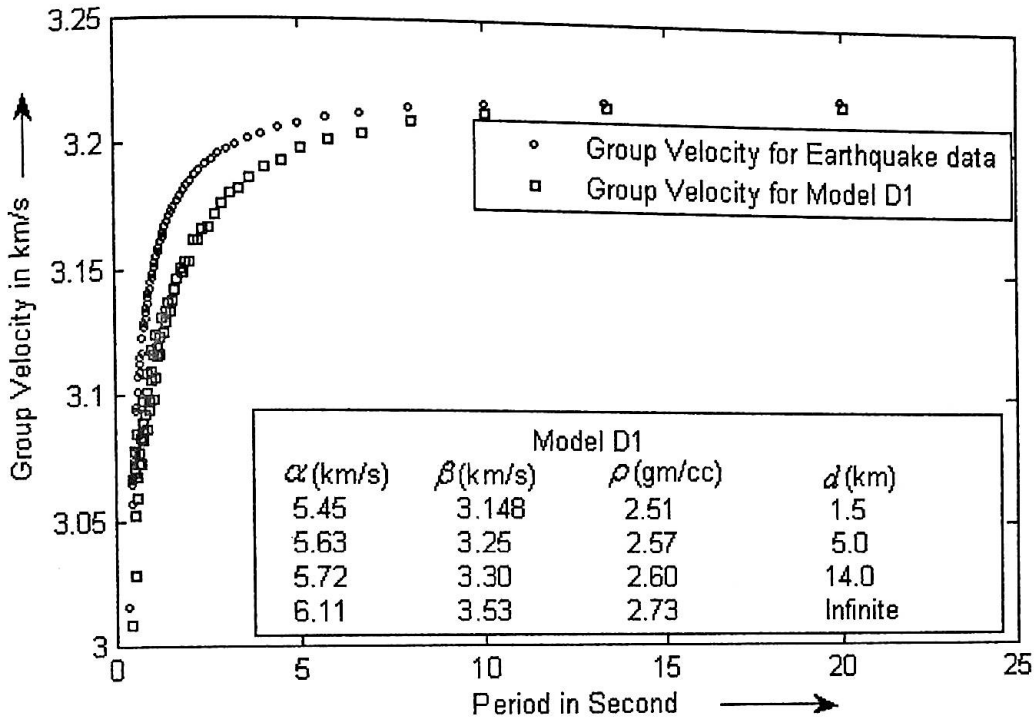
Fig. 6.4 The experimental and theoretical group velocity dispersion curves for the south-west of Daluchari, Chittagong earthquake data and model D1 respectively.
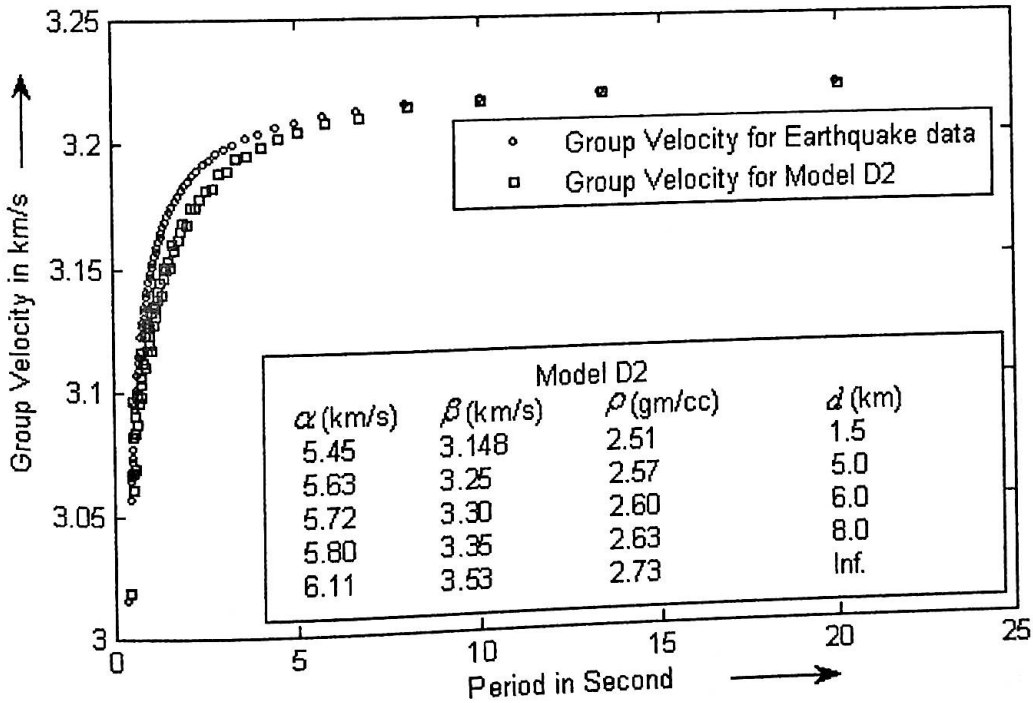
Fig. 6.5 The experimental and theoretical group velocity dispersion curves for the south-west of Daluchari, Chittagong earthquake data and model D2 respectively
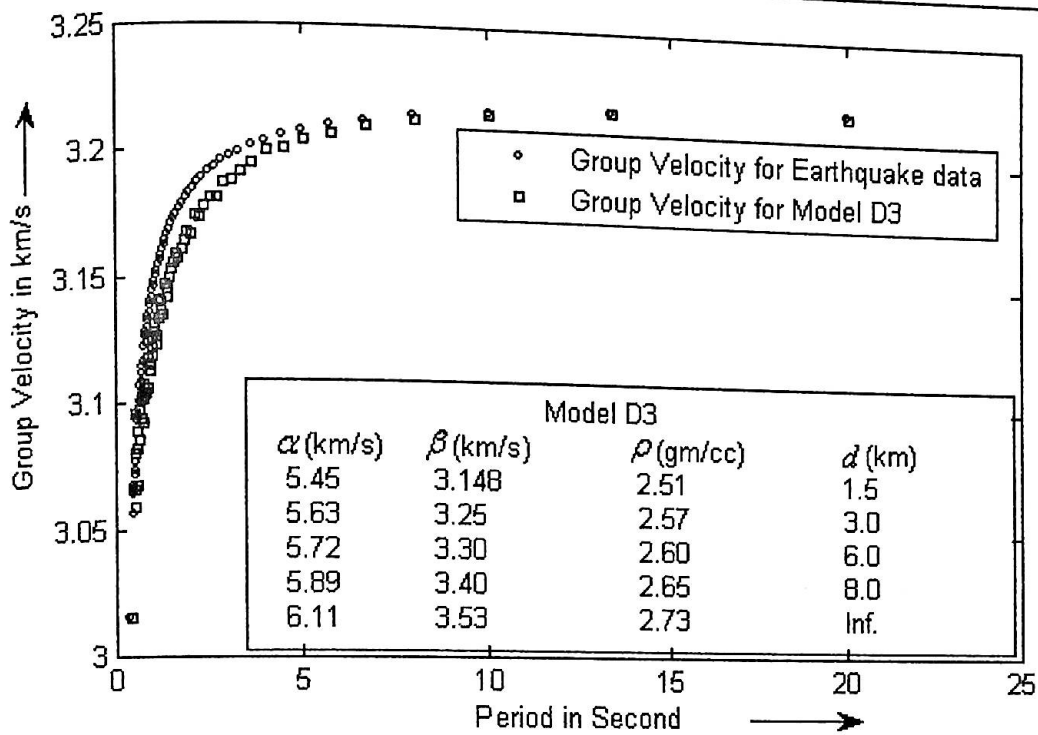
Fig. 6.6 The experimental and theoretical group velocity dispersion curves for the south-west of Daluchari, Chittagong earthquake data and model D3 respectively.
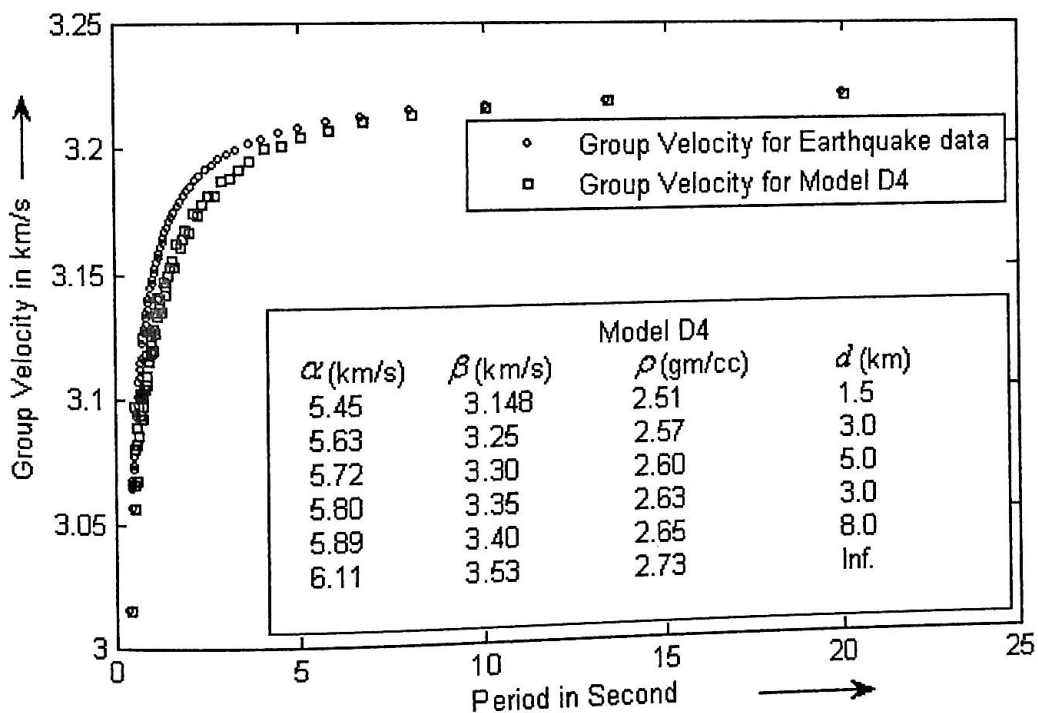
Fig. 6.7 The experimental and theoretical group velocity dispersion curves for the south-west of Daluchari, Chittagong earthquake data and model D4 respectively.

Six models have been considered to estimate the group velocity dispersion curve of the Kolabunia earthquake data. In order to minimize the error between the dispersion curves, model parameters have been changed and finally the crustal structure is

determined. The group velocity estimation of Kolabunia, Chittagong earthquake data are presented in Figs.6.8-13.
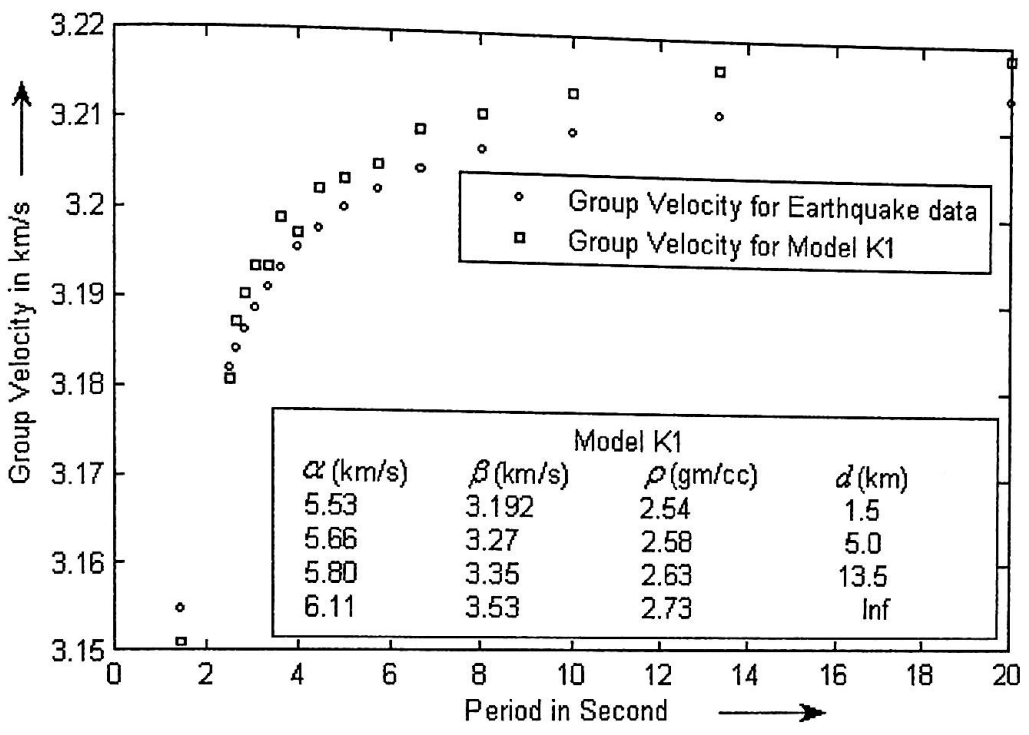
Fig. 6.8 The experimental and theoretical group velocity dispersion curves for Kolabunia, Chittagong earthquake data and model K1 respectively.
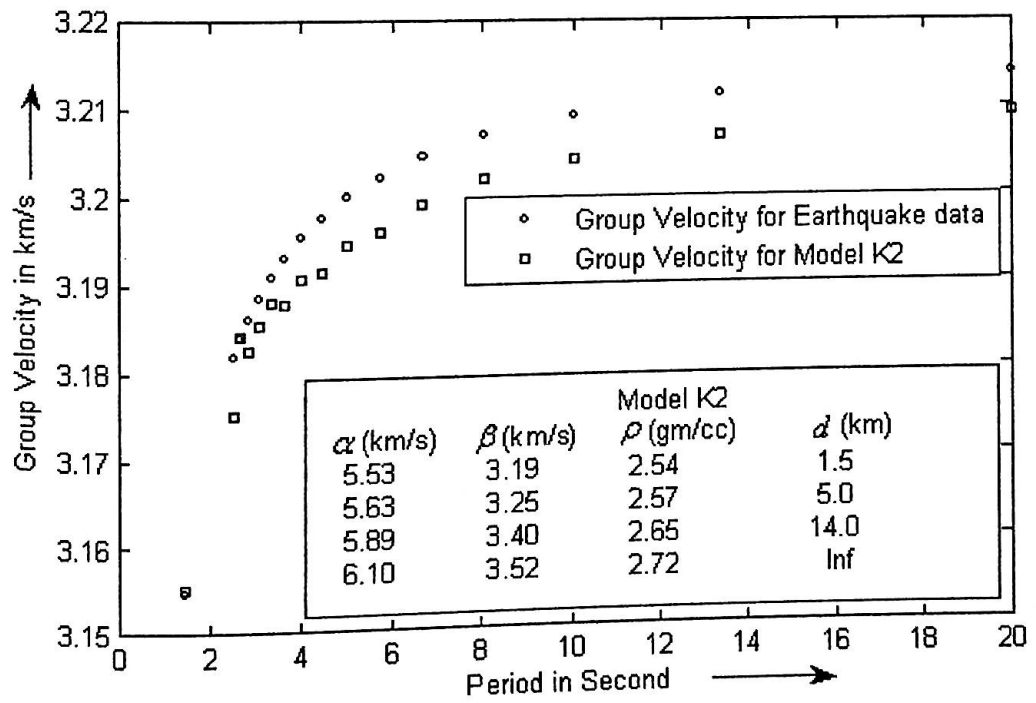
Fig. 6.9 The experimental and theoretical group velocity dispersion curves for Kolabunia, Chittagong earthquake data and model K2 respectively.
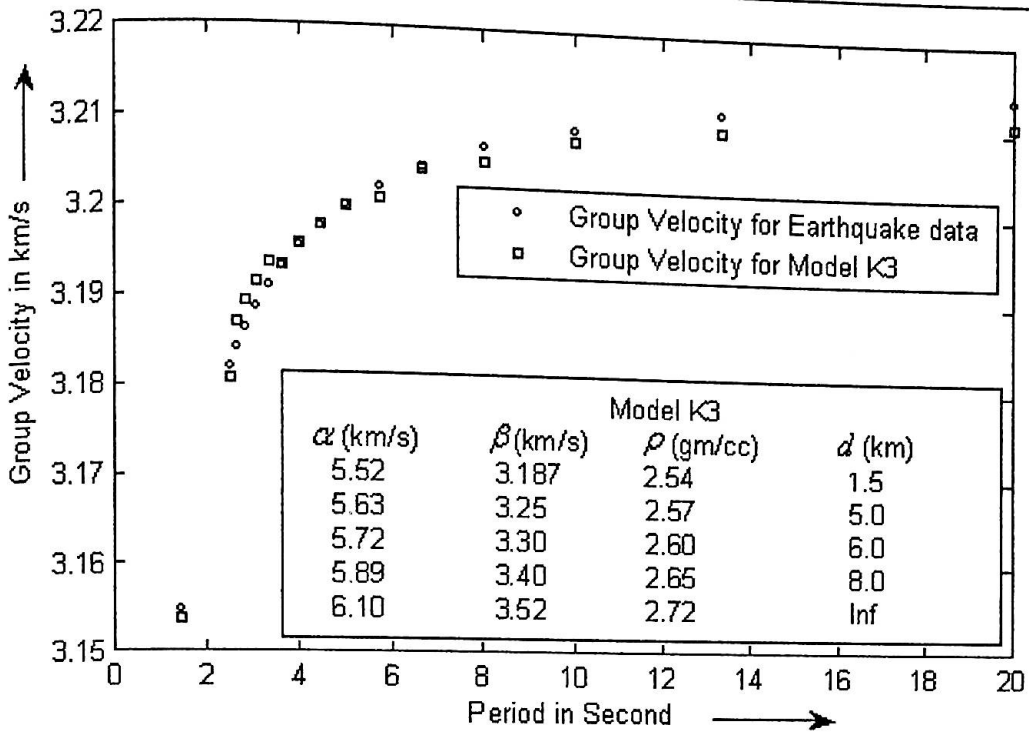
Fig. 6.10 The experimental and theoretical group velocity dispersion curves for Kolabunia, Chittagong earthquake data and model K3 respectively.

Model K3

α (km/s)	β (km/s)	ρ (gm/cc)	d (km)
5.52	3.187	2.54	1.5
5.63	3.25	2.57	5.0
5.72	3.30	2.60	6.0
5.89	3.40	2.65	8.0
6.10	3.52	2.72	Inf

Fig. 6.11 The experimental and theoretical group velocity dispersion curves for Kolabunia, Chittagong earthquake data and model K4 respectively.

Model K4

α (km/s)	β (km/s)	ρ (gm/cc)	d (km)
5.52	3.187	2.54	1.5
5.63	3.25	2.57	5.0
5.72	3.30	2.60	6.0
5.89	3.40	2.65	7.75
6.10	3.52	2.72	Inf

111

Fig. 6.12 The experimental and theoretical group velocity dispersion curves for Kolabunia, Chittagong earthquake data and model K5 respectively.

α (km/s)	β (km/s)	Model K5 ρ (gm/cc)	d (km)
5.52	3.187	2.54	1.5
5.63	3.25	2.57	3.0
5.72	3.30	2.60	5.0
5.80	3.35	2.63	6.0
5.89	3.40	2.65	8.0
6.10	3.52	2.72	Inf

Fig. 6.13 The experimental and theoretical group velocity dispersion curves for Kolabunia, Chittagong earthquake data and model K6 respectively

α (km/s)	β (km/s)	Model K6 ρ (gm/cc)	d (km)
5.52	3.187	2.54	1.5
5.63	3.25	2.57	3.0
5.72	3.30	2.60	5.0
5.80	3.35	2.63	3.0
5.89	3.40	2.65	8.0
6.10	3.52	2.72	Inf

The south of Meiktila, Myanmar earthquake data have also been used to study the crustal structure of the investigated area. In this regard six models have been considered to obtain the theoretical group velocity dispersion curves. The statistical

calculations of Mean Residual (MR), Average absolute Residual (AR), weighted Root Mean Square error (RMS) and the percent of Signal Power Fit (SPF) are taken into account to estimate the actual crustal structure. Models and curves are depicted in Figs. 6.14-6.19

α (Km/s)	β (Km/s)	ρ (gm/cc)	d (Km)
5.49	3.17	2.53	1.5
5.63	3.25	2.57	2.0
5.72	3.30	2.60	2.5
5.80	3.35	2.63	2.5
5.89	3.40	2.65	3.0
6.10	3.52	2.72	Inf.
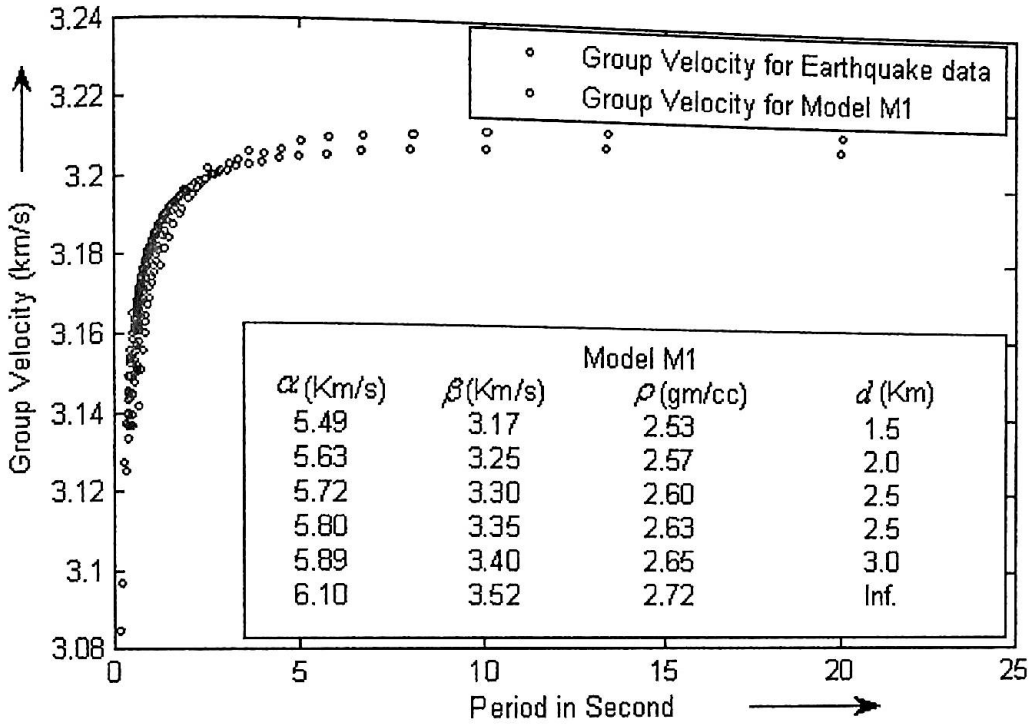
Fig. 6.14 The experimental and theoretical group velocity dispersion for the south of Meiktila, Myanmar earthquake data and model M1 respectively.

α (Km/s)	β (Km/s)	ρ (gm/cc)	d (Km)
5.49	3.17	2.53	1.5
5.63	3.25	2.57	2.0
5.72	3.30	2.60	2.5
5.80	3.35	2.63	3.0
5.89	3.40	2.65	3.5
6.10	3.52	2.72	Inf.
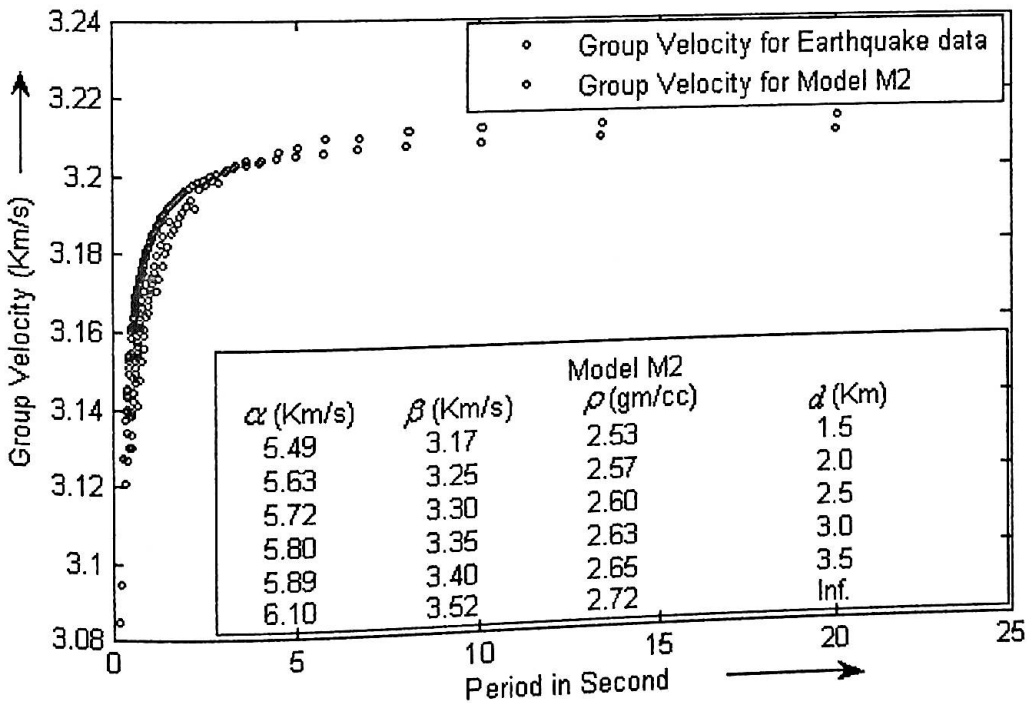
Fig. 6.15 The experimental and theoretical group velocity dispersion for the south of Meiktila, Myanmar earthquake data and model M2 respectively.

113

Model M3

α (Km/s)	β (Km/s)	ρ (gm/cc)	d (Km)
5.48	3.165	2.52	1.5
5.63	3.250	2.57	3.0
5.80	3.350	2.63	3.0
5.89	3.400	2.65	3.0
6.09	3.720	2.72	Inf.
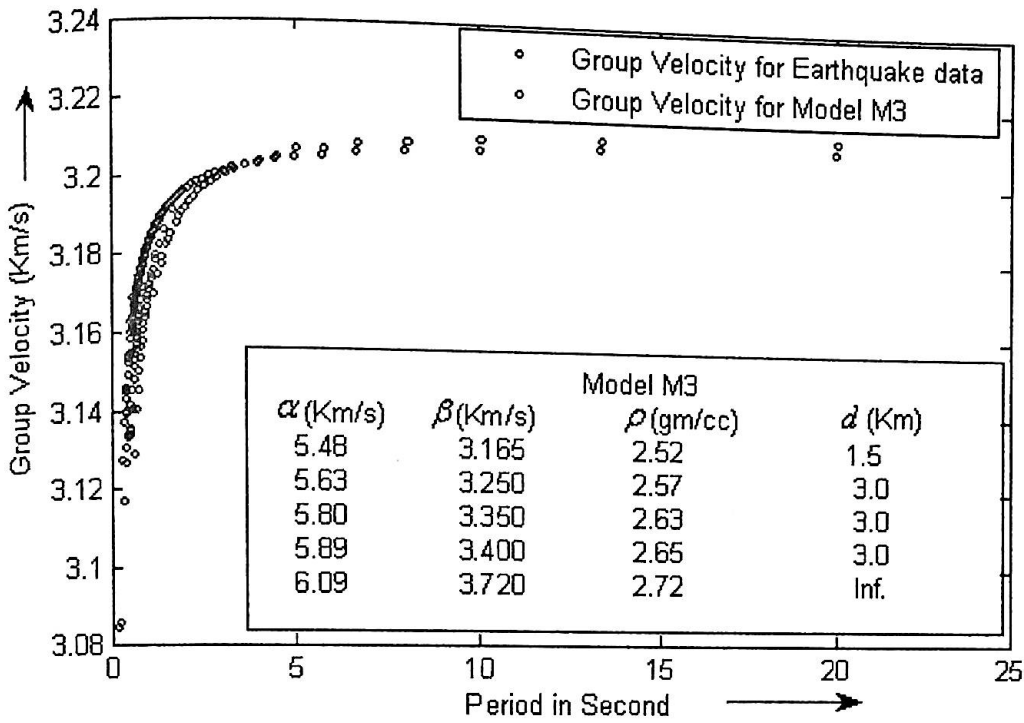
Fig. 6.16 The experimental and theoretical group velocity dispersion for the south of Meiktila, Myanmar earthquake data and model M3 respectively.

Model M4

α (Km/s)	β (Km/s)	ρ (gm/cc)	d (Km)
5.49	3.17	2.53	1.5
5.66	3.27	2.58	3.5
5.75	3.32	2.61	3.0
5.80	3.35	2.63	3.0
6.10	3.52	2.72	Inf.
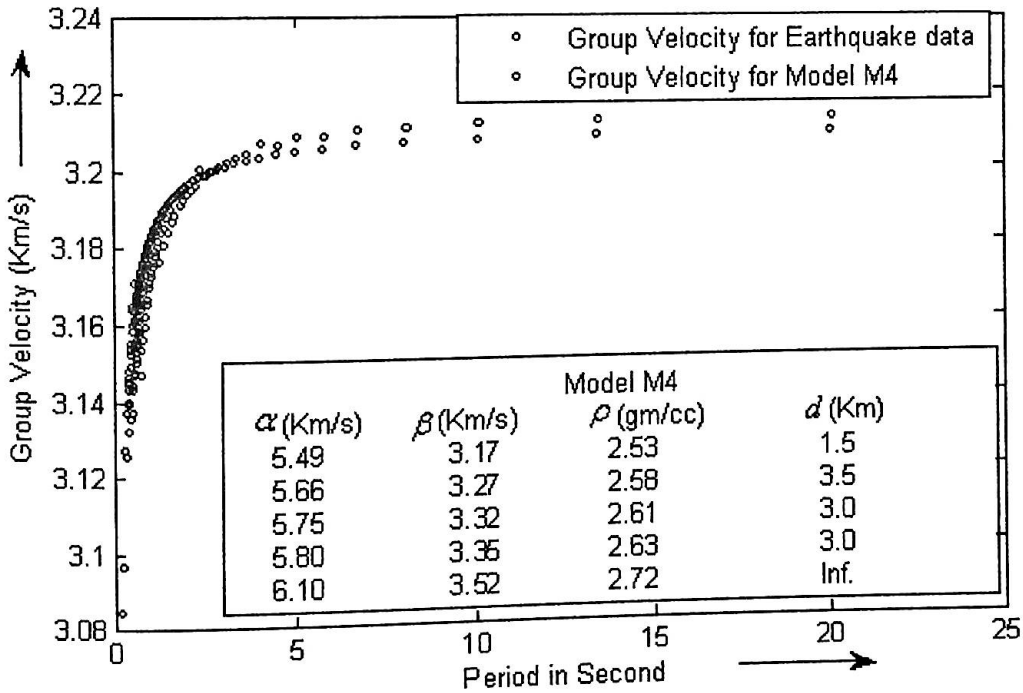
Fig. 6.17 The experimental and theoretical group velocity dispersion for the south of Meiktila, Myanmar earthquake data and model M4 respectively

114
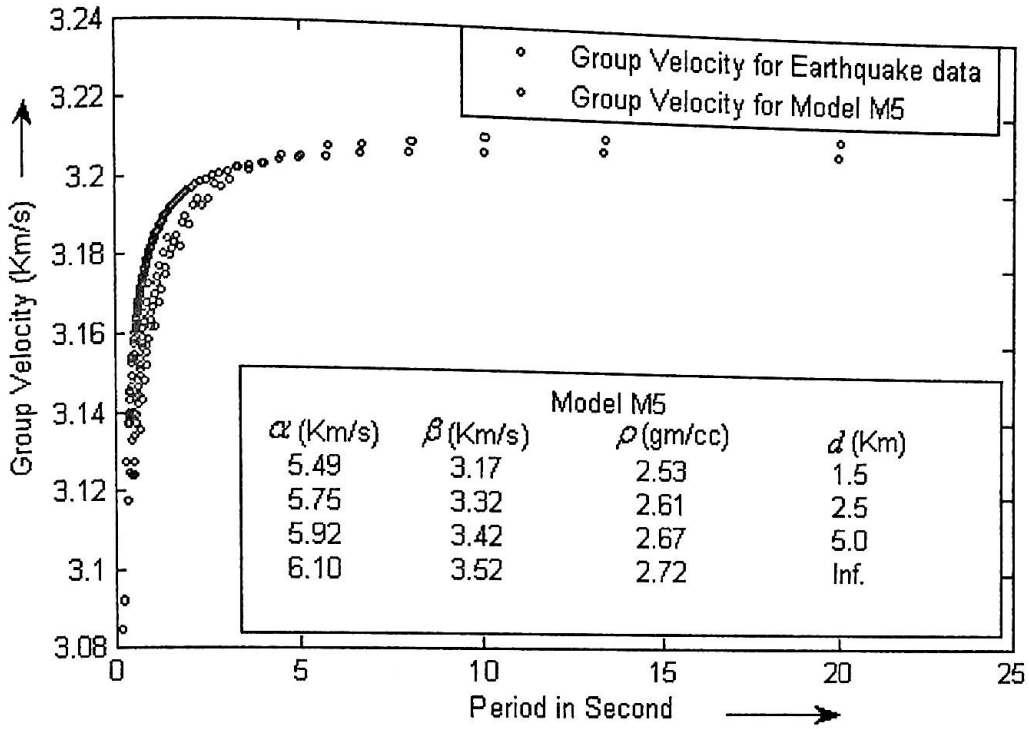
Fig. 6.18 The experimental and theoretical group velocity dispersion for the south of Meiktila, Myanmar earthquake data and model M5 respectively.

Model M5

α (Km/s)	β (Km/s)	ρ (gm/cc)	d (Km)
5.49	3.17	2.53	1.5
5.75	3.32	2.61	2.5
5.92	3.42	2.67	5.0
6.10	3.52	2.72	Inf.

Fig. 6.19 The experimental and theoretical group velocity dispersion for the south of Meiktila, Myanmar earthquake data and model M6 respectively.

Model M6

| α (Km/s)	β (Km/s)	ρ (gm/cc)	d (Km)
5.49	3.17	2.53	1.5
5.72	3.30	2.60	3.5
5.80	3.35	2.63	6.0
6.10	3.52	2.72	Inf.

115

6.4 Error Estimation

The aim of the current research is to study the shallow crustal structure of depth 23.5 km.

The S-wave velocities of the layers are free to change during the inversion. Consequently, the P-wave velocities are estimated using the relation $\alpha : \beta = 1 : 1.732$. Poisson's ratio (σ) in each layer was assumed to be .25 and the densities (ρ) are calculated applying the relation $0.32\alpha + 0.77$ (Ammon et al., 1990). Starting from initial estimates, the model parameters are iteratively improved until a good fit between the theoretical and experimental dispersion curves is obtained. During the inversion, a number of criteria were adapted to calculate the goodness of fit. These criteria are the standard error of estimate (SE), mean residual (MR), average absolute residual (AR), weighted root mean square error (RMS) and the percent of signal power fit (SPF). The mathematical relations used to compute the above statistical criteria are (Elenean et al., 2009):

$$SE = \sqrt{\frac{\sum_{i=1}^{N}(obs_i - mean)^2}{N-1}} \qquad \qquad 6.1$$

$$MR = \frac{\sum_{i=1}^{N}(obs_i - pred_i)}{N} \qquad \qquad 6.2$$

$$AR = \frac{1}{N}\left|\sum_{i=1}^{N}\frac{(obsi - predi)}{SE}\right| \qquad \qquad 6.3$$

$$RMS = \sqrt{\frac{\sum_{i=1}^{N}\frac{(obsi - predi)^2}{mean}}{N(N-1)}} \qquad \qquad 6.4$$

$$SPF = \left(1 - \frac{\left(\sum_{i=1}^{n}(obs_i - pred_i)\right)^2}{\sum_{i=1}^{N}(obs_i)^2}\right) X\,100 \qquad \qquad 6.5$$

Where 'obs' is the observed group velocity at each period, 'mean' is the mean of the observed group velocities, N is the number of observations at each period and 'pred' is the predicted group velocity of the current model. Estimated errors of the models are shown in table 6.1.

Table 6.1: Data fit criteria

Event Name	Model Name	SE	MR	AR	RMS (Km/s)	SPF (%)
26 July, 2003 SW of Daluchari, Chittagong Earthquake	D1	0.014983	0.022282	0.467639	0.001818	99.99339005
	D2	0.014983	0.008293	0.174056	0.000930	99.99826955
	D3	0.014983	0.009274	0.194643	0.000960	99.99815561
	D4	0.014983	0.009156	0.192216	0.000971	99.99811184
27 July, 2003 Kolabunia in Chittagong Earthquake	K1	0.014570	0.003179	0.218205	0.000575	99.9998444
	K2	0.014570	0.004246	0.291435	0.000676	99.9997851
	K3	0.014570	-.000055	0.003779	0.000259	99.9999684
	K4	0.014570	-.000283	0.019491	0.000264	99.9999670
	K5	0.014570	0.001013	0.069532	0.000260	99.9999680
	K6	0.014570	-.000704	0.048350	0.000300	99.9999574
21 September, 2003 S of Meiktila, Myanmar Earthquake	M1	0.022189	0.004040	0.182086	0.000503	99.9993866
	M2	0.022189	0.007497	0.337870	0.000673	99.9988432
	M3	0.022189	0.007818	0.352356	0.000688	99.9987911
	M4	0.022189	0.004002	0.180396	0.000490	99.9993549
	M5	0.022189	0.010629	0.479041	0.000861	99.9981079
	M6	0.022189	0.013365	0.602346	0.001019	99.9973480

6.5 Crustal Structure of South East Bangladesh from Models

The earthquake data of Daluchari, Kolabunia of Chittagong and Myanmar are processed and analyzed to study the crustal structure of south-eastern region of Bangladesh. Models for the different data sets are considered for computing the theoretical dispersion curves and the best fitting with the experimental dispersion curve yields the layer parameters of the curstal structure.

Considering the data fit criterion model D2, model K3 and model M4 might be considered as the shallow crustal structure of south-eastern Bangladesh. Finally it

could be said that model D2 / K3 and model M4 are representing the variation of crustal structure.
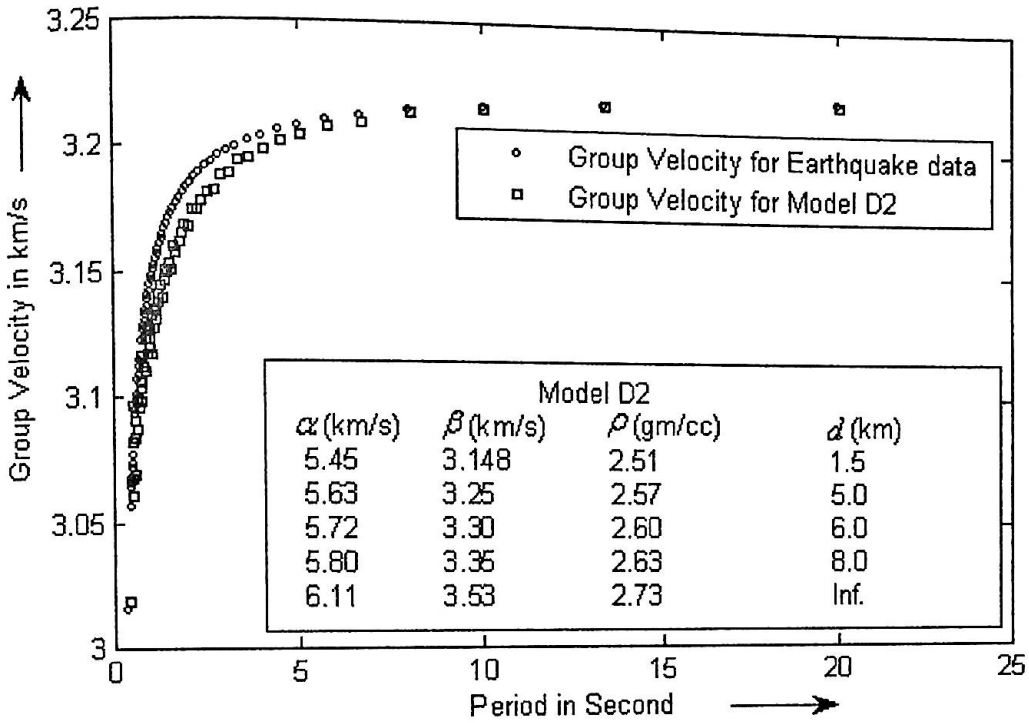
Fig. 6.20 The experimental and theoretical group velocity dispersion curves for the south-west of Daluchari, Chittagong earthquake data and model D2 respectively

Fig. 6.21 The experimental and theoretical group velocity dispersion curves for Kolabunia, Chittagong earthquake data and model K3 respectively.
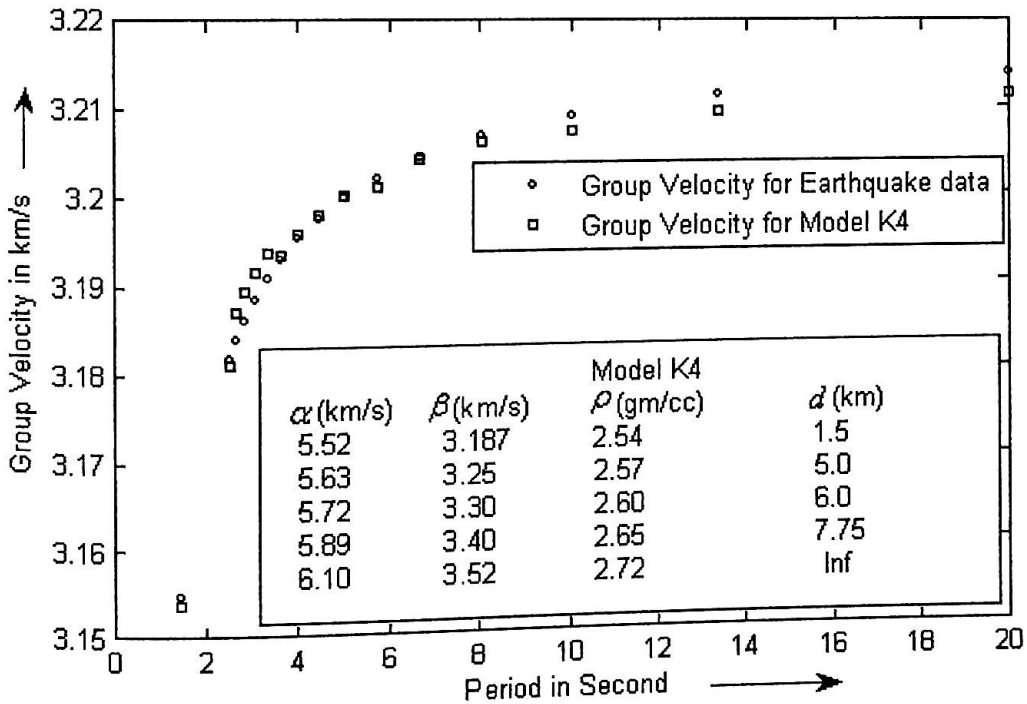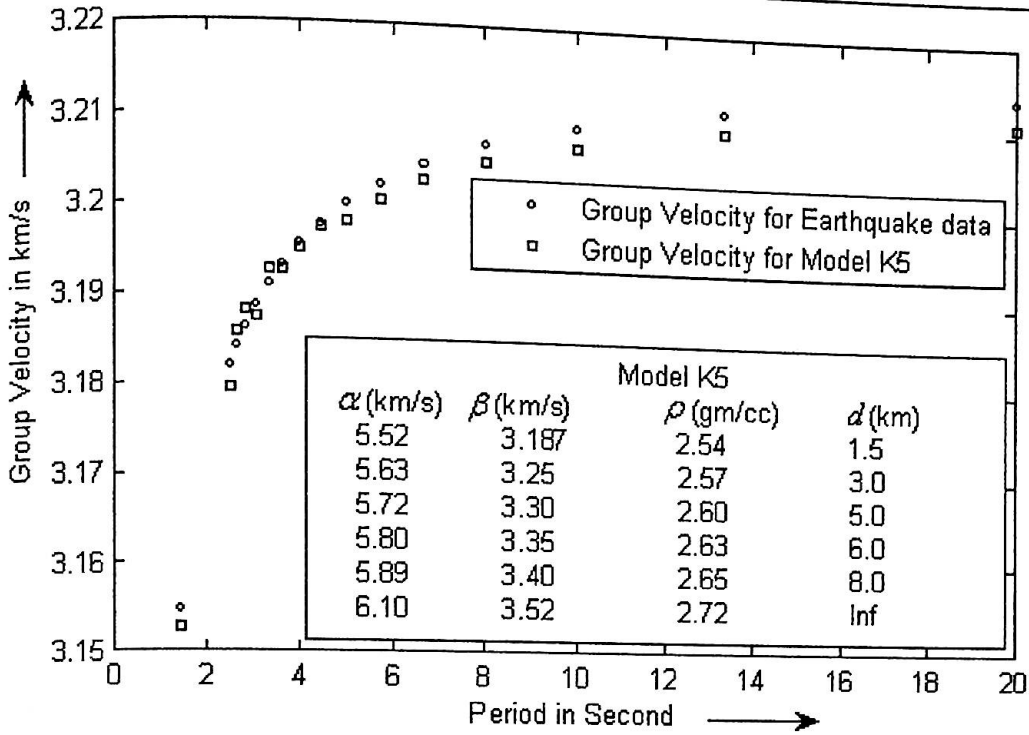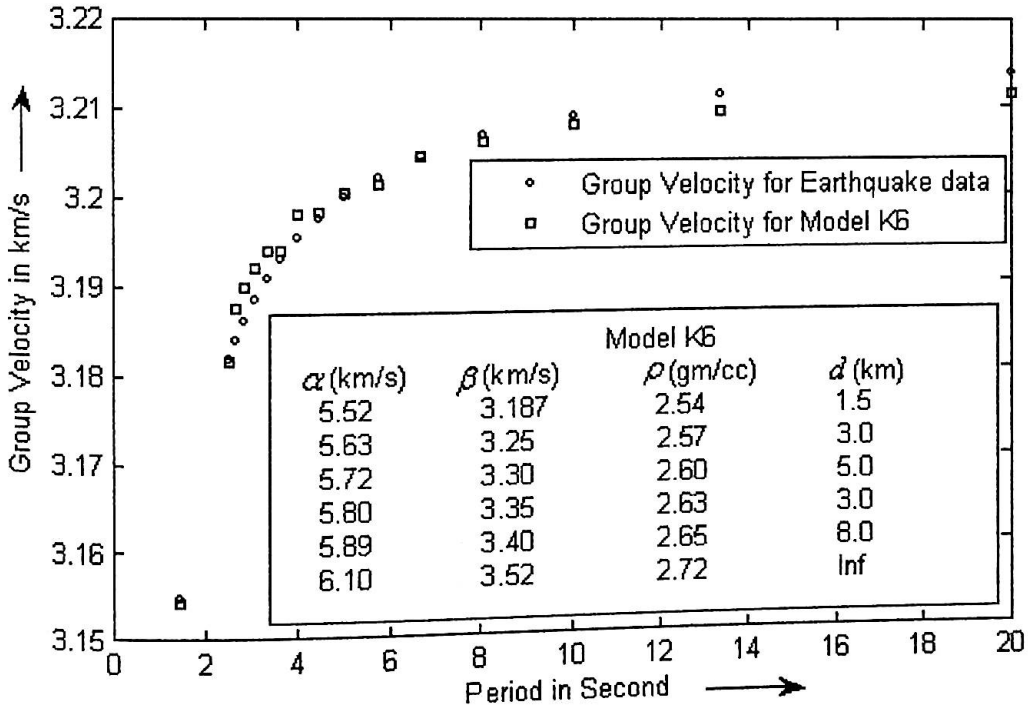
118

The figure contains the following table within the plot:

		Model M4	
α (Km/s)	β (Km/s)	ρ (gm/cc)	d (Km)
5.49	3.17	2.53	1.5
5.66	3.27	2.58	3.5
5.75	3.32	2.61	3.0
5.80	3.35	2.63	3.0
6.10	3.52	2.72	Inf.

Legend:
o Group Velocity for Earthquake data
o Group Velocity for Model M4

Axes: Group Velocity (Km/s) vs Period in Second
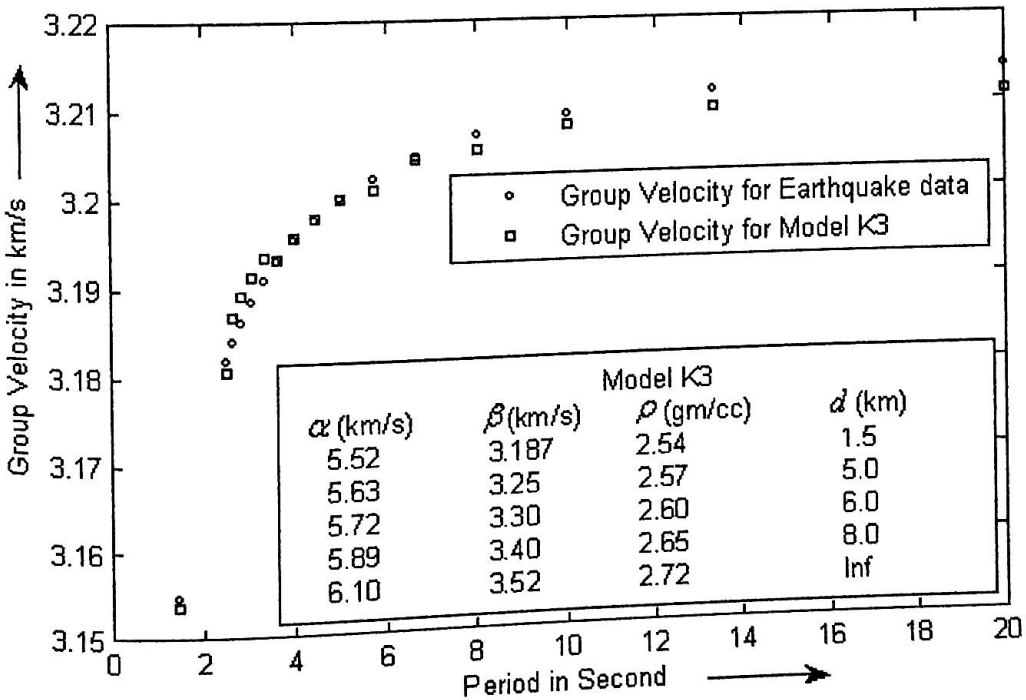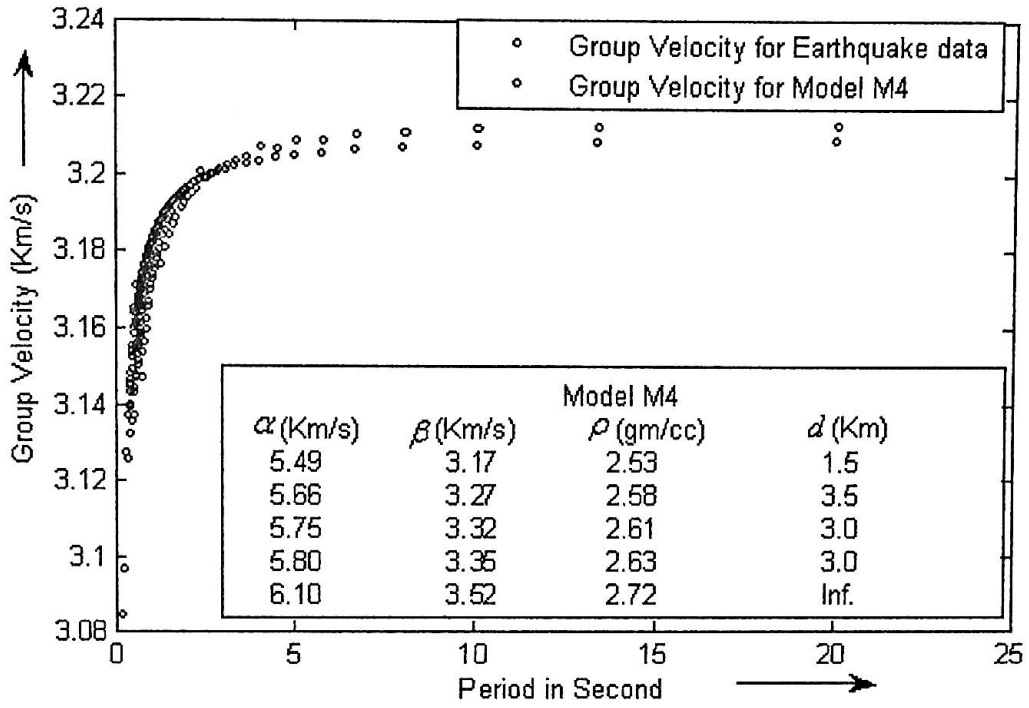
Fig. 6.22 The experimental and theoretical group velocity dispersion for the south of Meiktila, Myanmar earthquake data and model M4 respectively
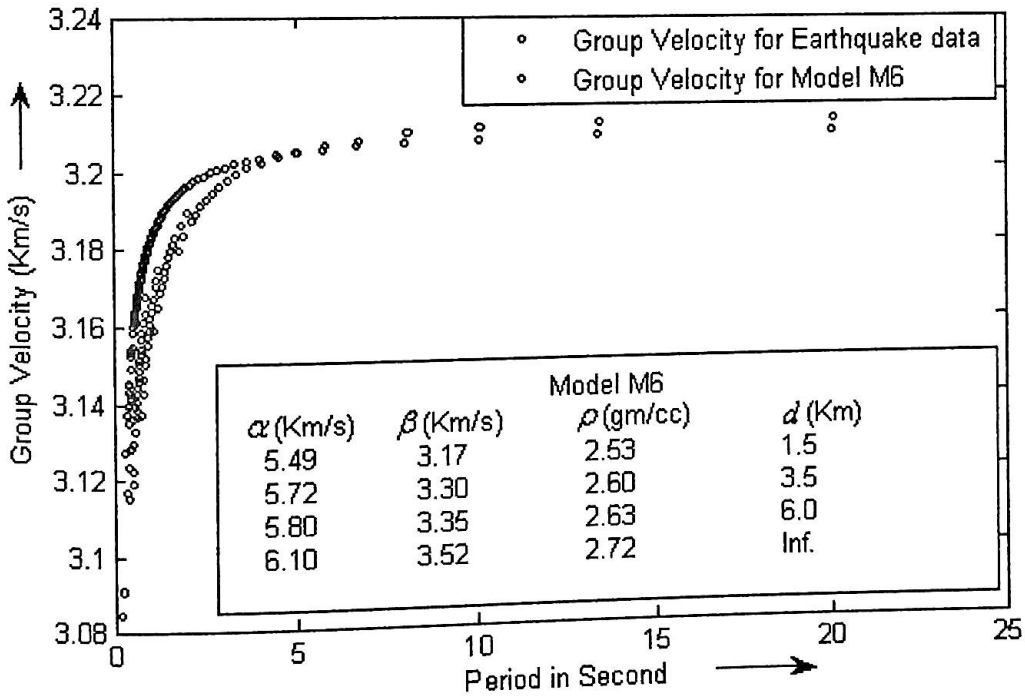
Chapter 7
Results and Discussions

Seismic surface wave analysis and modelling are being performed for studying the crustal structure of the south-eastern region of Bangladesh. The present research work is an effort to focus on the analysis of earthquake data and interpret the crustal structure.

Fig. 4.3 and Fig. 4.4 show that instantaneous frequency can be obtained from the seismic wave. This characteristic of the time frequency analysis is tried to use for the interpretation of geology from the seismological waves. Generally, the phase of a seismic wave will be changed when it propagates to or from one media to another. The changes of frequency with time of real data are to be found in Figs. 4.5-4.13 from the time frequency analysis. Frequency distributions are clearly evident, however, details are limited. The changes of frequencies as obtained in the above figures are not significant to identify the geologic features.

Since the variation of frequency with time does not seem a good characteristic of the earthquake waves, particularly for studying the crustal structure, in which the wave propagated. Amplitude has been tried to add over time frequency analysis and time frequency to amplitude ratio (TFA) has shown a good measure of studying earthquake wave as shown in Figs. 4.16-4.24.

It has been observed that frequency to amplitude ratio with time is different from time amplitude representation. But the analyses show that the frequency to amplitude effects are almost same pattern as recorded the amplitude with time (Figs.3.3-3.11) having one peak value in each case. However, the time position of the peak frequency to amplitude ratio has been shifted to a new time position. Sometimes the peak effects are found delayed. It is realistic to be considered that solely time amplitude plots are not enough to be used for detailed interpretation of the geology. It needs more

analysis and further work to attain interpretation from the point of the characterization of seismic wave. As time frequency to amplitude analysis of synthetic earthquake waves shown in Fig. 4.14 and Fig. 4.15, can be used for the characterization according to frequency to amplitude effects. Hence, time frequency to amplitude analysis of ground motion of seismic wave has been tried to use for studying the crustal structure. As amplitude is changed with time in the recorded seismic waves, another variable frequency of a seismic wave may be changed as media as thought to be dispersive. Although time-frequency analysis is not found more applicable in earthquake seismic wave, there must be relationship of crustal geology with frequency in which the wave propagates. Since it is wanted to see the variation of frequency along with the variation of amplitude, in the first phase ground motion seismic waves have been normalized to a unique maximum value to see uniform time frequency to amplitude effects. It is observed from the Figs. 4.16-4.24 that the peak time frequency to amplitude effect can be marked easily. The observations also show that the positions have been shifted to new times for peak effect in time frequency to amplitude analyses for earthquake waves.

Interfaces can be marked easily from the reflected time amplitude plot in exploration seismology but it becomes complicated for earthquake wave. When a wave propagated long distance through sub-surface, amplitude decreases exponentially. Frequency of the wave can be considered as better parameter for characterization of earthquake wave, when the amplitude is very low. So frequency to amplitude ratios is used to study the number of interfaces passed by the ground motion seismic wave. The magnitude and successive number of frequency to amplitude ratios as obtained in the time frequency to amplitude analysis can be used to study the degree of heterogeneity of the crustal structure.

In general the frequency to amplitude ratio can be shown exponentially decreasing manner. But the time frequency to amplitude ratio is found maximum and there is a huge frequency jump to a very low frequency of the propagated seismic wave. It can only happen when there is a very sharp acoustic impedance contrast present in the

path of the propagated seismic wave. However realistic modelling cannot be performed using TFA characteristics of the earthquake wave.

The research work is then extended for dispersion analysis. In this case, at first the experimental group velocity dispersion curve of earthquake data and the theoretical group velocity dispersion curves of the model parametric data (Table 5.2-5.4) have been made by using graphical method and modified Haskell matrix method respectively. Fig.5.3 shows the experimental dispersion curve and Figs.5.4-5.6 show the theoretical dispersion curves.

An initial earth's model has been considered to study the sensitivity of the model parameters. According to the model parameters, the dispersion curve has been made. For the change of value of each model parameters, dispersion curves have also been made and sensitivity observed. Figs. 5.7-5.10 show the sensitivity of the model parameters. It has been found that the S wave velocity and thickness are more sensitive than the other model parameters P wave velocity and density.

The theoretical dispersion curves have been matched with the experimental dispersion curves in order to estimate the crustal structure of the study area. For this purpose many models are created but a few of the models, which were found statistically close to the real condition, are only being considered. The group velocities obtained from earthquake data and from models have the similar characteristics as both are varying with period, and interpretations are made from model parameters. The statistical errors have been computed between the group velocities of dispersion curve. Considering statistical error analysis, it can be said that all the models are very nearer to an acceptable matching level, though the statistical confidence level SPF should be 95% but our results are above of that confidence level. In view of all errors studying in this research, sixteen models (Figs. 6.4-6.19) are seemed good enough for estimating the layer parameters. The detail statistical analysis between the experimental and theoretical group velocity dispersion curves are presented in table 6.1.

According to signal power fit the models of Figs. 6.20-6.22 are found more acceptable to represent the crustal structures. Hence from the analysis of Chittagong earthquake events four major sub-surface layers are identified within the depth of 20.5 km. The layer thicknesses are 1.5 km, 5.0 km, 6.0 km and 8.0 km with corresponding densities 2.54 gm/cc, 2.57 gm/cc, 2.60 gm/cc and 2.65 gm/cc. Also the south of Meiktila, Myanmar earthquake event indicates four layers of thicknesses 1.5 km, 3.5 km, 3.0 km, and 3.0 km of a total depth of 11.0 km (Fig 6.22). The densities are almost the same as found in the Chittagang events.

So from the analysis of earthquake surface waves it could be said that the model parameters of Fig. 6.21 are representing the crustal structure of the south-eastern region of Bangladesh.

Chapter 8
Conclusions

Seismology is playing an important role in the development process of geosciences in an effort to understand the structure and dynamics of the earth. When the ground moves violently, causing catastrophic loss of life as the earth surface disrupted and the building collapsed. Realistic crustal structure of an area is to be learned to mitigate catastrophic damages to reduce the threats of earthquake for the resources development and security. The present framework of knowledge of seismology is at a mature state but earthquake phenomenology is still not understandable. This thesis is an effort in the development process of seismological research through which crustal structure of the south-eastern region of Bangladesh is studied using surface wave analysis and modelling.

Time frequency to amplitude ratio, an extension of time frequency analysis, of the regional earthquake waves are studied for the characterization of crustal structure. It has seen few better characteristics from such analyses, but cannot obtain well correlation with the crustal variables. However, the analyses have successfully localized and obtained time frequency to amplitude effects as sequences on the recorded seismic surface waves.

So the dispersion analysis of group velocity distributions in the earth is introduced. Group velocity dispersions are computed and analyzed using graphical method for local earthquake seismic waves. Theoretical dispersion curves are also made according to modified Haskell matrix method. The computational algorithms of such dispersion curves of graphical method and extended Haskell matrix method are also furnished and some results are shown throughout the thesis.

An indirect model of the crustal structure has been constructed. The analysis of group velocities obtained from the earthquake wave and model parameters revealed the actual crustal structure of sub-surface. It was challenging to set up the model parameters. Most critical constraint was to consider the Poisson's ratio of 0.25. In real cases the ratio might be different for different subsurface layers and hence the interpreted crustal structure from model might not be appropriate. However for the computational advantages $\alpha : \beta$ ratio or Poisson's ratio were kept fixed at 1.732 or 0.25 respectively. Sensitivity of the constructed models has been studied and it is found that the S wave velocity and thickness of the layers are the vital factors. Therefore, S wave velocity and thickness setting in the model is also found very difficult. However, from the investigations it has been observed that the setting of total depth rather than individual thicknesses of the subsurface layers can provide more better and acceptable interpretations.

From the analysis and modelling of three earthquake events, the crustal structure of the south-eastern region of Bangladesh has revealed that there are four major crustal layers within the depth of 20.5 km. Layer thicknesses and densities of the area are respectively 1.5 km and 2.54 gm/cc; 5.0 km and 2.57 gm/cc; 6.0 km and 2.60 gm/cc; and 8.0 km and 2.65 gm/cc. Analysis and modelling of seismic surface wave presented in this thesis have demonstrated to be effective and have assessed the major crustal structure of the south-eastern region of Bangladesh.

References

Abo-Zena, A., (1979) Dispersion function computations for unlimited frequency values. Geophysical Journal of the Royal Astronomical Society, v. 58, pp. 91-105.

Aki, K., (1957) Space and time of stationary stochastic wave, with special reference to microtremors. Bulletin of the Earthquake Research Institute, v. 35, pp. 415-457.

Aki, K., (1965) Maximum likelihood estimation of b in the formula LogN=a-bM and its Confidence limits. Bulletin of the Earthquake Research Institute, University of Tokyo, v. 43, pp.237-239.

Alden, A., (2011) Earthquake Magnitudes Measuring the Big One.The New York Times Company, http://geology.about.com/cs/quakemags/a/aa060798.htm, downloaded as on 16 March 2011.

Allen, C.R., Amand, P.St., Richter, C.F. and Nordquist, J.M., (1965) Relationship between seismicity and geologic structure in the Southern California region. Bulletin of the Seismological Society of America, v. 55, pp. 753-797.

Allen, J.B. and Rabiner L., (1977) A unified approach to short-time-Fourier analysis and synthesis. Proceedings of Institute of Electrical and Electronics Engineers, v. 65(11), pp. 1558-1564,

Alterman, Z., Jarosch, H. and Pekeris, C.L., (1959) Oscillations of the Earth. Proceedings of Royal Astronomical Society, London, v. 252, pp. 80-95.

Ammon, C.J., Randall, G.E. and Zandt, G., (1990) On the nonuniqueness of receiver function inversions. Journal of Geophysical Research, v. 95, pp. 15303-15318.

Ammon, C.J. (ed.), (2010) Seismic Waves and Earth's Interior. http://eqseis.geosc.psu.edu/~cammon/HTML/Classes/IntroQuakes/Notes/waves_and_interior.html, downloaded as on 12 October 2010.

Amand, P.St., (1956) Two proposed measures of seismicity. Bulletin of the Seismological Society of America, v. 46, pp. 41-45.

References

Asiatic Society of Bangladesh (ASB), (2006) Banglapedia, CD edition February. http://www.banglapedia.org/english/copyright.html, downloaded as on 30 December 2010.

Bãth, M., (1956) A note on the measure of seismicity. Bulletin of the Seismological Society of America, v. 45, pp. 217-218.

Bender, B., (1983) Maximum likelihood estimation of b values for magnitude grouped data. Bulletin of the Seismological Society of America, v. 73(3), pp. 831-851.

Bender, F., (1983) Geology of Burma. Gebrüder Bornträger, Berlin, 260 p.

Benjamin, F. and Howell, Jr., (1990) An Introduction to Seismological Research, History and Development. Cambridge University Press, 201 p.

Ben-Menahem, A., (1995) A Concise History of Mainstream Seismology (Review), Origins, Legacy, and Perspectives. Bulletin of the Seismological Society of America, v. 85(4), pp. 1202-1225.

Bloch, S. and Hales, A.L., (1968) New techniques for the determination of surface wave phase velocities. Bulletin of the Seismological Society of America, v. 58, pp. 1021-1036.

Bloch, L., Hales, A.L. and Landisman, M., (1969) Velocities in the Crust and Upper Mantle of Southern Africa from Multi-Mode Surface-Wave Dispersion, Bulletin of the Seismological Society of America, v. 59, pp. 1599-1630.

Bolt, B.A., (1993) Earthquakes and Geological Discovery. Scientific American Library, W. H. Freeman and Company, 229 p.

Bowler, S., (1990) A simple model for planets' magnetic fields. New Scientist, v. 126, 32 p.

Braile, L.W. and Keller, G.R., (1975) Fine Structure of the Crust Inferred from Linear Inversion of Rayleigh-Wave Dispersion. Bulletin of the Seismological Society of America, v. 65, pp. 71-83.

Braile, L., (2004) Accessing current, recent and historical earthquake data. The IRIS Consortiam. http://web.ics.purdue.edu/%7Ebraile/edumod/eqdata/eqdata.pdf, downloaded as on 10 January 2010.

Brune, J. and Dorman, J., (1963) Seismic waves and earth structure in the Canadian Shield. Bulletin of the Seismological Society of America, v. 53, pp. 169-209.

Buchen, P. and Ben-Hador, R., (1996) Free-mode surface-wave computations. Geophysical Journal International, v. 124, pp. 869-887.

References

Bullen, K.E., (1963) An Introduction to the Theory of Seismology. Cambridge University Press, 381 p.

Campillo, M. and Paul, A., (2003) Long-range correlations in the diffuse seismic coda. Science, v. 299, pp. 547-549.

Carcione, J.M., Herman, G.C. and Kroode, P.E., (2002) Y2K Review Article Seismic Modeling. Geophysics, v. 67, pp. 1304-1325.

Chakraborty, A. and Okaya, D., (1995) Frequency-time decomposition of seismic data using wavelet-based methods. Geophysics, v. 60(6), pp. 1906-1916.

Chouhan, R.K.S., (1970) On the Frequency-Magnitude relation $\log N = a - b$ M. Pure and Applied Geophys, v. 81(IV), pp. 119-123.

Christova, C. and Vanék, J., (1990) Variation of seismic activity and b-value in the Wadati–Benioff zone of the Hellenic arc, Stuia. Geophysics, v. 34, pp. 197-207.

Classen, T. and Macklenbrauker, W., (1980) The Wigner distribution-A tool for time-frequency signal analysis, 3 Parts. Philips Journal of Research, v. 35(3-6), pp. 217-250, 276-300, 372-389.

Cohen, A., Daubechies, I., Jawerth, B. and Vial, P., (1993) Multiresolution analysis, wavelets and fast wavelet transform on an interval. Comptes rendus de Académie des sciences Série 1 Mathématique, v. 316, pp. 417-421.

Dain, E., Tapponnier, A.Y. and Molnar, P., (1984) Active Faulting and Tectonics of Burma and Surrounding Regions. Journal of Geophysical Research, v. 89(B1), pp. 453-472.

DasGupta, S., (1984) Tectonic trends in Surma basin and possible genesis of folded belt. Memoirs of the Geological Survey of India, v. 113, pp. 58-61.

Davison, C., (1927) The Founders of Seismology. Cambridge University Press, 240 p.

Deshpande, A., (2010) Richter Magnitude Scale. http://www.buzzle.com/articles/richter-scale-explained.html, downloaded as on 5 August, 2010.

Dewey, J. and Byerly, P., (1969) The Early History of Seismometry (to 1900). Bulletin of the Seismological Society of America, v. 59(1), pp. 183-227.

Dorman, J., Ewing, M. and Oliver, J., (1960) Study of Shear-Velocity Distribution in the Upper Mantle by Mantle Rayleigh Waves. Bulletin of the Seismological Society of America, v. 50, pp. 87-115.

Dorman, J. and Ewing, M., (1962) Numerical Inversion of Seismic Surface Wave Dispersion Data and Crust-Mantle Structure in the New York-Pennsylvania Area. Journal of Geophysical Research, v. 67, pp. 5227-5241.

Dost, B., (1994) The ORFEUS Data Center, Annali Di Geofisica, v. 37(5), pp. 1071-1074.

Dunkin, J., (1965) Computation of modal solutions in layered elastic media at high frequencies. Bulletin of the Seismological Society of America, v. 55, pp. 335-358.

Dziewonski, A.M. and Hales, A.L, (1972) Numerical analysis of dispersive seismic waves, in Methods in Computational Physics, edited by B.A. Bolt. Academic Press, v. 11, pp. 217-295.

Dziewonski, A., Mills, J. and Bloch, S., (1972) Residual dispersion measurements; a new method of surface wave analysis. Bulletin of the Seismological Society of America, v. 62, pp. 129-139.

Dziewonski, A.M. and Hales, A.L, (1972) Numerical analysis of dispersive seismic waves, in Methods in Computational Physics, edited by B.A. Bolt. Academic Press, v. 11, pp. 217-295.

Dziewonski, A., Mills, J. and Bloch, S., (1972) Residual dispersion measurements; a new method of surface wave analysis. Bulletin of the Seismological Society of America, v. 62, pp. 129-139.

Evans, P., (1964) The tectonic framework of Assam. Journal of the Geological Society of India, v. 5, pp. 80-96.

Ewing, M. and Press, F., (1952) Crustal structure and surface wave dispersion; Part 1, Solomon Islands earthquake of July 29, 1950. Bulletin of the Seismological Society of America, v. 42, pp. 315-325.

Ewing, M., Jardetsky, W. and Press, F., (1957) Elastic Waves in Layered Media. McGraw-Hill Book Company, New York, 380 p.

Elenean, K.M.A., Aldamegh, K.S., Zharan, H.M. and Hussein, H.M., (2009) Regional waveform inversion of 2004 February 11 and 2007 February 09 Dead Sea earthquakes. Geophysical Journal International, v. 176, pp. 185–199.

Fathom, (2002) A Brief History of Seismology. Fathom Knowledge Network, http://www.fathom.com/feature/122149/, downloaded as on 16 November 2010.

References

Ganguly, S., (1997) Petroleum Geology and Exploration History of the Bengal Basin in India and Bangladesh. Indian Journal of Geology, v. 69(1), pp. 1-25.

Gregory, C., (2006) Earthquake Nation. The Cultural Politics of Japanese Seismicity, 1868–1930. University of California Press, Berkeley, 331 p.

Gubin, I.E., (1964b) Earthquake forecasting II. Bulletin of the Academy of Sciences USSR, Geophysical Survey, v. 9, pp. 783-787.

Gubin, I.E., (1966a) Single-element seismic zoning maps. Academy of Science, USSR, Physics of the Solid Earth, v. 6, pp. 372-376.

Gubin, I.E., (1966b) Multiple-element seismic zoning maps. Academy of Science, USSR, Physics of the Solid Earth, v. 7, pp. 424-429.

Gumbel, E.J., (1958) Statistics of Extremes, Columbia Union Press, New York, 375 p.

Gutenberg, B. and Richter, C.F., (1954) Seismicity of the Earth and associated phenomena. Princeton University Press, New Jersey, 310 p.

Gutenberg, B. and Richter, C.F., (1956c) The energy of earthquake. Quarterly Journal of the Geological Society of London. v. 112, pp. 1-14.

Haskell, N.A., (1953) The dispersion of surface waves in multilayered media. Bulletin of the Seismological Society of America, v. 43, pp. 17-34.

Hayes, M.H., (1996) Statistical Digital Signal Processing and Modeling. John Wiley & Sons, New York, 608 p.

Hiller, K., (1988) On the Petroleum Geology of Bangladesh. Bundesanstalt fur Geowissenschaften und Rohstoffe und Geologische Landesamter in der Bundes Republic Deutsch, Hannover, 351 p.

Hu, J. F., Su, Y.J. and Zhu, X.G., (2002) S wave velocity and Poisson's ratio structure of crust in Yunnan and its implication. Science in China (Ser. D) (in Chinese), v. 33(8), pp. 714-722.

Istituto Nazionale de Geofisica e Valcanologia (INGV), (2009) Seismology, Bologana Branch, Bologana, Italy. http://www.bo.ingv.it/contents/scientific-research/Seismology.html, downloaded as on 23 October 2009.

Incorporated Research Institutions for Seismology (IRIS), (2011) Data Types, Data Management Center. http://www.iris.edu/data/types.htm, downloaded as on 10 July 2011.

Incorporated Research Institutions for Seismology (IRIS), (2011) PASSCAL Instrument Center. http://www.passcal.nmt.edu, downloaded as on 1 August 2011.

References

International Union of Geodesy and Geophysics (IUGG), (2007) Geosciences. http://www.iugg.org/publications/reports/, The Future, 2007, 106 p.

Jia-Fu, H., Yi-Li, H., Jin-Yu, X., Yun, C., Hong, Z. and Hai-Yan, H., (2008) Crust-Mantle Velocity Structure of S Wave and Dynamic Process Beneath Burma Arc and its Adjacent Regions. Chinese Journal of Geophysics, v. 51(1), pp. 105-114.

Johnson, S.Y. and Alam, A.M.N., (1991) Sedimentation and Tectonics of the Sylhet Trough, Bangladesh. Bulletin of the Geological Society of America, v. 103, pp. 1513-1527.

Kan, R.J. and Lin, Z.Y., (1986) A preliminary study on crustal and upper mantle structures in Yunnan. Earthquake Research in China (in Chinese), v. 2(4), pp. 50-61.

Kaila, K.L., Rao, N.M. and Narain, H., (1974) Seismotectonic maps of southwest Asia region comprising eastern Turkey, Caucasus, Persian plateau, Afghanistan and Hindu Kush. Bulletin of the Seismological Society of America, v. 64(3), pp. 657-669.

Kaila, K.L. and Rao, N.M., (1975) Seismotectonic maps of European area, Bulletin of the Seismological Society of America, v. 65(6), pp. 1721-1732.

Kanamori, H. and Brodsky, E.E., (2004) The physics of earthquakes. Reports on Progress in Physics, v. 67, pp. 1429-1496.

Kay, S.M., (1988) Modern spectral estimation, Theory and application. Prentice-Hall, USA, 543 p.

Kelly, K.R. and Marfurt, K.J. (Eds.), (1990) Numerical modeling of seismic wave propagation. Society of Exploration Geophysicists, v. 67, pp. 171-177.

Kennett, B.L.N., (1974) Reflection, rays and reverberations. Geophysical Journal of the Royal Astronomical Society, v. 64, pp. 1685-1696.

Kennett, B.L.N. and Kerry, N.J., (1979) Seismic waves in a stratified half-space. Geophysical Journal of the Royal Astronomical Society, v. 57, pp. 557-583.

Kennett, B.L.N., (1983) Seismic Wave Propagation in Stratified Media. Cambridge University Press, London, 288 p.

Khan, A.A., (1991) Tectonics of the Bengal Basin. Journal of Himalayan Geology, v. 2(1), pp. 91-101.

Khan, A.A., (2010) Earthquake, Tsunami and Geology of Bangladesh. UGC. Publication, Bangladesh, 332 p.

Khin, J., (1990) Geological, petrological and geochemical characteristics of granitoid rocks in Burma with special reference to the associated W-Sn mineralization and there tectonic setting. Journal of Southeast Asian Earth Sciences, v. 4(4), pp. 293-304.

Klein, F.W., (1978) Hypocenter location program HYPOINVERSE. U. S. Geological Survey, Open-File Report 78-694, 102 p.

Knopoff, L., (1961) Green's function for eigenvalue problems and the inversion of Love wave dispersion data. Geophysical Journal International, v. 4, pp. 161-173.

Knopoff, L., (1964) A matrix method for elastic wave problems. Bulletin of the Seismological Society of America, v. 54, pp. 431-438.

Knopoff, L., Mueller, S. and Pilant, W.L., (1966) Structure of the crust and upper mantle in the Alps from the phase velocity of Rayleigh waves. Bulletin of the Seismological Society of America, v. 56, pp. 1009-1044.

Koeing, W., Dunn, H. and Lacy, L., (1946) The sound spectrograph. Journal of the Acoustical Society of America, v. 18(1), pp 19-49.

Kovach, R.L., (1978) Seismic surface waves and crustal and upper mantle structure. Reviews of Geophysics and space physics, v. 16, pp.1-13.

Kozlovsky, Y.A. (Ed.), (1987) The Super deep Well of the Kola Peninsula. Springer Verlag, Berlin, 558 p.

Kradolfer, U., (1993) Automating the Exchange of Earthquake Information. EOS Transactions American Geophysical Union, v. 74(39), 442 p.

Kradolfer, U., (1996) AutoDRM–The First Five Years. Seismological Research Letter, v.67, pp. 30-33.

Lahr, J.C., (1989) HYPOELLIPSE/Version 2.0. A computer program for determining local earthquakes hypocentral parameters, magnitude, and first-motion pattern. U. S. Geological Survey, Open-File Report 89-116, 92 p.

Landisman, M., Dziewonski, A. and Sata, Y., (1969) Recent improvements in the analysis of surface wave observations. Journal of Geophysical Research, v. 17, pp. 369-403.

Larson, E.W. and Ekström, G., (2001) Global models of surface wave group velocity. Pure and Applied Geophysics, v. 158, pp. 1377-1400.

Lay, T. (eds.), (2009) History of the Theory of Elasticity. Cambridge University Press, v. I, pp. 627-634.

Lee, A.W., (1932) The determination of thicknesses of the continental layers from travel times of seismic waves. Geophysical Journal International, v. 3, pp. 13-21.

Lee, W.H.K. and Lahr, J.C., (1972) HYPO71. A computer program for determining hypocenter, magnitude, and first motion pattern of local earthquakes. U.S. Geological Survey, Open-File Report 135-171, 120 p.

Lee, W.H.K. (ed.), (1994) Digital Seismogram Analysis and Waveform Inversion IASPEI software Library Volume 3. Seismological Society of America, 183 p.

Lilwall, R.C. and Douglas, A., (1984) Global seismicity in terms of short period magnitude M_b based on individual station magnitude-frequency distributions, A.W.R.E. Rep., 023/84, HMSO, London.

Lomnitz, C., (1974) Global Tectonics and Earthquake Risk. Developments in Geotectonics 5, Elsevier Scientific Publication Company, 320 p.

Love, A.E.H., (1911) Some Problems of Geodynamics. Cambridge University Press, 180 p.

Luco, J.E., and Apsel, R.J., (1983) On the Green's function for a layered half-space, part I. Bulletin of the Seismological Society of America, v. 73, pp. 909-929.

Mallat, S., (1989) A theory for multiresolution signal decomposition: the wavelet representation. Institute of Electrical and Electronics Engineers, Transactions on Pattern Analysis and Machine Intelligence, v. 11(7), pp. 674-693.

Marple, S.L., (1987) Digital spectral analysis, with applications. Prentice-Hall, 492 p.

McEvilly, T.V., (1964) Central U. S. Crust-Upper Mantle Structure from Love and Rayleigh Wave Phase Velocity Inversion. Bulletin of the Seismological Society of America, v.54, pp. 1997-2015.

Medalia, J. (ed.), (2008) Comprehensive Nuclear Test-Treaty. CRS Report for Congress, www.fas.org/sgp/crs/nuke/RL34394.pdf, downloaded as on 10 July, 2010.

Mitchell, A.H.G., (1993) Cretaceous-Cenozoic Tectonic Events in the Western Myanmar (Burma)-Assam Region. Journal of the Geological Society (London), v. 150, pp. 1089-1102.

Mitra, S., Hazarika, N., Priestley, K. and Gaur, V. K., (2006) Lithospheric structure across the eastern Himalayan collision from the Bengal basin to southern Tibet. Journal of Asian Earth Sciences, v. 26, 151 p.

References

Mitra, S., Bhattacharya, S.N. and Nath, S.K., (2008) Crustal Structure of the Western Bengal Basin from Joint Analysis of Teleseismic Receiver Functions and Rayleigh-Wave Dispersion. Bulletin of the Seismological Society of America, v. 98(6), pp. 2715-2723.

Morgan, J.P. and Mcintire, W.G., (1959) Quaternary Geology of the Bengal Basin, East Pakistan and India. Bulletin of the Geological Society of America, v. 70, pp. 319-342.

Nandy, D.R., (1980) Tectonic Patterns in Northeastern India. Indian Journal of Earth Sciences, v. 7(1), pp. 103-107.

Nandy, D.R., Dasgupta, S., Sarkar, K. and Ganguly, A., (1983) Tectonic Evolution of Tripura-Mizoram Fold Belt, Surma Basin, Northeast India. Quarterly Journal of the Geological, Mining and Metallurgical Society of India, v. 55(4), pp. 186-194.

Nandy, D.R., (2001) Geodynamics of Northeastern India and the adjoining region. ACB, Calcutta, India, 209 p.

National Aeronautics and Space Administration, (NASA), (2011) Solar System Exploration, 11 May 2011. http://solarsystem.nasa.gov/planets/profile.cfm?Object = Earth&Display=Facts, downloaded as on 11 July 2011.

National Research Council (NRC), (2001) Basic Research Opportunities in Earth Sciences. http://books.nap.edu/catalogphp?record_id=9981, National Academic Press, Washington, 153 p.

National Research Council (NRC), (2008) Origin and Evolution of Earth, Research Questions for a Changing Planet. http://www.nap.edu/openbook.php?record_id=12161, National Academic Press, Washington, 137 p.

Novotny, O., (1999) Seismic Surface Waves, Lecture notes for post-graduate Studies. nstituto de Fisica, Salvador, Bahia, 156 p.

Orfeus, (2011) Observatories and Research Facilities for European Seismology, Seismological Software Library. http://www.orfeus-eu.org/Software/softwarelib.html, downloaded as on 24 May 2011.

Park, C.B., Miller, R.D. and Xia, J., (1999) Multichannel analysis of surface waves. Geophysics, v. 64, pp. 800-808.

References

Percival, D.B. and Walden, A.T., (1993) Spectral analysis for physical applications-Multitaper and conventional univariate techniques. Cambridge University Press, 580 p.

Pesquet, J.C., Krim, H. and Carfatan, H., (1996) Time-invariant orthonormal wavelet representations. Institute of Electrical and Electronics Engineers, Transactions on Signal Processing, v. 44(8), pp. 1964-1970.

Pestel, E. and Leckie, F.A., (1963) Matrix Methods in Elasto-Mechanics. McGraw–Hill, New York, 451 p.

Peter, B., Klaus, K. and Seigfruid, W., (2009) Data Analysis and Seismogram Interpretation. ebooks.gfz-potsdam.de/pubman/item/escidoc:4002.../Chapter_1_rev1.pdf, downloaded as on 3 May 2009.

Pivnik, D.A., Nahm, J., Tucker, R.S., Smith, G.O., Nyein, K., Nyunt, M. and Maung, P.H., (1998) Polyphase deformation in a fore-arc/back-arc basin, Salin subbasin, Myanmar (Burma). Bulletin of the American Association of Petroleum Geologists, v. 82, pp. 1837-1856.

Rahman, S.M., Islam, M.R., Keramat, M. and Islam, M.S., (2007) Seismic attribute analysis for the characterization of Tibetan Bright Spots: INDEPTH Seismic Profiles Tibet 9 and 10, Journal of the Geological Society of India, v. 69(4), pp. 739-745.

Reid, H.F., (1914) The Lisbon earthquake of November 1, 1755. Bulletin of the Seismological Society of America, v .4, pp. 53-80.

Ritsema, A.R., (1954) The seismicity of the Sunda Arc in space and time, Indonesia. Madjalah ilmu alam untuk Indonesia, v. 110, pp. 41-49.

Ritzwoller, M.H. and Levshin, A.L., (2002) Estimating shallow shear velocities with marine multi-component seismic data. Geophysics, v. 67, pp. 1991-2004.

Riznichenko, Yu.V., (1958) The study of seismic conditions. Bulletin of the Academy of Sciences of the U.S.S.R., Geophysics Series, v. 9, pp. 615-622.

Riznichenko, Yu.V., (1959) On quantitative determination and mapping of seismic activity. Annall Geofisica (Rome), v. 12, pp. 227-237.

Satŏ, Y., Landisman, M. and Ewing, M., (1960) Love waves in a heterogeneous, spherical earth, Parts 1 and 2. Journal of Geophysical Research, v. 65, pp. 2395-2404.

Schwab, F.A., (1970) Surface-wave dispersion computations, Knopoff's method. Bulletin of the Seismological Society of America, v. 60, pp. 1491-1520.

Schwab, F.A. and Knopoff, L., (1970) Surface-wave dispersion computations. Bulletin of the Seismological Society of America, v. 60, pp. 321-344.

Schenkova, Z. and Karnik, V., (1970) The probability of occurrence of largest earthquakes in the European area- part II. Pure and Applied Geophysics, v. 80 (III), pp.152-161.

Schwab, F.A. and Knopoff, L., (1972) Fast surface wave and free mode computations, edited by B. A. Bolt, Methods in Computational Physics. Academic Press, New Youk, pp. 87-180.

Schenkova, Z. and Prochazkova, D., (1976) Correlation of statistical estimations of the largest possible earthquakes. Acta Geophysica, v. 24(2), pp. 11-116.

Shearer, P.M., (1999) Introduction to Seismology. Cambridge University Press, 260 p.

Smith, W.D., (1986) Evidence for precursory changes in the frequency-magnitude b-value. Journal of Geophysical Royal Astronomical Society, v. 86, pp. 815-838.

Snieder, R.K., (1987) Surface wave holography in Seismic Tomography With Applications in Global Seismology and Exploration Geophysics edited by G. Nolet. D. Reidel Publication, Norwell, Mass, U.S.A., pp. 323-337.

Steeghs, P. and Drijkoningen, G., (2001) Seismic sequence analysis and attribute extraction using quadratic time-frequency representations. Geophysics, v. 66(6), pp. 1947-1959.

Talukdar, S.N., (1982) Geology and hydrocarbon prospects of east coast basins of India and their relationship to evolution of the Bay of Bengal. Offshore SE Asia, Singapore Conference, Expl I, Abs., v. 1, pp 1-8.

Taner, M.T., Koehler, F.and Sheriff, R.E., (1979) Complex seismic trace analysis. Geophysics, v. 44, pp. 1041-1063.

Thomson, W.T., (1950) Transmission of elastic waves through a stratified solid medium. Journal of Applied Physics, v. 21, pp. 89-93.

Thrower, E.N., (1965) The computation of the dispersion of elastic waves in layered media. Journal of Sound and Vibration, v. 2(3), pp. 210-226.

Todhunter, I. and Pearson, K., (1893) A History of the Theory of Elasticity and of the Strength of Materials. Cambridge University Press, v. 2(1), 936 p.

References

Uddin, A. and Lundberg, N., (1998a) Cenozoic history of the Himalayan-Bengal system, Sand composition in the Bengal basin, Bangladesh. Bulletin of the Geological Society of America, v. 110, pp. 497-511.

United States Geological Survey (USGS), (2009) Regional & Whole-Earth Structure. http://earthquake.usgs.gov/research/structure/, downloaded as on October 26 2009.

Utsu, T., (1965) A method for determining the value of b in relation for earthquakes. Bulletin of the Earthquake Research Institute, University of Hokkaido, Japan, v. 13, pp. 99-103.

Wang, J.H., (1988) b values of shallow earthquakes in Taiwan, Bulletin of the Seismological Society of America, v. 78(3), 1254 p.

Watson, T.H., (1970) A Note on Fast Computation of Rayleigh Wave Dispersion in the Multilayered Elastic Half-Space. Bulletin of the Seismological Society of America, v. 60(1), pp. 161-166.

Welch, P.D., (1967) The Use of Fast Fourier Transform for the Estimation of Power Spectra. A Method Based on Time Averaging Over Short, Modified Periodograms. Institute of Electrical and Electronics Engineers, Trans Audio Electroacoustics, v. (AU-15), pp. 70-73.

Willmore, P.L. (ed.), (1979) Manual of Seismological Observatory Practice. Technical Report SE-20, World Data Center A for Solid Earth Geophysics. NOAA, Boulder, Colorado, USA., 150 p.

Xia, J., Miller, R.D. and Park, C.B., (1999) Estimation of near-surface shear-wave velocity by inversion of Rayleigh waves. Geophysics, v. 64, pp. 691-700.

Zebrowski, E.Jr., (1997) Perils of a Restless Planet, Scientific Perspectives on Natural Disasters. Cambridge University Press, 302 p.

Appendix 1

The Richter scale, also known as the Richter magnitude scale is used to measure the magnitude of earthquakes. This scale was developed by Charles F. Richter of the California Institute of Technology in 1935. It is a logarithmic scale that ranges from 0 to over 10. The original Richter scale formula that is used to calculate the magnitude of any earthquake is as follows (Deshpande, 2010):

$$M_L = \log_{10} A - \log_{10} A_0 \left(\delta \right)$$

Where

A = Maximum excursion, or the greatest deviation on the Wood-Anderson seismograph

A_0 = Distance of the epicenter; δ = Location of the earthquake

M_L = Richter scale range

The magnitude of an earthquake is measured using the instrument known as seismograph. The magnitude is determined by the Richter scale from the logarithm of the amplitude of the waves that are recorded by the seismograph. In this scale 6 magnitude earthquake is 10 times greater than an earthquake of magnitude 5.

Today seismic events may be measured based on body waves or surface waves.

Body-wave magnitude is (Alden, 2011):

$$M_b = \log\left(\frac{A}{T} \right) + Q(D, h)$$

Where

A = ground motion in microns,

T = wave's period in seconds, and

Q(D,h) = correction factor that depends on distance to the quake's epicenter D in degrees and focal depth h in kilometers.

Surface-wave magnitude is

$$M_s = \log\left(\frac{A}{T}\right) + 1.66 \log D + 3.30$$

This moment magnitude, M_w, is not based on seismometer readings at all but on the total energy released in a quake, the seismic moment M_0 in dyne-centimeters:

$$M_w = \frac{2}{3}\log(M_0) - 10.7$$

The formula for M_w is such that below magnitude 8 it matches M_s and below magnitude 6 it matches M_b.

The magnitude of earthquakes are based on the Richter scale and also describe the effects of earthquakes of various magnitude near the epicenter as shown in the following table (Deshpande, 2010):

Richter Magnitude	Description	Effects	Frequency of Occurrence
0 - 2.0	Micro	Not felt	About 8,000 per day
2.0 - 2.9	Minor	Not felt but recorded	About 1,000 per day
3.0 - 3.9	Minor	Often felt, but causes no damage	49,000 per year
4.0 - 4.9	Light	Often felt with shaking and rattling noises, but causes no significant damage	6,200 per year
5.0 - 5.9	Moderate	Can cause major damage, specially to poorly constructed buildings	800 per year
6.0 - 6.9	Strong	Can be destructive in areas up to about 160 km	120 per year
7.0 - 7.9	Major	Can cause serious damage	18 per year
8.0 - 8.9	Great	Causes serious damage over large areas	1 per year
9.0 - 9.9	Great	Can be very destructive in areas several miles across	1 per year
10.0 - more	Epic	Has never been recorded	Extremely Rare

List of Publications

M. O. Faruk, S. M. Rahman, M. A. Hashem and M. Keramat, Time frequency analysis of earthquake seismic wave, Proceedings of the ICECC, 27-29 June, University of Rajshahi, Bangladesh, 2008.
Related chapter: 3, 4.

M. M. Mahabub, S. M. Rahman, M. I. Mehedi, **M. O. Faruk**, Sediment Distribution of Continental Margin of the Southern Brazil Basin in the Southwest Atlantic Ocean, J. Soil Nature, v. 3(1), pp. 04-15, 2009.
Related chapter: 4.

M. O. Faruk, S. M. Rahman, M. A. Hashem and M. Keramat, Sequence Analysis of Ground Accelerated Earthquake Wave for studying Geology of the Earth, Online Journal of Earth Science, v. 4(1), pp. 56-62, 2010.
Related chapter: 3, 4.

M. O. Faruk, S. M. Rahman, M. A. Hashem and M. Keramat, Group Velocity Dispersion Analysis of Daluchari Chittagong Earthquake for Studying the Crustal Thickness, The IUP Journal of Earth Sciences, v. 5(2), pp. 26-39, 2011.
Related chapter: 3, 5 and 6.

M. O. Faruk, S. M. Rahman, M. A. Hashem and M. Keramat, Group Velocity Dispersion Analysis of Kolabunia Chittagong Earthquake for Studying the Crustal Thickness, Proceedings of the National Geoscience Conference, 11-12 June, The Puteri Pacific Johor Bahru, Johor, Malaysia 2011.
Related chapter: 3, 5, 6.

140